SGP-TR-59

FLOW CHARACTERISTICS AND RELATIVE PERMEABILITY FUNCTIONS FOR TWO PHASE GEOTHERMAL RESERVOIRS FROM A ONE DIMENSIONAL THERMODYNAMIC MODEL

Anthony J. Menzies

August 1982

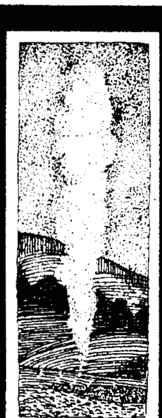

Stanford Geothermal Program
INTERDISCIPLINARY RESEARCH
IN ENGINEERING AND EARTH SCIENCES
Stanford University, Stanford, California

A

Stanford Geothermal Program
Interdisciplinary Research in
Engineering and Earth Sciences
STANFORD UNIVERSITY
Stanford, California

SGP-TR-59

FLOW CHARACTERISTICS AND RELATIVE PERMEABILITY FUNCTIONS FOR TWO PHASE GEOTHERMAL RESERVOIRS FROM A ONE DIMENSIONAL THERMODYNAMIC MODEL

By

Anthony J. Menzies

August 1982

Financial support was provided through the Stanford Geothermal Program under Department of Energy Contract No. DE-AT03-80SF11459 and by the Department of Petroleum Engineering, Stanford University.

ABSTRACT

Theoretical flow characteristics for a fractured geothermal reservoir have been obtained by modelling the system with a one dimensional thermodynamic model. The model includes the effect of heat transfer from the rock to the fluid and irreversible processes, such as friction, by using an effective isentropic efficiency term. By approching the problem in this manner it has not been necessary to define the flow geometry or to define such parameters as the two phase friction factor.

By comparing the theoretical characteristics generated by the model with field data it is possible to estimate the flow area and an effective fracture width for the two phase flow into the wellbore from the reservoir. It is also possible to calculate under what conditions choking will occur in the reservoir and hence, the maximum exploitation rate for the reservoir/well system.

Field examples are included to illustrate how the flow area and effective fracture width are calculated. It was further found that certain characteristics of the field flow data could be explained by the concept of choked or critical flow.

From the data generated by the model it was possible to derive a unique set of relative permeability curves, independent of the reservoir temperature. They were derived as functions of the inplace liquid saturation and could therefore be used in present geothermal simulators. They have been compared with a number of other relative permeability functions and it is concluded that the relative permeability functions developed here are probably more consistent for fractured geothermal reservoirs.

TABLE OF CONTENTS

LIST OF FIGURES

LIST OF TABLES

1. INTRODUCTION

Study of the flow characteristics of geothermal wells has been largely limited to either liquid dominated reservoirs where flashing occurs in the wellbore, Nathenson(1974), Ryley(1980), or to vapor dominated systems, Rumi(1972). In both these cases flow in the reservoir is single phase and essentially isothermal. The reservoir behaviour can therefore be analyzed using flow equations developed in the groundwater hydrology or petroleum engineering literature. When two phase flow occurs in the reservoir the situation is more complex and cannot be analyzed in the same manner. The interactions between the two phases and the flow system become important in describing the flow behaviour. These interactions are accounted for in petroleum reservoir engineering by the use of the concept of relative permeability.

Geothermal applications have an additional complication since the two phase flow of oil and gas is essentially isothermal whereas a two phase flow of steam and water is not. Temperature drops as high as 50°C have been measured in geothermal reservoirs. In spite of this, relative permeability curves, particularly those developed by Corey(1954) for oil reservoirs, are still used in simulation models of geothermal reservoirs.

Two phase compressible flow has been studied in detail, particularly in nuclear reactor engineering, but very little of this research has been applied to geothermal systems. Choked or critical flow has formed a central part of this research effort and although it forms the basis of the James(1962) method for measurement of output parameters in geothermal wells, the idea that choked flow could occur in reservoir flow systems, thereby limiting the systems' output, has not been widely discussed.

The purpose of this research was to study the flow characteristics of two phase geothermal reservoirs, particularly the potential problem of choked or critical flow. As a result of the study it has also been possible to generate relative permeability functions to account for the observed flow characteristics.

2. TWO PHASE GEOTHERMAL RESERVOIRS

2.1 Flow Characteristics

The flow characteristics of geothermal reservoirs are inferred from the measurement of enthalpy, total massflow and concentration of chemical components as functions of the wellhead pressure. By plotting these characteristics under both transient and steady state conditions the general processes occurring in the reservoir can be inferred. In this study only the enthalpy and massflow changes are considered although the chemical changes are also important.

Figures 2.1 and 2.2 show specific examples of measured output characteristics from the Tungonan geothermal field, the Philippines and from the Larderello field in Italy, Rumi (1972). They illustrate the major differences in measured flow characteristics between single phase water, single phase steam and two phase geothermal reservoirs. The important characteristics of the two phase system are the almost constant massflow and increasing enthalpy at low wellhead pressures.

Figure 2.3 shows a crossplot of the enthalpy and massflow data for the two phase well, showing how the enthalpy rises very quickly over a small change in massflow. This is in disagreement with the observation of Sorey, Grant and Bradford(1980): "In two phase wells these measurements usually show enthalpy varying linearly with massflow (to a first approximation)". This characteristic is difficult to explain and is a central aspect of this research effort.

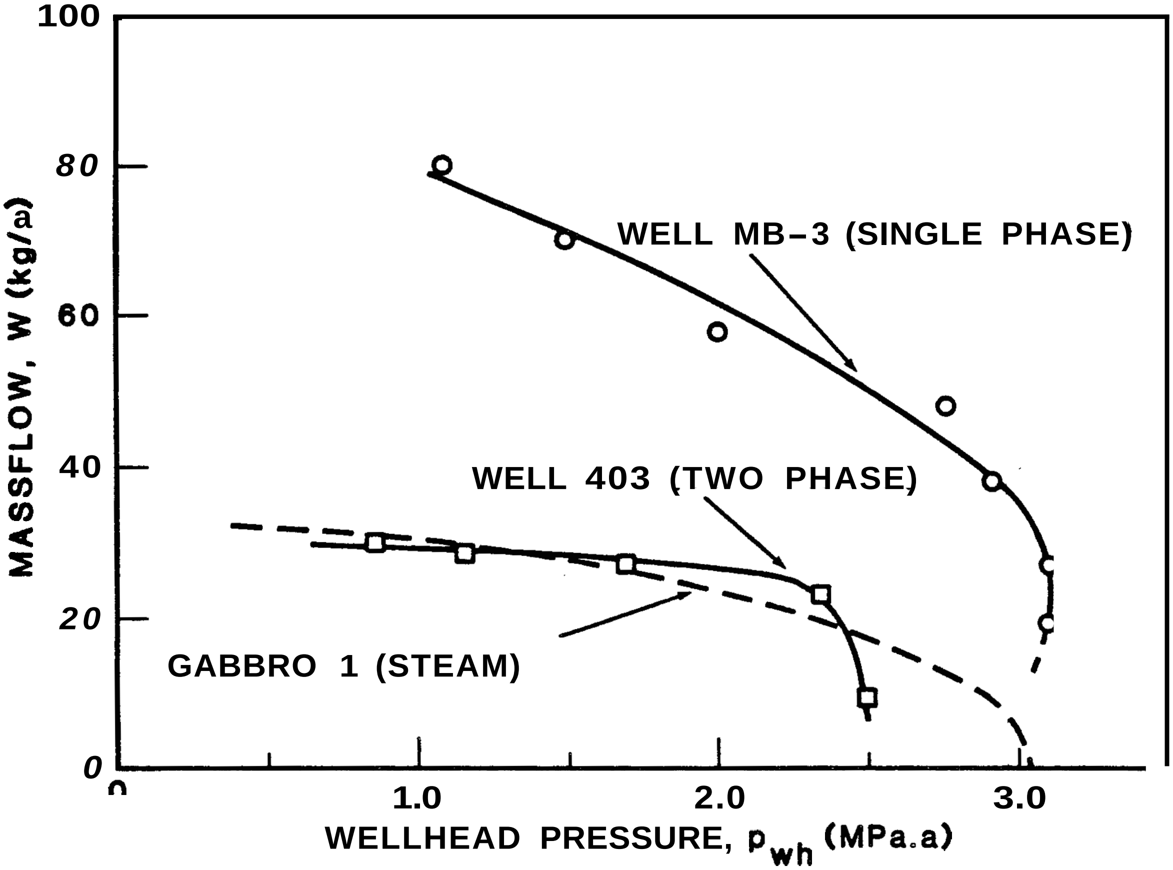

FIGURE 2.1: MASSFLOW CHARACTERISTICS OF TYPICAL GEOTHERMAL WELLS

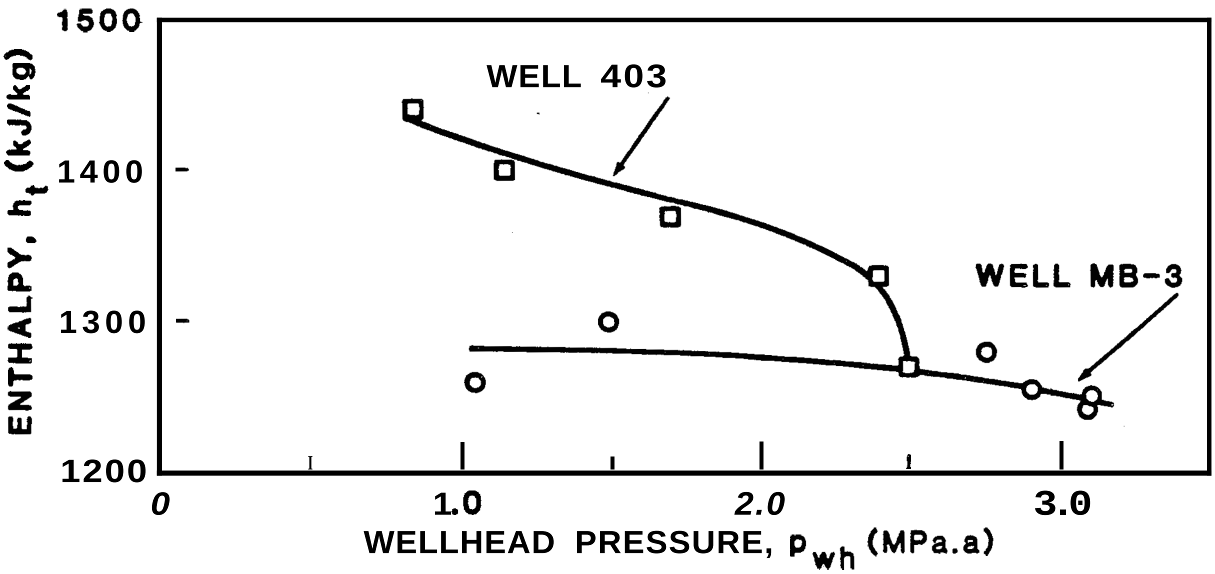

FIGURE 2.2: ENTHALPY CHARACTERISTICS OF TYPICAL GEOTHERMAL WELLS

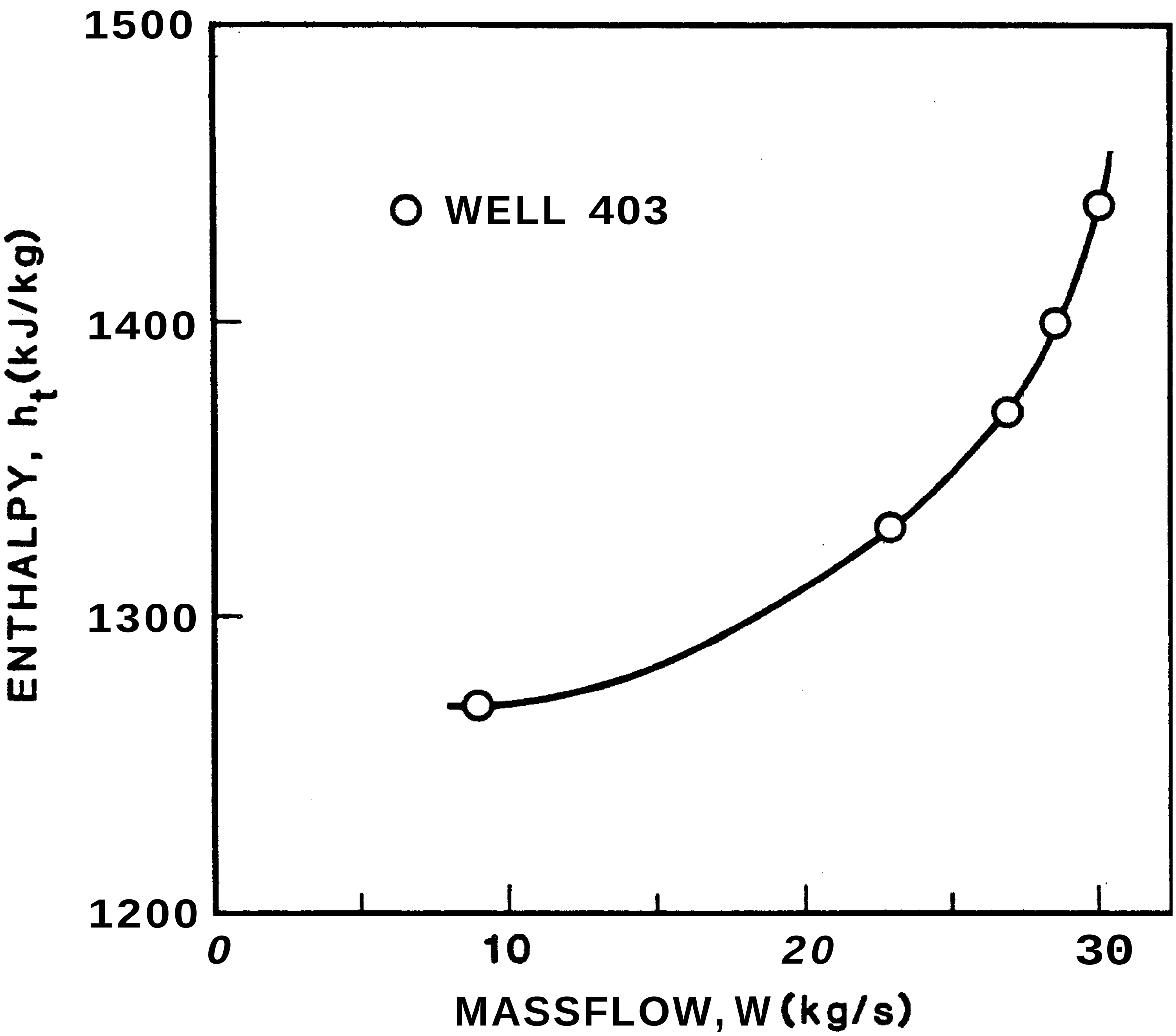

FIGURE 2.3: ENTHALPY, MASSFLOW CROSSPLOT FOR TWO PHASE GEOTHERMAL WELL

2.2 Relative Permeability Functions

A petroleum engineering approach to two phase flow in reservoirs is the use of relative permeability functions. Their basic use is to account for the interactions between one fluid and the other and also with the surroundings. Corey(1954) developed formulas to relate the oil and gas relative permeabilities to the inplace liquid saturation based on numerous measurements of the flow of oil and gas through consolidated sedimentary cores.

Tsang and Wang(1980) reviewed the current practice in simulation of geothermal recovery processes and observed that all the two phase models use the relative permeability functions developed by Corey(1954). This is in spite of the fact that few geothermal reservoirs are sedimentary and most are highly fractured volcanics. The rational for using the Corey equations in models of fractured geothermal reservoirs is that if a large enough control volume is used the heterogeneities due to the fractures will average out. However, this is only true when the two phase conditions are widespread over the reservoir and is likely to be in serious error where local changes in flow conditions occur. In addition, another major problem is that the relative permeability functions for steam and water are not well eshablished.

In terms of steam and water the Corey type relative permeability functions are (Sorey et al.(1980)):

$$k_{rw} = [S^*]^4 \qquad (2.2\text{-}1)$$

$$k_{rs} = [1 - (S^*)^2][(1 - S^*)^2] \qquad (2.2\text{-}2)$$

where:

$$S^* = \frac{(S - S_{rw})}{(1 - S_{rw} - S_{rs})} \qquad (2.2\text{-}3)$$

and: S_{rw}= residual water saturation

S_{rs}= residual steam saturation

A major problem with the use of these functions is the determination of S_{rw} and S_{rs}.

Experimental work by Counsil(1979) has defined relative permeability functions for steam and water flow, based on measurements in consolidated cores. These functions have not received widespread use in geothermal simulation.

A further method of defining the relative permeability functions is to use measured flow characteristics. The basic approach is described by Sorey et al.(1980) and Horne and Ramey(1978) and Shinohara(1978) present relative permeability curves calculated from procedures based on this approach. Using production data from wells in the Wairakei geothermal field in New Zealand, they were able to obtain relative permeability curves as functions of the flowing water mass fraction. The Corey relative permeability curves are functions of the inplace liquid saturation (vol. basis) and the field derived curves need to be converted to this basis before being used in present geothermal simulators. This is usually not possible.

The problem involved in converting from flowing to inplace saturations is discussed by Miller(1951). In his paper he states: "the weight fraction of gas in the mixture instantaneously at x is quite different from the weight fraction of gas in the mixture passing x in unit time". This arises because the vapor has a higher mobility and hence a higher velocity than the liquid. The ratio between the vapor and liquid velocities is called the "slip ratio" and it must be known to convert from flowing to inplace saturations. This is clearly not possible in a field situation.

This study therefore set out to investigate theoritically the two phase flow of steam and water mixtures in fractures in an attempt to derive relative permeability curves more appropriate to geothermal reservoir applications.

The next section deals with the selection and description of the thermodynamic model used in this research.

3. STREAMTUBE MODEL

3.1 Selection of Model

In an attempt to better understand the processes involved in the two phase flow of steam and water in a fractured geothermal reservoir, a model of steam/water flow in a confined conduit was sought.

There are a number of existing one dimentional models for the study of two phase vapor liquid flow. They are normally classified as homogeneous, slip or separated flow models, depending on the assumptions made in their derivation. The homogeneous models assume that the vapor and liquid phases have the same velocity, hence no meaningful relative permeability functions can be derived.

The model found to be *most* appropriate to this research was the "streamtube" model of Wallis and Richter(1978). This model overcomes the difficulties inherent in the usual slip flow theory by allowing the velocity and thermodynamic state to vary normal to the flow direction. It does this by considering the two phase flow field to be distributed between a number of discrete streamtubes, hence the name streamtube model. The streamtube model has been found to predict critical flow in nozzles more accurately than other slip models.

The text of Wallis and Richter's paper is reproduced as Appendix A.

3.2 Description of Model

The model uses a series of discrete pressure steps to approximate the continuous flashing. After each pressure step a streamtube is created. In this newly created streamtube initially only saturated steam flows. At the same time the steam in streamtubes that already existed is assumed to expand isentropically. When this occurs some of the steam condenses; this small amount of liquid is assumed to have the same velocity as the steam. Thus within each streamtube the homogeneous model is assumed to apply. This basic process is shown in Figure 3.1. There is assumed to be no interaction between the streamtubes and thus no transfer of energy, mass or momentum. Each streamtube has a different velocity, hence a velocity profile exists normal to the flow direction. The first vapor streamtube has the highest velocity and the liquid streamtube has the lowest velocity. The effective slip ratio is found from the ratio of the average vapor velocity to the liquid velocity.

In the original form of the model, the energy balance only considered the changes in enthalpy and velocity while the assumption of isentropic expansion required that the overall process be reversible. Thus the decrease in enthalpy must be equal to the increase in velocity. This implies that the system is frictionless and other energy changes such as gravitational effects have not been taken into account. In studies on nozzles these assuptions have been found to be valid. However, for geothermal reservoir applications heat transfer to the fluid is important and must be included in the model formulation.

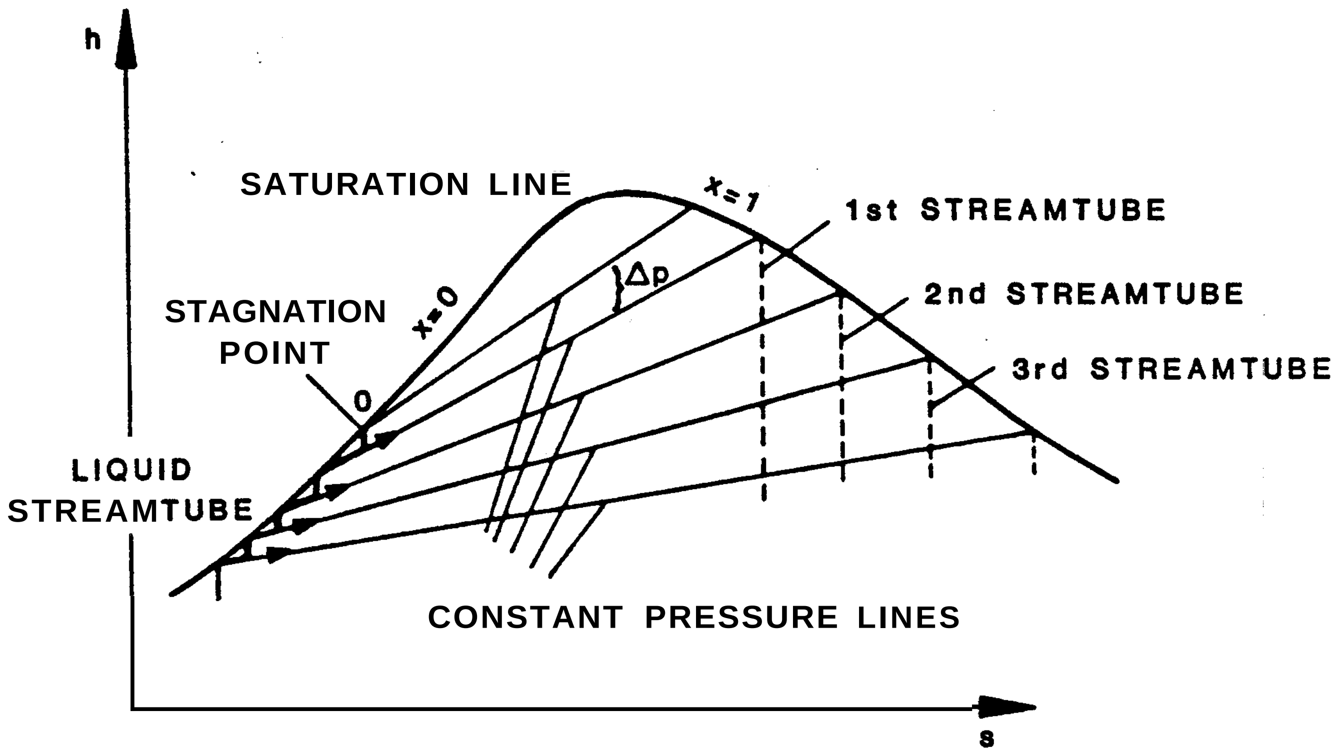

FIGURE 3.1: ENTHALPY/ENTROPY DIAGRAM SHOWING FORMATION OF STREAMTUBES (WALLIS AND RICHTER, 1978)

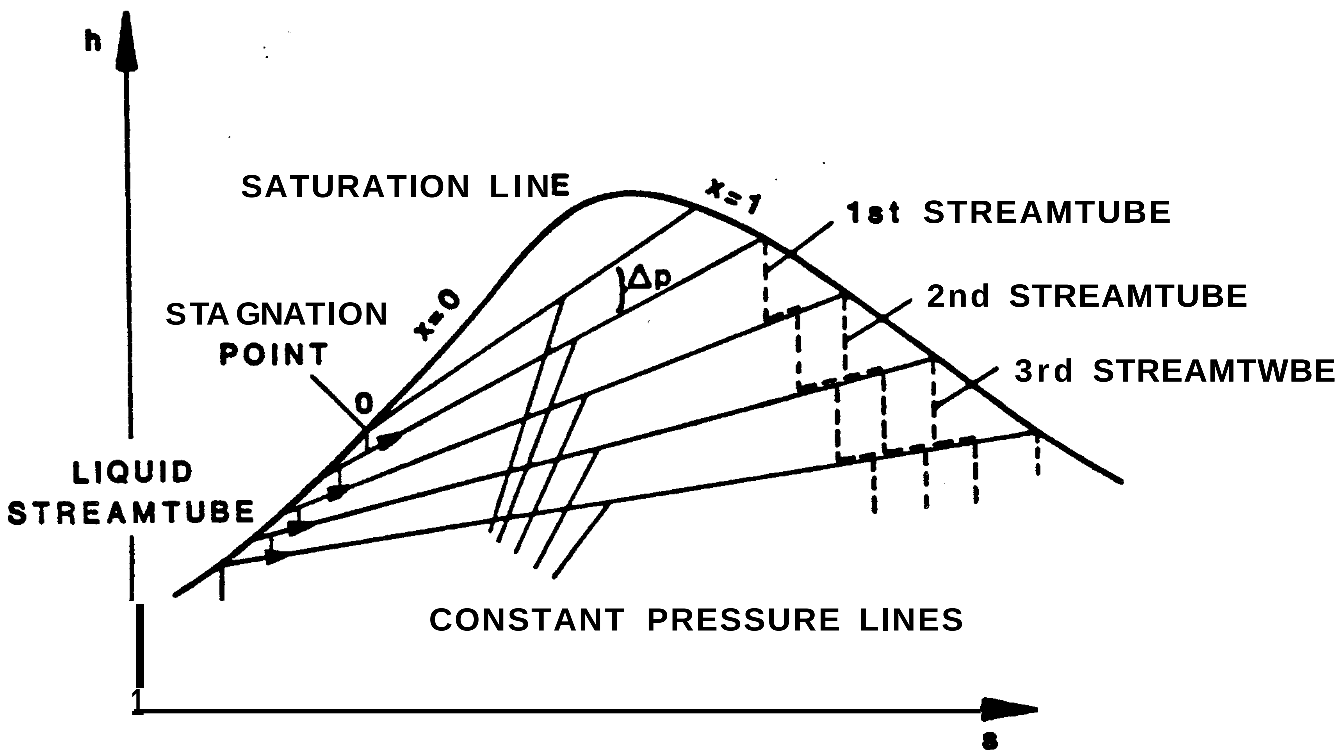

FIGURE 3.2: ENTHALPY/ENTROPY DIAGRAM SHOWING FORMATION OF STREAMTUBES, INCLUDING EFFECT OF HEAT TRANSFER (AFTER WALLIS AND RICHTER, 1978)

Using basic thermodynamic relationships, this energy gain is given by:

$$Q = C_p(T_0 - T_f)(1 - \eta_s) \qquad (3.2-1)$$

where:

η_s = the effective isentropic efficiency

The isentropic efficiency term is used since not all the heat. transferred results in an increase in the fluids internal energy. Some is used to counteract the irreversible processes not included in the energy balance of the basic model.

This heat transfer step changes the basic model as indicated in Figure 3.2. It extends the basic model by allowing the flashing process to be approximated by a two step process rather than the basic single step process.

3.3 Mathematical Formulation

The basic steps involved in the model are shown in Figure 3.3. This shows the formation of the first two vapor streamtubes and as the pressure continues to decline further streamtubes are formed and expand in the same fashion. To simplify the computation, the model is normalized on the basis of unit massflow ie. $Y_i + y_i = 1$.

If we consider the first isentropic expansion step (labelled 1 in Figure 3.3) we have a liquid massflow, Y_0, with enthalpy, h_0, entropy, s_0, and velocity, v_0, calculated from:

$$v_0^2 = 2(p_0 - p_{sat})/\rho_f \qquad (3.3-1)$$

expanding to a liquid massflow, Y_1, with properties h_1', s_1', v_1 and a vapor massflow, y_1, with properties h_1'', s_1'' and v_1. Note that the liquid and vapor streamtubes are assumed to have the same velocity, when the vapor streamtube is first formed.

Applying the usual conservation equations,

mass:

$$Y_0 = Y_1 + y_1 \qquad (3.3\text{-}2)$$

and energy:

$$Y_0\left(h_0' + \frac{v_0^2}{2}\right) = Y_1\left(h_1' + \frac{v_1^2}{2}\right) + y_1\left(h_1'' + \frac{v_1^2}{2}\right) \qquad (3.3\text{-}3)$$

and the assumption of isentropic expansion:

$$Y_0 s_0' = Y_1 s_1' + y_1 s_1'' \qquad (3.3\text{-}4)$$

we get from (3.3-2) and (3.3-4):

$$y_1 = Y_0 \frac{s_0' - s_1'}{s_1'' - s_1'} \qquad (3.3\text{-}5)$$

and from (3.3-2) and (3.3-3):

$$v_1^2 = v_0^2 + 2\left[h_0' - h_1' - \frac{y_1}{Y_0}(h_1'' - h_1')\right] \qquad (3.3\text{-}6)$$

It is a simple matter to extend these equations to their more general form. (see Appendix A for the more general derivation).

As indicated in Figure 3.3, the liquid and vapor streamtubes now undergo heat transfer which increases both the liquid and vapor enthalpy and entropy. The basic equations are:

$$Q = C_p(T_0 - T_1)(1 - \eta_s) \tag{3.3-7}$$

$$\Delta h = Q \tag{3.3-8}$$

$$\Delta s = \frac{Q}{T_1} \tag{3.3-9}$$

The actual change will depend on the effective isentropic efficiency and the specific heat of the fluid in each particular streamtube. It is also assumed that the fluid velocities remain constant during the heat transfer step.

During the second isentropic expansion a new vapor streamtube is created. At the same time the first vapor streamtube expands and some of the vapor may condense resulting in a steam mass fraction of:

$$x_{1,2} = \frac{s_{1,1}^* - s_2'}{s_2'' - s_2'} \tag{3.3-10}$$

if $x_{1,2} < 1$:

$$h_{1,2} = x_{1,2}h_2'' + (1 - x_{1,2})h_2' \tag{3.3-11}$$

if $x_{1,2} > 1$:

$$h_{1,2} = h_2'' + T_2(s_{1,1}^* - s_2'') \tag{3.3-12}$$

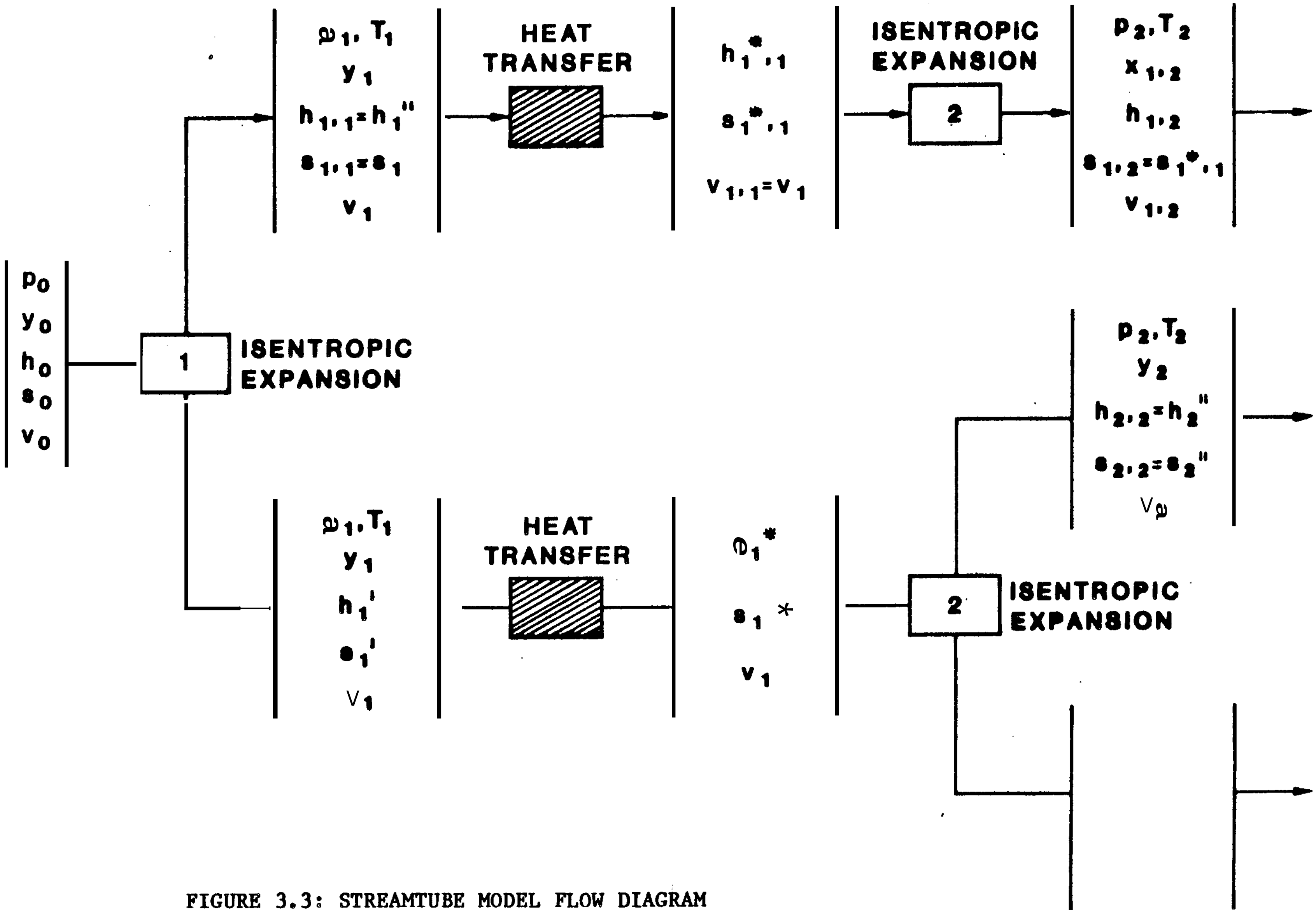

FIGURE 3.3: STREAMTUBE MODEL FLOW DIAGRAM

The homogeneous mixture is assumed to have a uniform velocity and this is calculated from:

$$v_{1,2}^{2} = 2(h_{1,1}^{*} - h_{1,2}) + v_{1,1}^{2} \qquad (3.3\text{-}13)$$

The two vapor streamtubes and the liquid streamtube then undergo heat transfer, thereby increasing their respective enthalpies and entropies before the next isentropic expansion. This process is continued until the total pressure drop is reached, at which stage there will be n vapor streamtubes where n is the number of pressure steps.

Defining i as the streamtube number and n as the total number of pressure steps, the homogeneous density in the i^{th} streamtube is:

$$\rho_{i,n} = \frac{1}{\dfrac{(1 - x_{i,n})}{\rho_n} + \dfrac{x_{i,n}}{\rho_n''}} \qquad (3.3\text{-}14)$$

and the total massflux can be calculated from:

$$G = \left[\sum_{i=1} \frac{y_i}{\rho_{i,n} v_{i,n}} + \frac{Y_n}{\rho_n' v_n}\right]^{-1} \qquad (3.3\text{-}15)$$

From the generated velocity profile average vapor and liquid velocities can be calculated, from which an effective slip ratio can be found:

$$\bar{v}_{s,n} = \frac{\sum_{i=1}^{n} y_i v_{i,n} x_{i,n}}{\sum_{i=1}^{n} y_i x_{i,n}} \qquad (3.3\text{-}16)$$

$$\bar{v}_{w,n} = \frac{\left[\sum_{i=1}^{n} y_i v_{i,n} (i - x_{i,n})\right] + Y_n v_n}{\left[\sum_{i=1}^{n} y_i (1 - x_{i,n})\right] + Y_n} \qquad (3.3\text{-}17)$$

and:

$$\varepsilon_n = \frac{\bar{v}_{s,n}}{\bar{v}_{w,n}} \qquad (3.3\text{-}18)$$

In addition the flowing enthalpy can be found from:

$$\bar{h}_t = \left[\sum_{i=1}^{n} y_i h_{i,n}\right] + Y_n h_n \qquad (3.3\text{-}19)$$

3.4 Calculation of Relative Permeabilities

The liquid saturation after n pressure drops can be calculated from the slip ratio and the liquid mass fraction; after Miller(1951):

$$\frac{S_{w,n}}{1-S_{w,n}} = \frac{1}{\left(\frac{1 - Y_n}{Y_n}\right)\left(\frac{1}{\varepsilon_n}\right)\left(\frac{\rho_n'}{\bar{\rho}_n''}\right)} \qquad (3.4\text{-}1)$$

where :

$$\bar{\rho}_n'' = \frac{\sum_{i=1}^{n} y_i \rho_{i,n}}{1 - Y_n} \qquad (3.4-2)$$

The ratio of relative permeabilities can then be calculated from:

$$\frac{k_{rw}}{k_{rs}} = \left(\frac{1}{\varepsilon_n} \right)\left(\frac{\mu_w}{\mu_s} \right)\left(\frac{S_{w,n}}{1 - S_{w,n}} \right) \qquad (3.4-3)$$

This is equivalent to the more common formula derived in Grant and Sorey(*1979):*

$$\frac{k_{rw}}{k_{rs}} = \left(\frac{\nu_w}{\nu_s} \right)\left(\frac{h_n'' - \bar{h}_t}{\bar{h}_t - h_n'} \right) \qquad (3.4-4)$$

The streamtube model assumes no interaction between the streamtubes which implies:

$$k_{rw} + k_{rs} = 1 \qquad (3.4-5)$$

Where flow is controlled by a fracture system the assumption that the phases do not interact is generally thought to be reasonable.

Using Equation *(3.4-1)* the model calculates the inplace liquid saturation and from Equations *(3.4-3)* and *(3.4-5)* the corresponding values of **the** water and steam relative permeabilities are calculated.

3.5 Computer Program (GEOFLOW)

A computer program has been written to solve the streamtube model equations and generate the relative permeability values. A listing of the program with a typical output is included as Appendix B.

Input to the program involves the following variables:

PI:	reservoir pressure (MPa.a)
PS:	saturation pressure (MPa.a)
DP:	pressure step size (kPa)
N:	number of pressure steps
EIE:	effective isentropic efficiency, η_s

At present it is assumed by the program that the reservoir pressure is greater than or equal to the saturation pressure but it only requires minor modifications for GEOFLOW to accept two phase initial conditions.

After each pressure/heat transfer step the program prints out the following variables:

PRESS:	pressure (MPa.a)
TEMP:	saturation temperature (°C)
MASS FLUX:	total mass flux (kg/m^2s)
SLIP RATIO:	effective slip ratio
ENTHALPY:	total flowing enthalpy (kJ/kg)
YW:	liquid flowing mass fraction
SATW:	liquid inplace volume fraction
KS:	steam relative permeability
KW:	water relative permeability

To calculate the thermodynamic properties needed by the program, subroutines developed by Reynolds(1979) were used. In the calculation of the heat transfer and relative permeabilities values of the specific heat and dynamic viscosity were required. Curve fits were developed for these properties, at saturation conditions, based on the data presented in Schmidt(1969).

Before using the program to study the system of interest, it was tested against an example presented in Wallis and Richter(1978). Using a pressure step of 100 kPa, initial temperature of 250°C with no heat transfer, GEOFLOW was run and the results compared in Figures *3.4* and 3.5. The slight differences are believed to be due to the fact that different thermodynamic correlations were probably used by Wallis and Richter.

The next section presents the data generated by GEOFLOW for a range of input conditions.

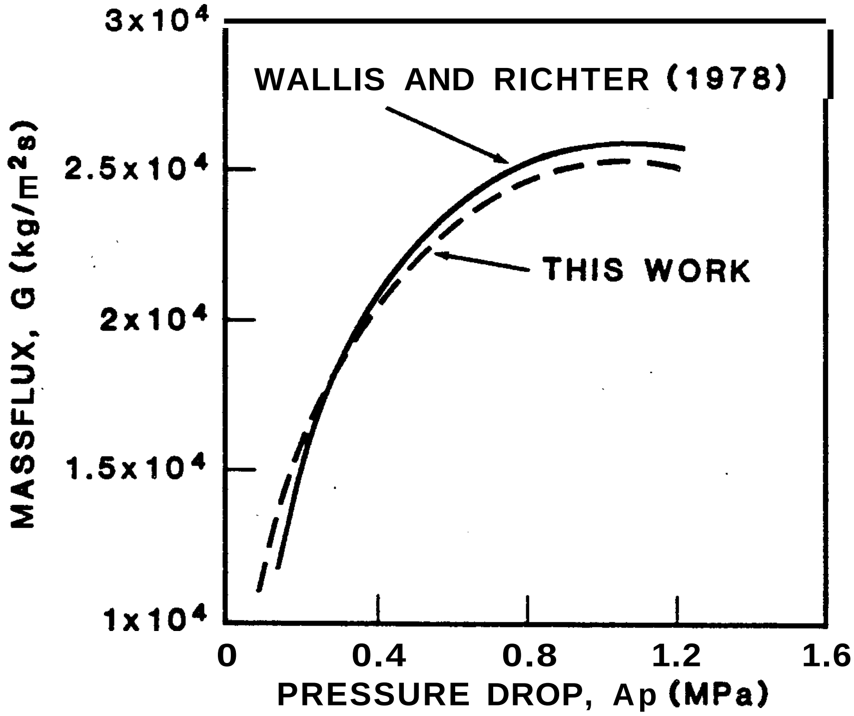

FIGURE 3.4: MASSFLUX VS PRESSURE DROP - COMPARISON WITH WALLIS AND RICHTER

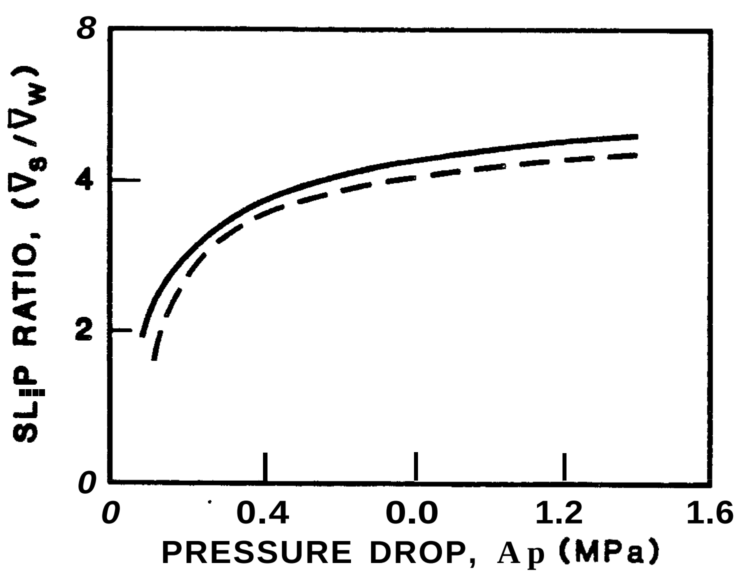

FIGURE 3.5: SLIP RATIO VS PRESSURE DROP - COMPARISON WITH WALLIS AND RICHTER

4. FLOW CHARACTERISTICS

Using the computer program, GEOFLOW, theoritical curves of massflux and enthalpy as functions of the production zone flowing pressure can be generated. The initial reservoir conditions and the effective isentropic efficiency were used as input variables. A constant pressure step of 50 kPa was used for this study.

4.1 Effect of Reservoir Pressure

The effect of reservoir pressure is shown, for reservoir temperatures of 250°C and 300°C, in Figures 4.1 and 4.2. The graphs indicate that within the two phase region the reservoir pressure has negligible effect on the calculated massflux. If the reservoir pressure is greater than the saturation pressure the data can be extrapolated into the single phase region by assuming that the massflux is zero when the well flowing pressure is equal to the reservoir pressure. In this case the effect of the reservoir pressure is important, as shown in Figure 4.3.

If the reservoir pressure is greater than the saturation pressure it has no effect on the increase in flowing enthalpy as heat transfer only occurs after flashing has started.

These results imply that meaningful comparisons between field and model data can be made even when the reservoir pressure is not accurately known, provided it is greater than the saturation pressure. This is important as the reservoir temperature is normally known more accurately than the initial reservoir pressure.

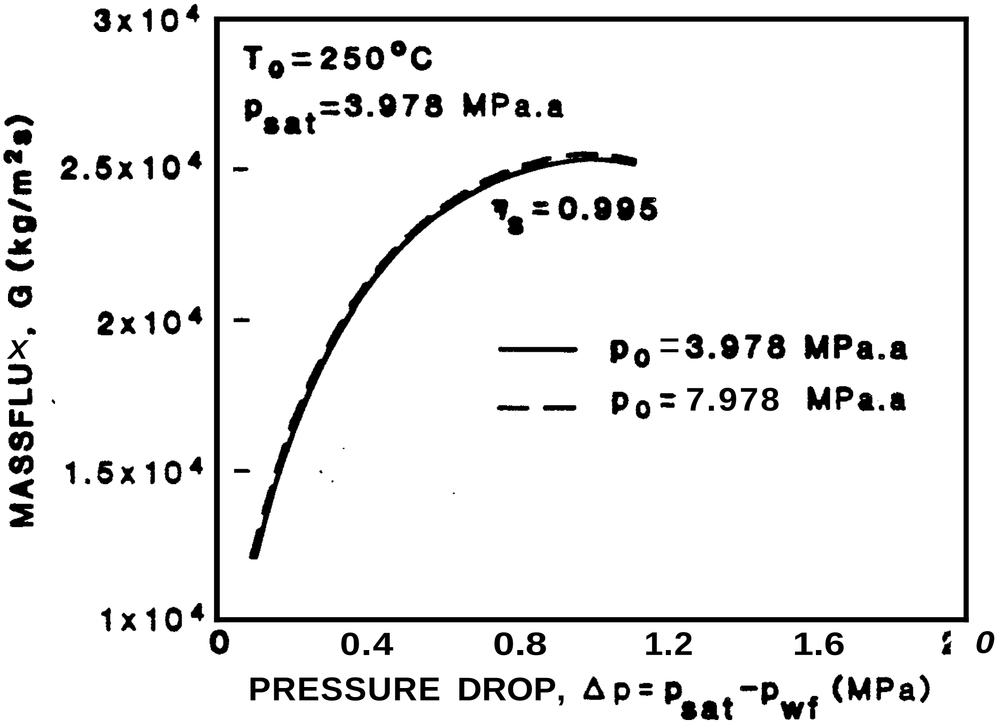

FIGURE 4.1: MASSFLUX VS PRESSURE DROP, T_0=250°C

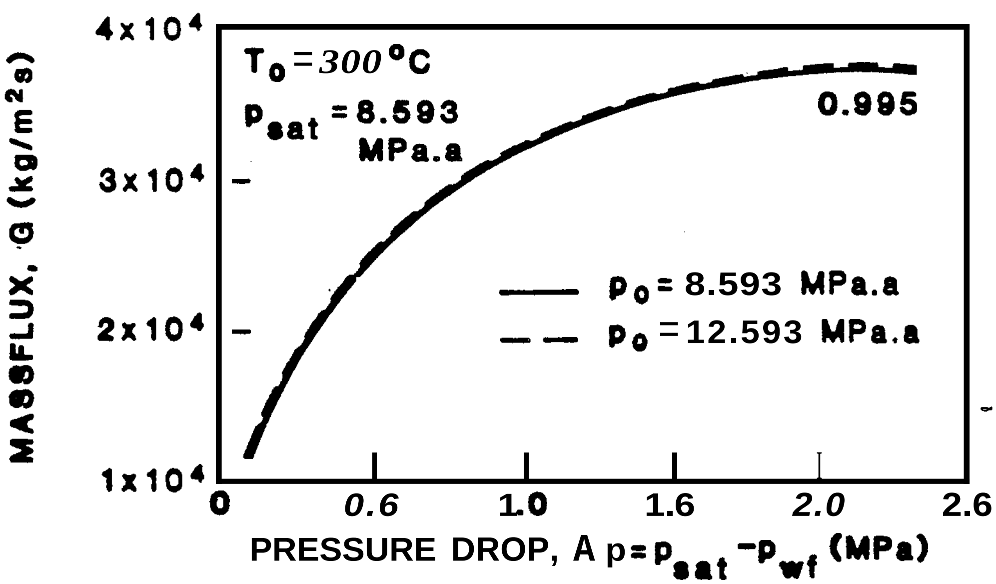

FIGURE 4.2: MASSFLUX VS PRESSURE DROP, T_0=300°C

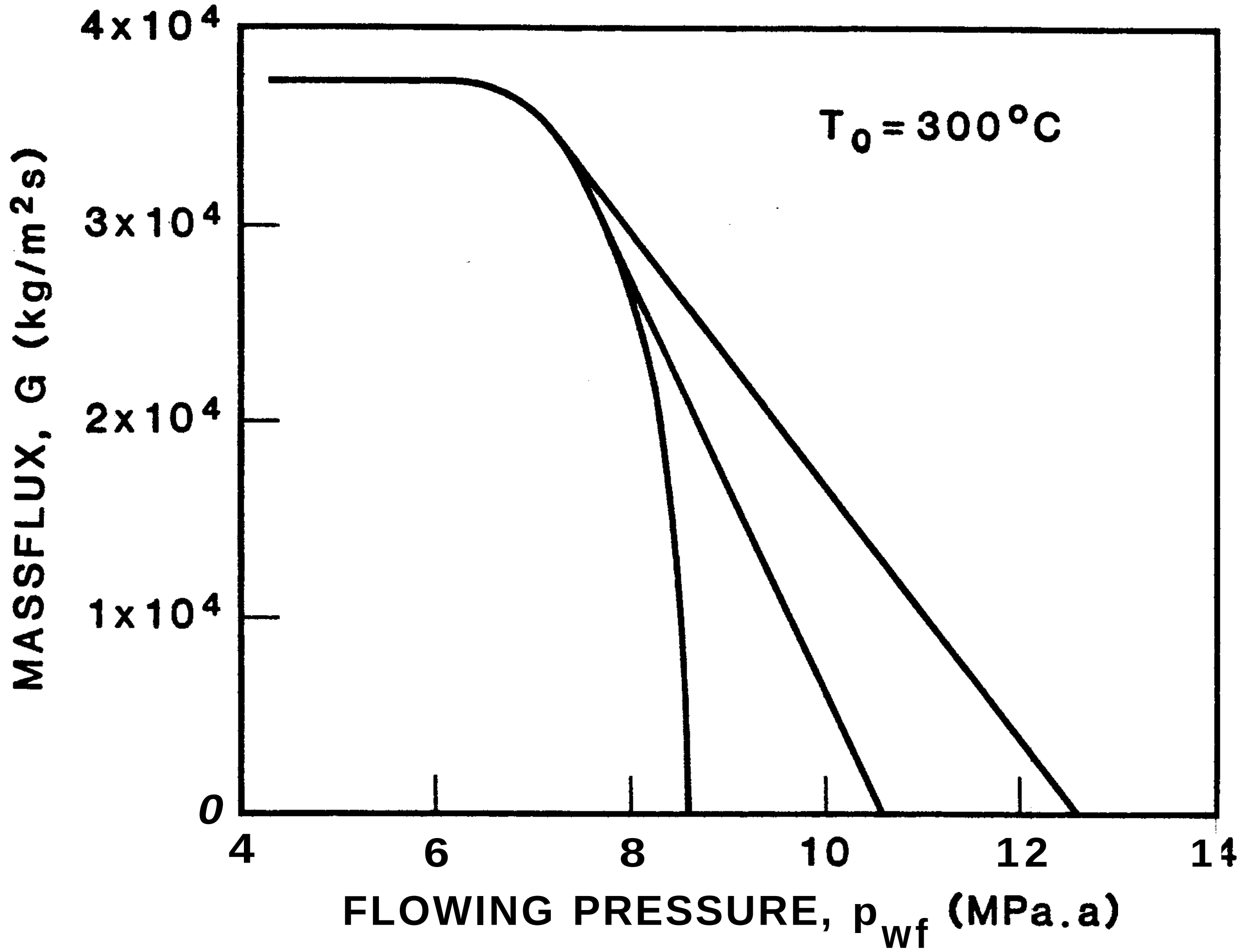

FIGURE 4.3: MASSFLUX VS FLOWING PRESSURE, T_0=300°C

4.2 Choked Flow

The data generated by GEOFLOW have been plotted (Figures 4.4 to 4.9) as graphs of massflux and enthalpy vs the pressure drop based on the saturation pressure. The choked flow condition is indicated by the dashed horizontal lines.

The data from GEOFLOW showed the massflux increasing as the pressure drop increased, until a maximum value was reached. After that point the calculated massflux started to decline. This is a characteristic of the thermodynamic models but the phenomena is not observed in practice, Moody(1965). The choked massflux is taken to be the maximum predicted value; the value where $\partial G/\partial p = 0$.

The graphs (Figures 4.4 to 4.9) indicate that as the effective isentropic efficiency decreases the choked massflux decreases and choking occurs at a lower value of pressure drop. This is in agreement with the statement from Reynolds and Perkins(1977): "for a given flowrate there is a maximum heat input for which the prescibed flow can be passed by the duct. Compressible flows therefore exhibit choking due to heating". The water saturation at which this occurred was found to be 0.6 - 0.7.

The output from GEOFLOW is in terms of the massflux and to convert this to a massflow for comparison with field data, the flow area is required. Conversely if the model is being used to study field data it is possible to calculate the flow area from the ratio of the measured massflow to the calculated massflux. This procedure is described in the next section.

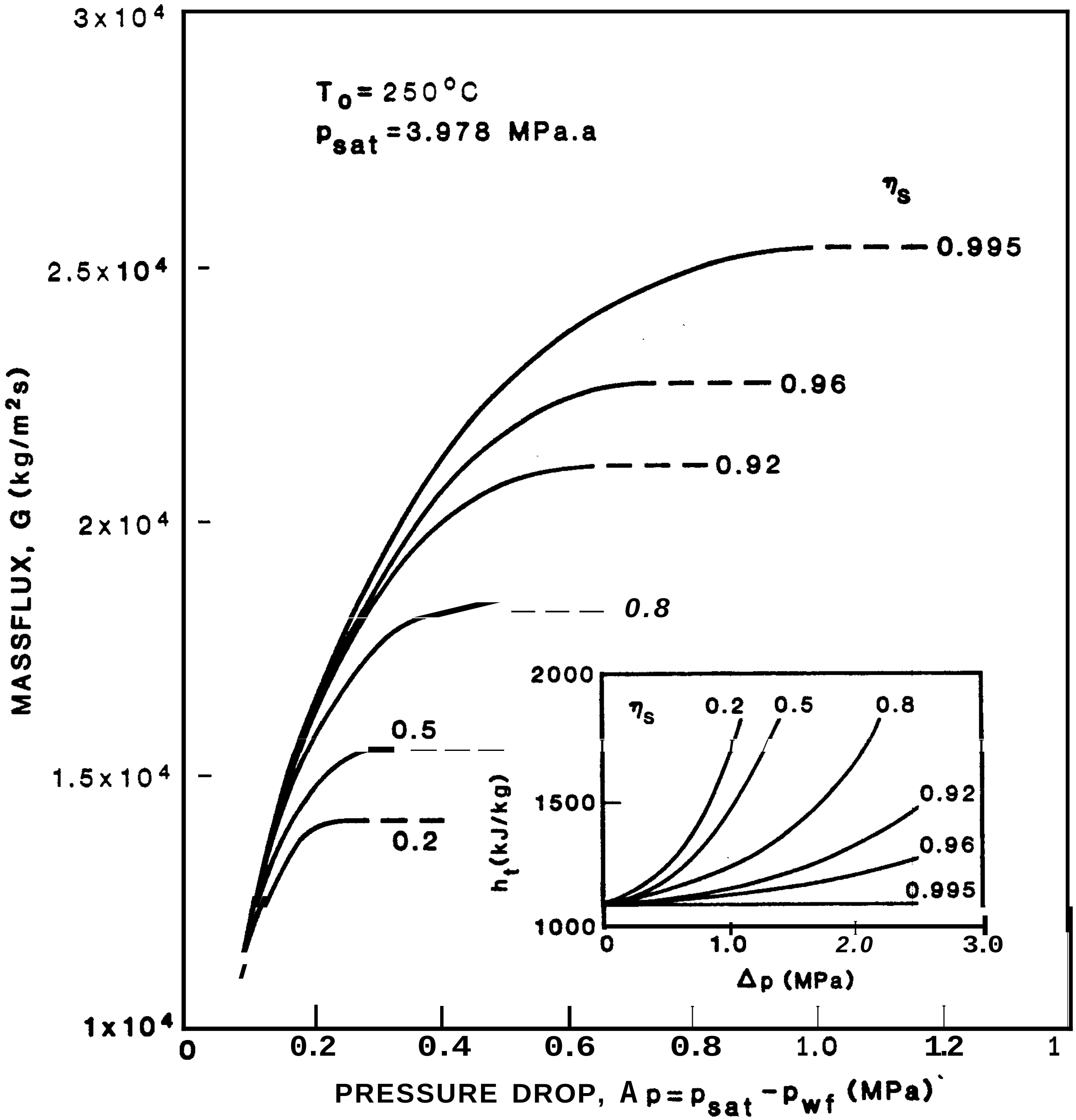

FIGURE *4.4:* MASSFLUX AND ENTHALPY VS PRESSURE DROP, T_0=250°C

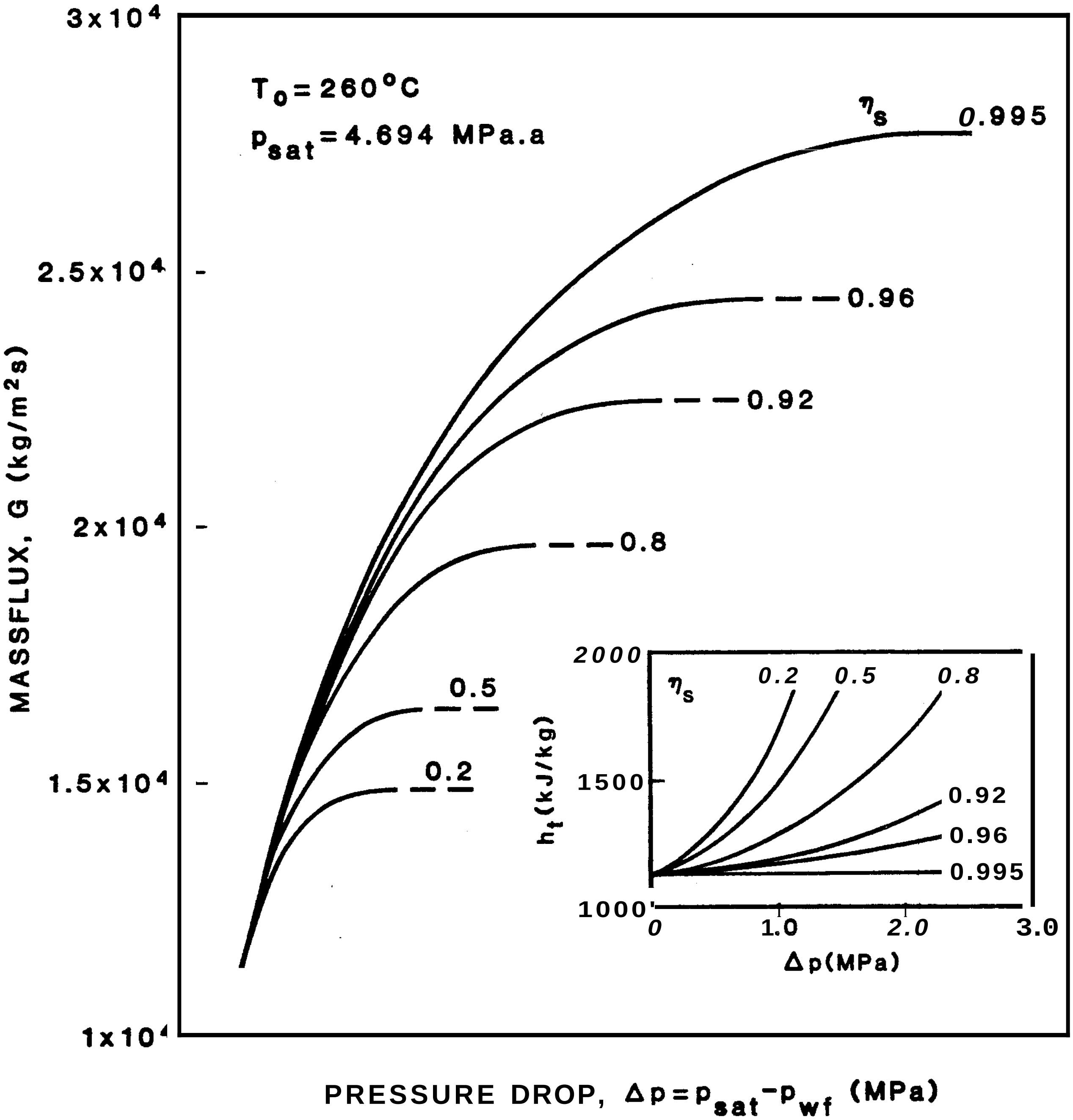

FIGURE 4.5: MASSFLUX AND ENTHALPY VS PRESSURE DROP, T_0=260°C

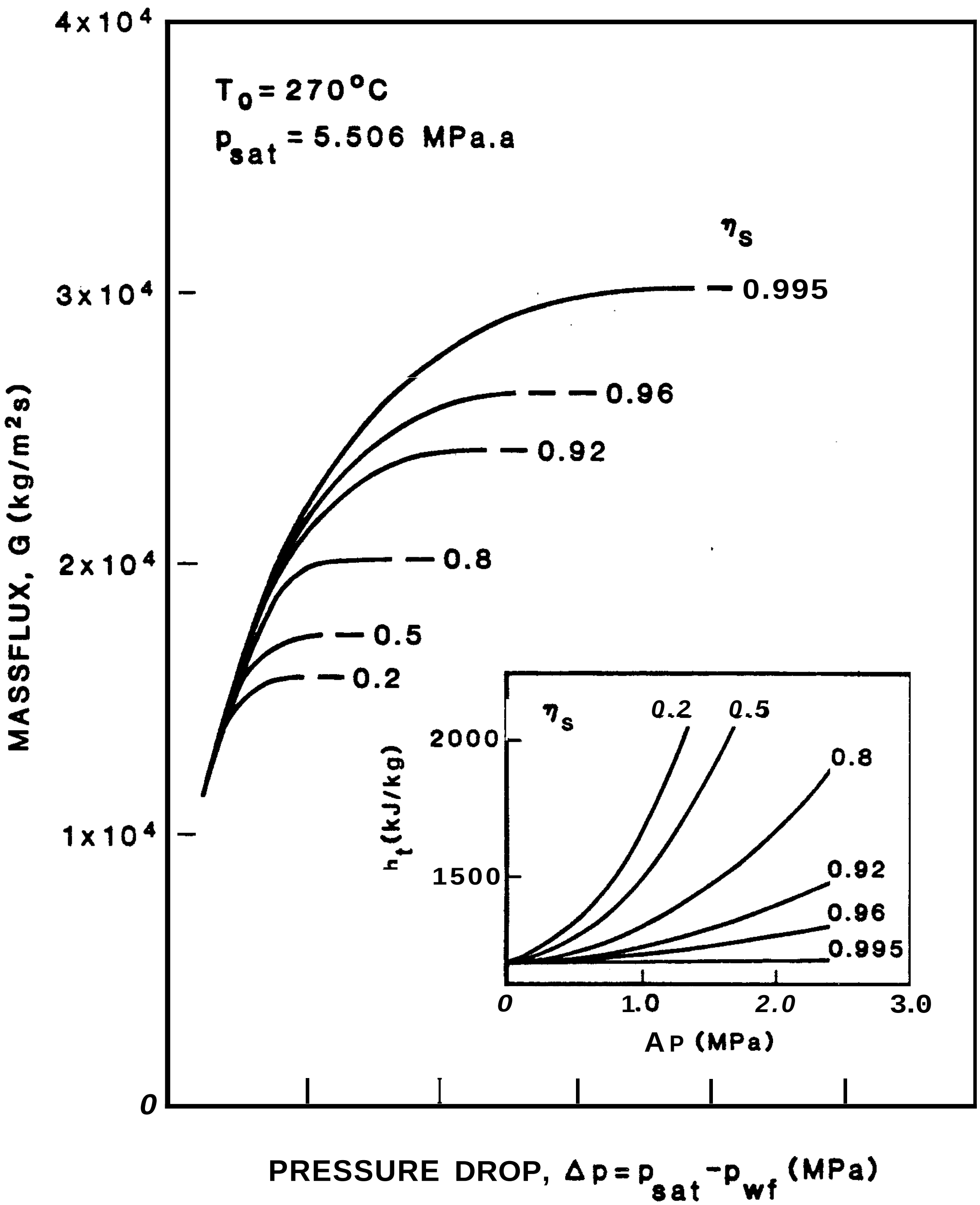

FIGURE 4.6: MASSFLUX AND ENTHALPY VS PRESSURE DROP, T_0=270°C

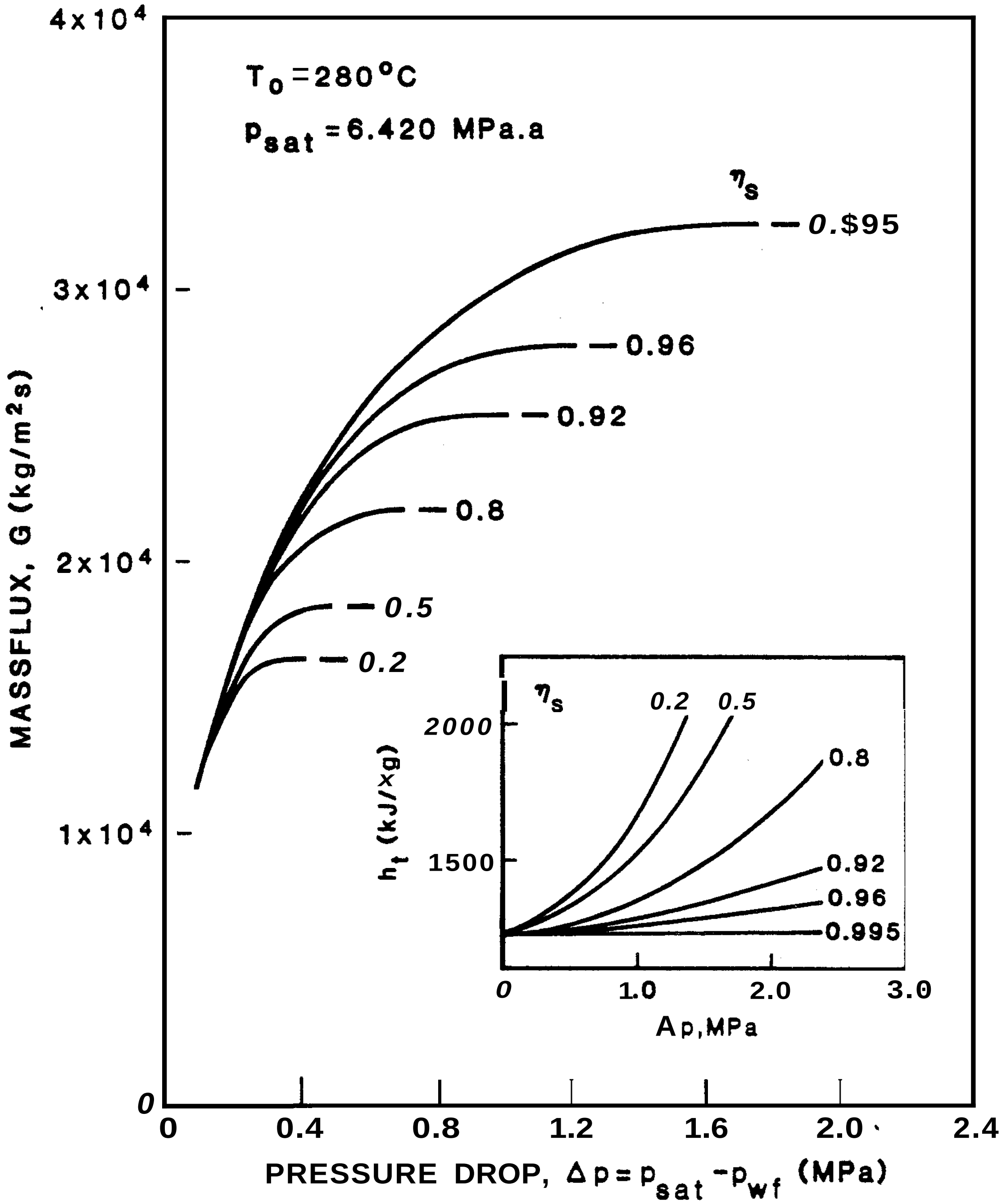

FIGURE 4.7: MASSFLUX AND ENTHALPY VS PRESSURE DROP, T_0=280°C

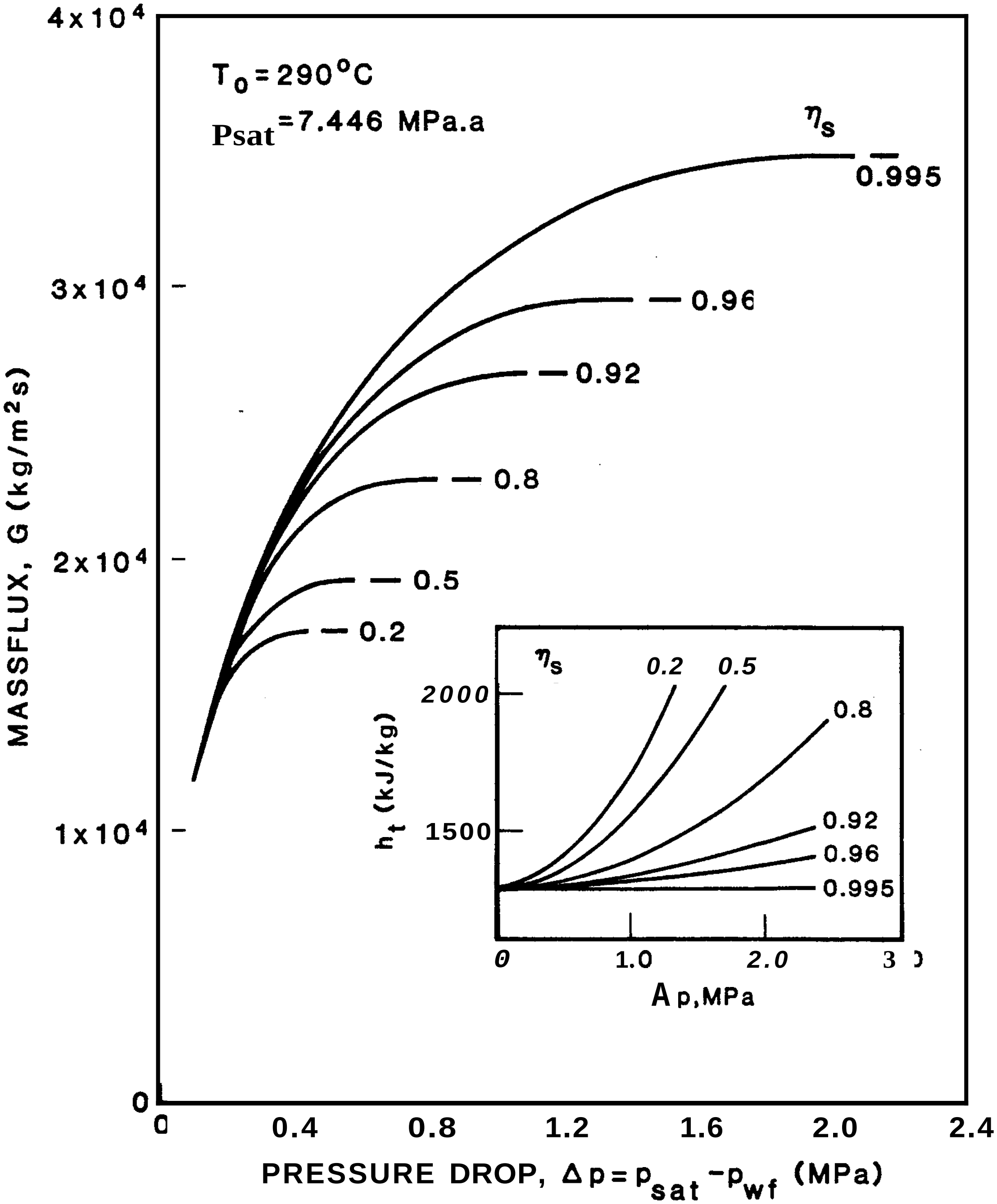

FIGURE 4.8: MASSFLUX AND ENTHALPY VS PRESSURE DROP, T_0=290°C

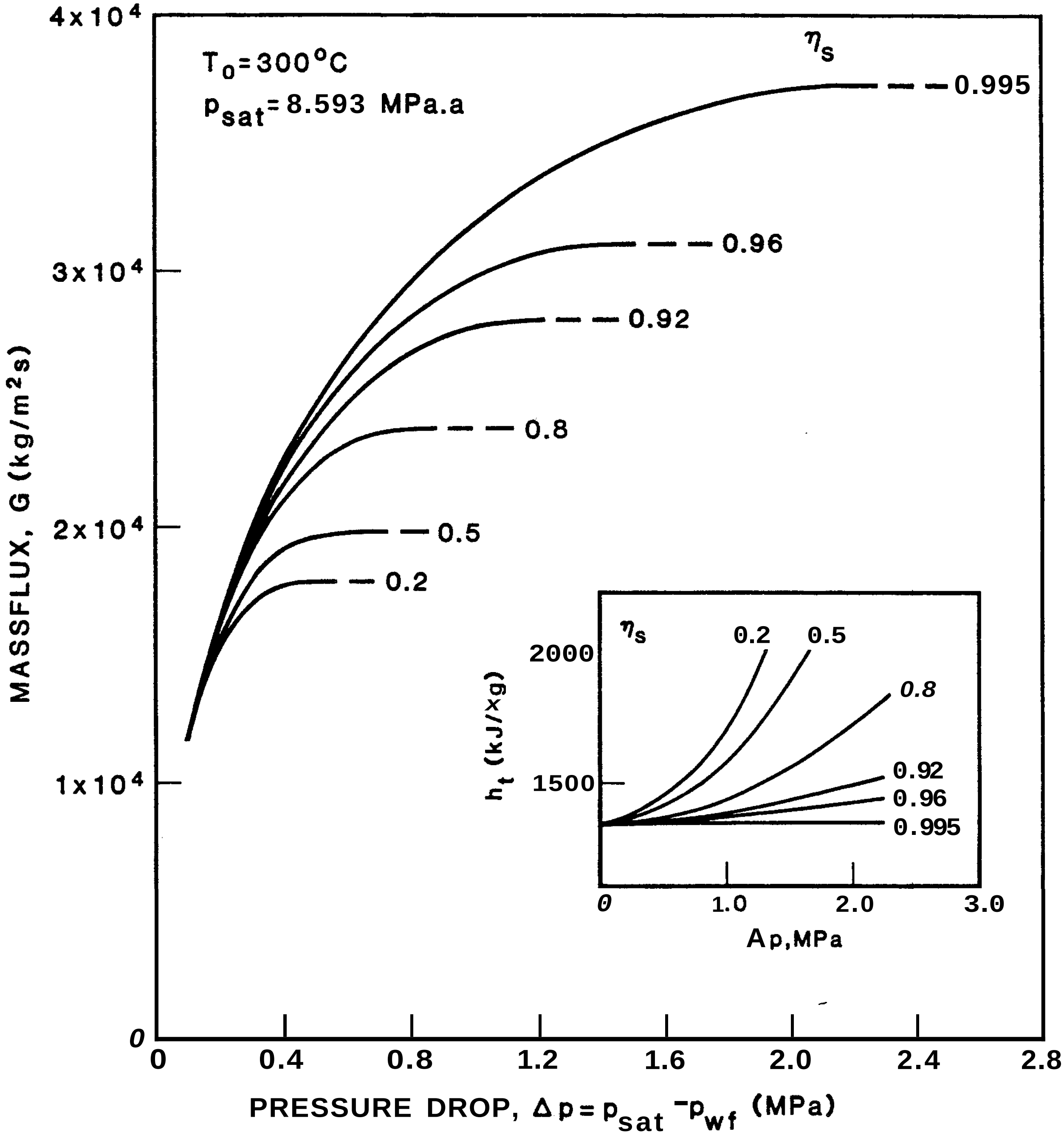

FIGURE *4.9:* **MASSFLUX AND** ENTHALPY **VS** PRESSURE DROP, T_0=300°C

4.3 Flow Geometry

One use of the graphs in Figures 4.4 to 4.9 is to compare field and model data to obtain information on the flow geometry as the fluid enters the well. Knowing the reservoir temperature, flowing pressure at the production zone and the measured enthalpy it is possible to calculate the flow area. By assuming a fracture orientation and borehole geometry it is further possible to estimate an effective fracture width. In this study a single fracture perpendicular to the borehole is assumed, as shown in Figure 4.10.

The first step in estimating the flow area is to select the graph applicable to the field data. Using the enthalpy/pressure drop plot the appropriate value of the effective isentropic efficiency is estimated and the corresponding massflux is found from the massflux/pressure drop graph, using the effective isentropic efficiency as a parameter. The flow area is then calculated from the ratio of the measured massflow to the calculated massflux. Note that the pressure drop is defined with respect to the saturation pressure and not the reservoir pressure.

Using the fracture/borehole geometry shown in Figure 4.10, an effective fracture width can be estimated. The effect of fracture orientation is included in the effective isentropic efficiency, hence a horizontal fracture orientation should be used in the estimation of the effective fracture width.

If the flowing pressure and/or the flowing enthalpy are unknown, an approximate estimation of the flow area can be found using the massflux/temperature graph of Figure 4.11.

Knowing the flow area it is possible to convert the calculated massflux values to massflows and compare the calculated massflow and enthalpy relationships with the field data.

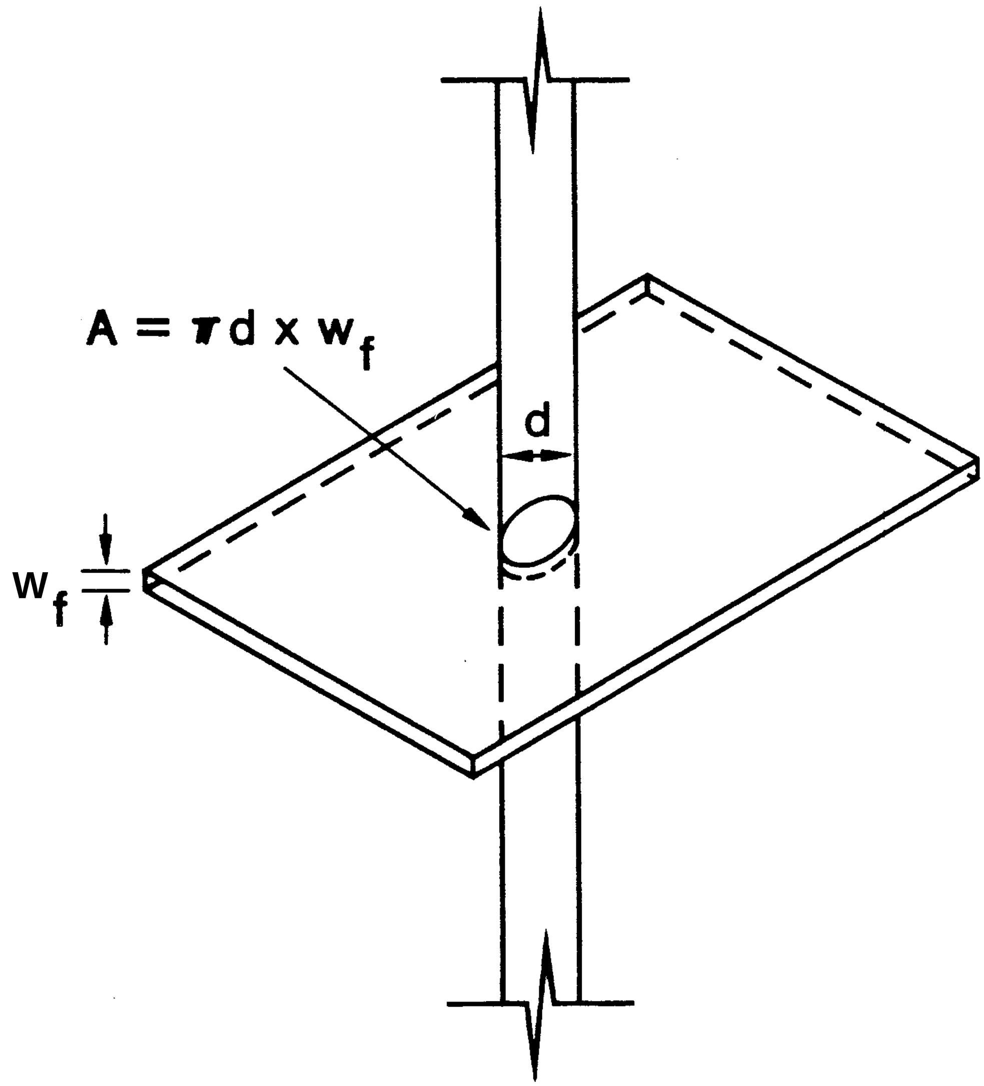

FIGURE 4.10: FRACTURE/BOREHOLE ORIENTATION USED FOR CALCULATION OF EFFECTIVE FRACTURE WIDTH

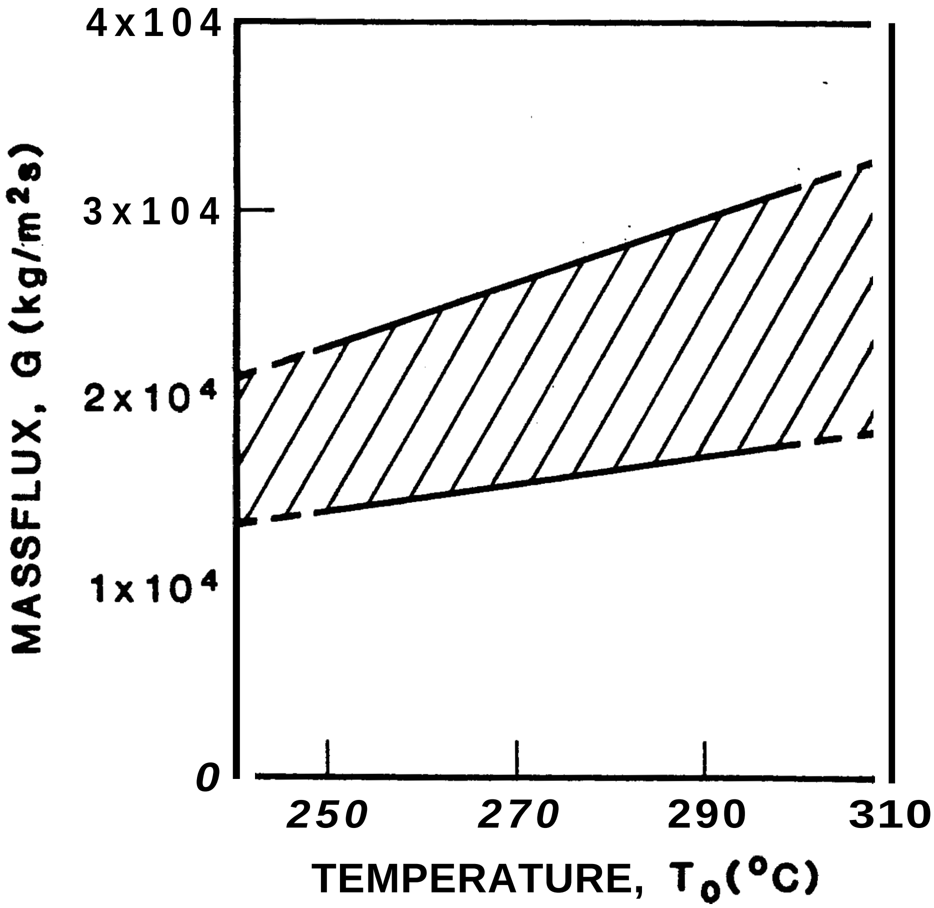

FIGURE 4.11: MASSFLUX VS TEMPERATURE, FOR ESTIMATION OF FLOW AREA WHEN FLOWING SURVEYS UNAVAILABLE

The estimated values of effective fracture width can be compared with earlier approximate methods, provided data is available under conditions of both single and two phase flow. These methods were proposed by James(1975) and Bodvarsson(1981) and they relate the pressure drop and massflow to the effective fracture width, under conditions of single phase incompressible flow:

James(1975):

$$w_f^3 = \frac{W^{1.85} \mu_w^{0.15}}{10^6 \Delta p \, d^{0.85} \rho_w} \qquad (4.3-1)$$

after Bodvarsson(1981):

$$(2d2106\Delta p \, \rho_w) w_f 3 - \left(\frac{W^2}{r} \right) w_f - \frac{W^2 f d}{2r^2} = 0 \qquad (4.3-2)$$

where f = friction factor

Both derivations are based on a horizontal fissure of constant thickness but James assumes that all the kinetic energy is converted to static pressure, hence the kinetic energy term is dropped from the equation.

The next section considers data from four geothermal wells and compares the calculated flow characteristics to the characteristics measured in the field. Effective fracture widths have also been calculated to see if "reasonable" values could be obtained.

5. COMPARISON OF FLOW CALCULATIONS WITH FIELD AND EXPERIMENTAL DATA

GEOFLOW was used to investigate the flow characteristics and flow geometry of four geothermal wells from fields with widely differing reservoir conditions. The flow data from Arihara(1974) for two phase steam/water flow in consolidated cores has also been studied to find the effective flow area of the core and to compare this with the flow areas obtained from the field data.

The output from GEOFLOW for the four field examples is reproduced as Appendix C.

5.1 Field Data

A summary of the well and reservoir conditions for the four wells studied is presented in Table 5.1. The flow characteristics have been calculated using GEOFLOW and where possible compared with the measured massflow and enthalpy characteristics.

To obtain the flow characteristics from GEOFLOW, a value for the flowing pressure opposite the production zone was required and also the corresponding enthalpy and massflow measurements. The lowest pressure available was generally used as this corresponded to the highest value of massflow. GEOFLOW was run, using a trial and error technique, until the value of effective isentropic efficiency gave the required value of enthalpy at the measured flowing pressure. The flow area was determined from the ratio of measured massflow to the corresponding calculated massflux and the effective fracture width estimated as described in Section 4.2.

Using the calculated flow area, the massflux values were converted to massflows and plotted as a function of the flowing downhole pressure. The

TABLE 5.1: FIELD DATA - SUMMARY OF WELL AND RESERVOIR DATA

WELL NAME	FIELD	TOTAL DEPTH(m)	MAJOR D. ZONE(m)	BORE DIA.(m)	RESERVOIR TEMP (°C)	RESERVOIR PRESS (MPa.a)	SATURATION PRESS.(MPa.a)	REFERENCE
"UTAH-STATE" 14-2	ROOSEVELT HOT SPRINGS	1[illegible]60	884-915	0.[illegible]	[illegible]	9.84[illegible]	4.[illegible]94	BUTZ AND PLOOSTER(1979)
BR-21	BROADLANDS, NEW ZEALAND	1120	490	0.[illegible]	[illegible]-260	4.6	[illegible]	GRANT(1[illegible]2)
KG-12	KRAFLA, ICELAND	2[illegible]00	1600-1700	0.22*	3[illegible]	12.[illegible]	11.289	STEFANSSON AND STEINGRIMSSON(19[illegible]0)
403	TUNGONAN, PHILIPPINES	24[illegible]0	2000-2200	0.22	[illegible]5	11.68	8.0	PNOC(1981)

* assumed value based on liner diameter

calculated enthalpies were plotted in a similar fashion. Both graphs and the crossplot of enthalpy and massflow could then be compared with the measured field data.

5.1.1 Well "Utah-State" 14-2, Roosevelt Hot Springs, Utah, USA

Two flow tests have been reported on this well; the first in May 1978 and the second in May 1979. Flowing pressure surveys were conducted at a number of massflows, but problems with the flow measuring equipment precluded the measurement of the total fluid enthalpy. The flowrate measurements are said to have an accuracy of ±15%, Butz and Plooster(1979). The measured flow data is presented in Table 5.2.

TABLE 5.2: MEASURED FLOW DATA, WELL "UTAH-STATE" 14-2

DATE	FLOWING PRESSURE, p_{wf} (MPa.a)	MASSFLOW, W (kg/s)
May 1978	4.79	57.2
	(5.99)	45.0
	6.08	46.5
	(6.72)	32.1
May 1979	2.59	73.1
	3.52	55.8
	(4.22)	63.6
	6.41	40.9
	6.90	35.8

( ): estimated pressure

In the calculations using GEOFLOW, a value of $\eta_s = 0.995$ was assumed. This resulted in the expansion process being virtually isenthalpic.

There were two flowrates at which flashing occurred in the reservoir and this data was used with the output of GEOFLOW to calculate the flow area and effective fracture width.

Single phase flow data was also available in this well ($p_{wf} > p_{sat}$) and effective fracture widths were calculated using the formulas of James(1975) and Bodvarsson(1981). A friction factor of 1.0 was used in Bodvarsson's formula. This is the limiting value suggested by Smith and Ponder(1982) for self propped fractures.

The results of the calculations for effective fracture width are shown in Table 5.3:

TABLE 5.3: CALCULATED EFFECTIVE FRACTURE WIDTH FOR WELL "UTAH-STATE" 14-2

p_{wf} (MPa.a)	W (kg/s)	G (kg/m^{2}s)	A (m^2)	w_f (mm)
2.59	73.1	27695.76	0.00264	3.8[1]
4.22	63.6	22560.94	0.00282	4.1[1]
6.08	46.5		0.00505	7.3[2]
			0.00311	4.53
6.90	35.8		0.00470	6.8[2]
			0.00282	4.1[3]

1 calculated from GEOFLOW

2 calculated from James(1975)

3 calculated from Bodvarsson(1981)

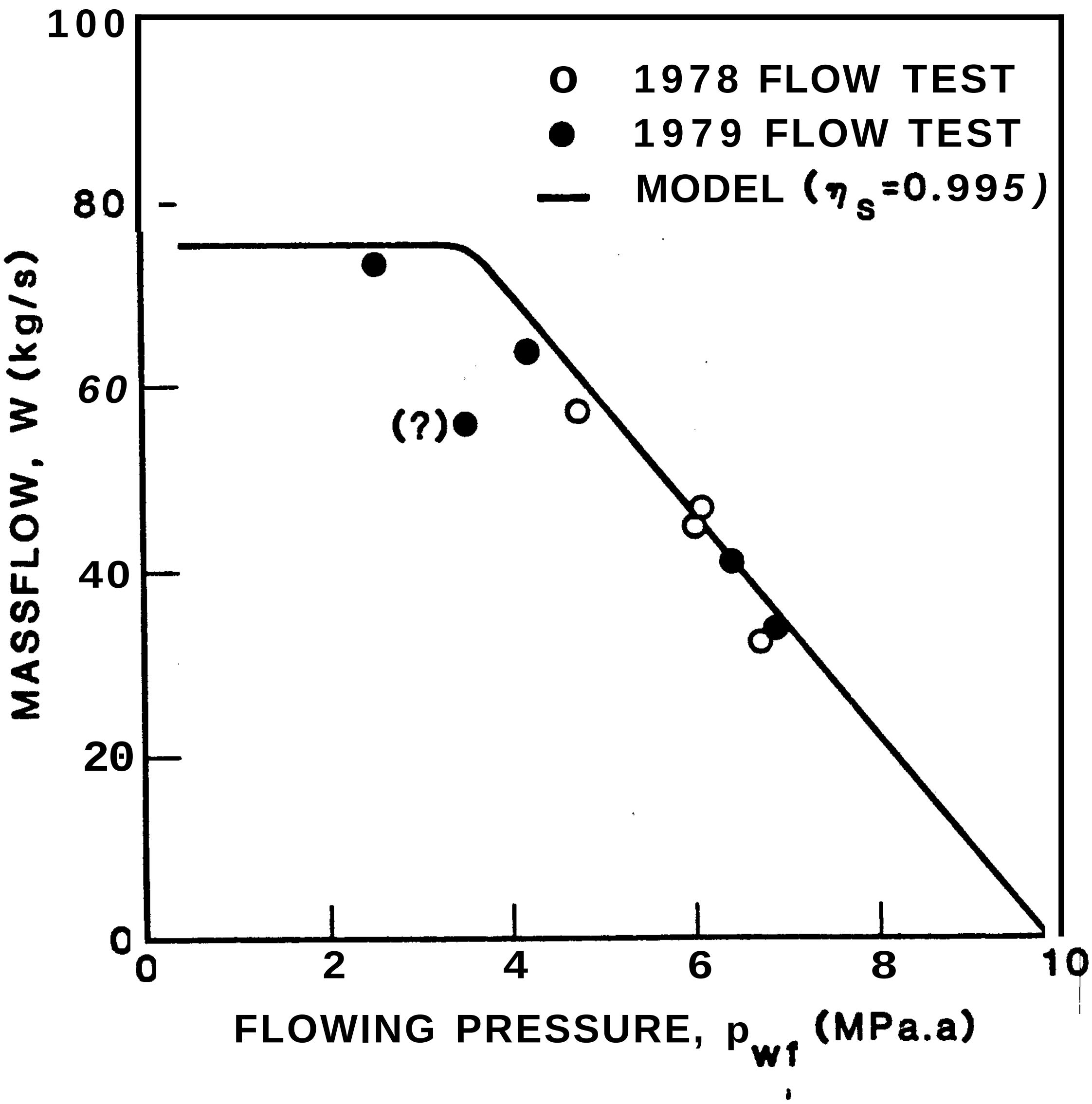

FIGURE 5.1: MASSFLOW VS FLOWING DOWNHOLE PRESSURE, WELL "UTAH-STATE" 14-2

Using the average flow area from GEOFLOW the massflow/flowing pressure curve was calculated and is compared with the field data in Figure 5.1. The data has been extrapolated into the single phase region by assuming that the massflow is zero when the flowing pressure is equal to the reservoir pressure (when p_{wf} = 9.845 MPa.a).

GEOFLOW predicted that choking would occur when the flowing pressure was less than 3.44 MPa.a, suggesting that the maximum flowrate available from "Utah-State" 14-2 would be approximately 75 kg/s.

5.1.2 Well BR-21, Broadlands Geothermal Field, New Zealand

This well has been tested a number of times since it was completed in June 1970. The latest series of tests were conducted in March/April 1982 as part of a study on high enthalpy wells, Grant(1982).

Enthalpy and pressure data were available at a single flowrate and this was used in GEOFLOW to obtain the effective isentropic efficiency and hence, the flow characteristics. The reservoir pressure is equal to the saturation pressure, suggesting that the fluid is either saturated water or a two phase steam/water mixture. GEOFLOW assumes that the fluid is saturated water. If the inplace fluid is in fact a steam/water mixture, the inplace enthalpy will be greater than the saturation enthalpy assumed by GEOFLOW, resulting in a higher value for the effective isentropic efficiency. The effective isentropic efficiency was found to be 0.58, substantially lower than the value for the other field examples, suggesting that two phase conditions do in fact exist in the reservoir. This would also mean that the calculated flow area and effective fracture width would be maximum values as the calculated massflux values will be lower than the true values.

The calculation of the effective fracture width is summarized in Table 5.4. As single phase flow does not occur in the reservoir the calculation methods of James(1975) and Bodvarsson(1981) cannot be used.

TABLE 5.4: CALCULATED EFFECTIVE FRACTURE WIDTH FOR WELL BR-21

P_{wf} (MPa.a)	W (kg/s)	G (kg/m^{2}s)	A (m^2)	w_f (mm)
3.51	21.7	16857.47	0.00129	2.0

The calculated flow characteristics for massflow and enthalpy, as functions of the flowing pressure are shown in Figures 5.2 and 5.3. No reliable measured flow characteristics are available at lower massflows as the well did not stabilise during the flow test, Grant(1982).

Choking was predicted to occur at a flowing pressure of 4.2 MPa.a but this is probably a high estimate because of the initial conditions used in the calculation by GEOFLOW.

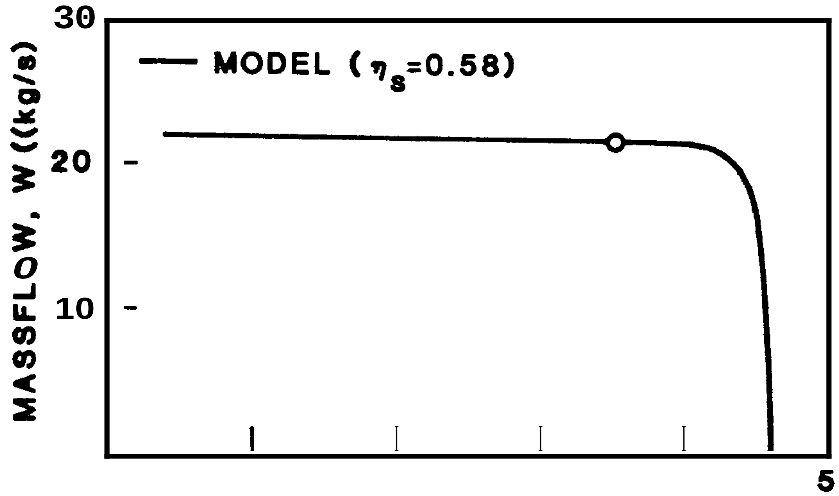

FIGURE 5.2: MASSFLOW VS FLOWING DOWNHOLE PRESSURE, WELL BR-21

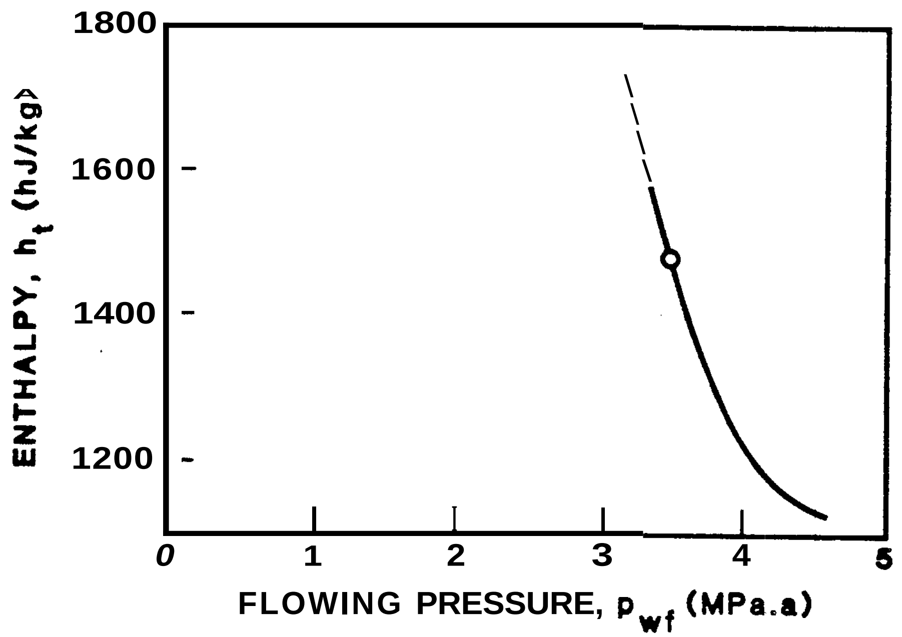

FIGURE 5.3: ENTHALPY VS FLOWING DOWNHOLE PRESSURE, WELL BR-21

5.1.3 Well KG-12, Krafla Geothermal Field, Iceland

The Krafla field is a liquid dominated field which produces saturated and superheated steam in a number of wells. The measured massflows are low, with KG-12 producing 6.7 kg/s but no decrease in massflow is seen as the wells are back pressured, Stefansson and Steingrimsson(*1980).*

A flowing pressure survey was available from KG-12 and the corresponding enthalpy was estimated to be 3000 kJ/kg. Using this data, GEOFLOW was found to fit with an effective isentropic efficiency of ***0.95.***

The calculation of flow area and effective fracture width is summarised in Table ***5.5:***

TABLE ***5.5:*** CALCULATED EFFECTIVE FRACTURE WIDTH FOR WELL KG-12

p_{wf} (MPa.a)	W (kg/s)	G (kg/m^2s)	A (m^2)	w_f (mm)
2.10	*6.7*	*32580.45*	0.00021	*0.3*

Based on the calculated flow area, the flow characteristics were calculated and are shown in Figures ***5.4*** and ***5.5.***

The massflow/flowing pressure curve indicates that choking occurs when the flowing pressure is less than ***9.6*** MPa.a, resulting in a constant massflow which is independent of the flowing pressure. This is consistent with the observed well characteristics.

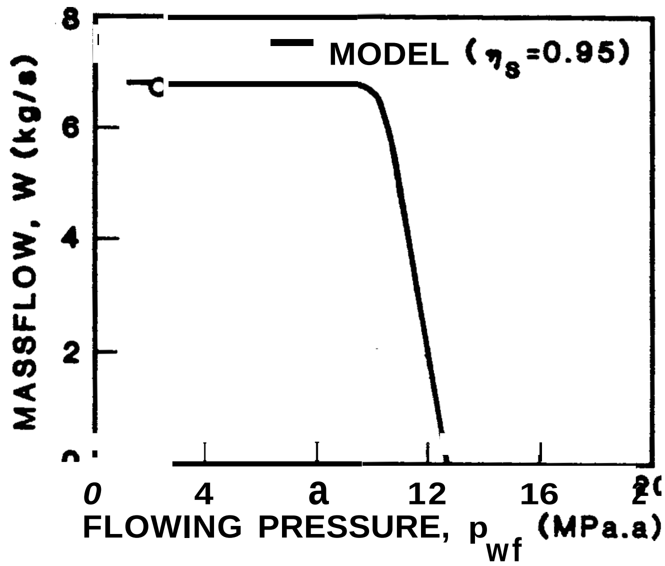

FIGURE *5.4:* **MASSFLOW** VS FLOWING DOWNHOLE **PRESSURE, WELL** KG-12

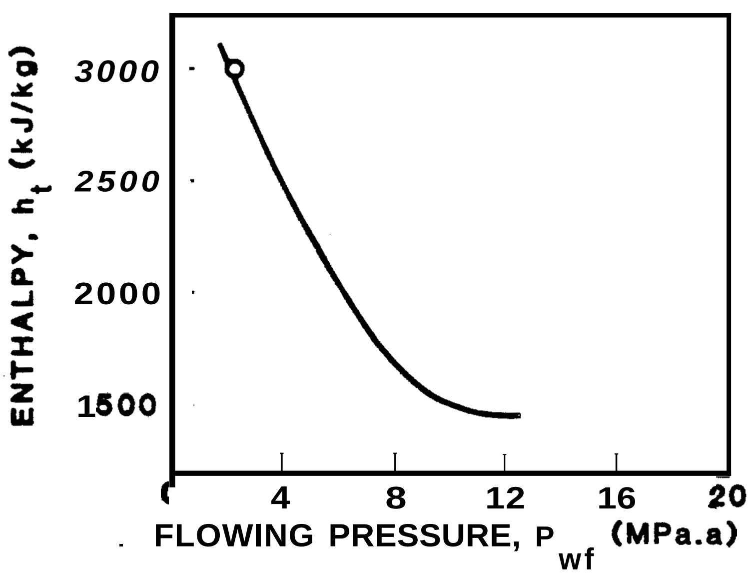

FIGURE 5.5: **ENTHALPY** VS FLOWING **DOWNHOLE PRESSURE,** WELL **KG-12**

5.1.4 Well 403, Tungonan Geothermal Field, the Philippines

Flow characteristics for this well are available from a flow test and from flowing pressure and temperature surveys conducted between August 1980 and Feburary 1981.

The data from these tests is summarized in Table 5.6:

TABLE 5.6: MEASURED FLOW DATA FROM WELL 403

WELLHEAD PRESSURE, p_{wh} (MPa a)	FLOWING PRESSURE, p_{wf} (MPa a)	MASSFLOW, W (kg/s)	ENTHALPY, h_t (kJ/kg)
0.95		30.2	1440
1.26	3.73*	28.8	1400
1.80		26.6	1370
2.46	7.20	22.8	1330
2.58	11.33	9.0	1270

* estimated from flowing temperature survey

The saturation water enthalpy at 295°C is 1317 kJ/kg; greater than that measured at the lowest massflow. This suggests that, although the production zone at 2000-2200 m is the predominant zone, other lower enthalpy zones do feed into the well under high wellhead pressure. Unfortunately this is a common problem when trying to analyze geothermal well behaviour. This data was used to calculate the effective fracture width using James(1975) and Bodvarsson(1981) but is not included in the graphs of flow characteristics.

The calculation of fracture width is summarized in Table 5.7. To obtain the data from GEOFLOW, an effective isentropic efficiency of 0.987 was used.

TABLE 5.7 : CALCULATED EFFECTIVE FRACTURE WIDTH FOR WELL 403

p_{wf} (MPa.a)	W (kg/s)	G (kg/m^2s)	A (m^2)	w_f (mm)
3.73	28.8	34088.31	0.00084	1.2[1]
7.20	22.8	29063.45	0.00078	1.11
11.33	9.0		0.00420	6.1[2]
			0.00240	3.53

1 calculated from GEOFLOW

2 calculated from James(1975)

3 calculated from Bodvarsson(1981)

The discrepancy between the GEOFLOW and the James/Bodvarsson results, is probably due to error in the assumed reservoir pressure, This would not affect the GEOFLOW calculations but does influence the results from James and Bodvarsson.

Using the average flow area from GEOFLOW, the flow characteristics were calculated and plotted in Figures 5.6 and 5.7. A crossplot of the enthalpy and massflow data was also prepared and is compared with the field data in Figure 5.8.

Choking was calculated to occur when the well flowing pressure is less than 6.15.MPa.a; indicating that the total system massflow would be limited to approximately 28 kg/s.

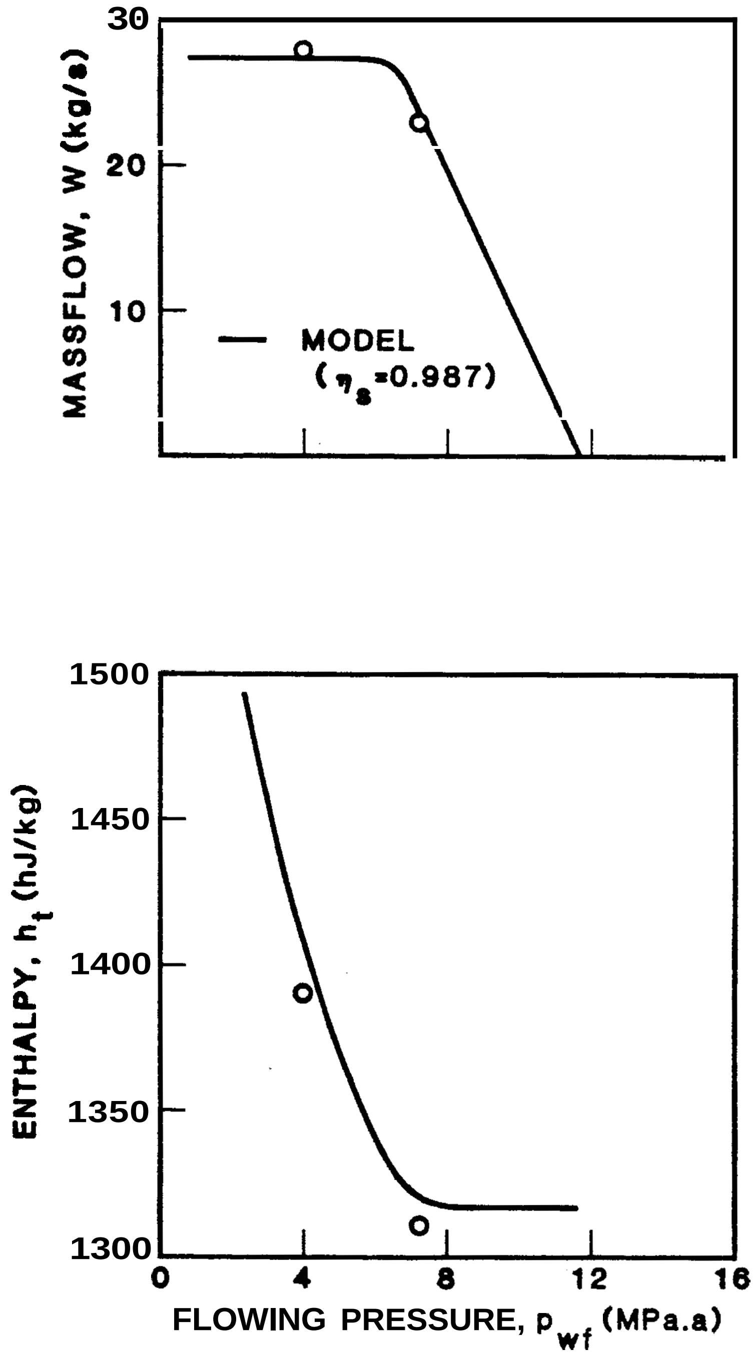

FIGURE 5.7: ENTHALPY VS FLOWING WWNHOLE PRESSURE, WELL *403*

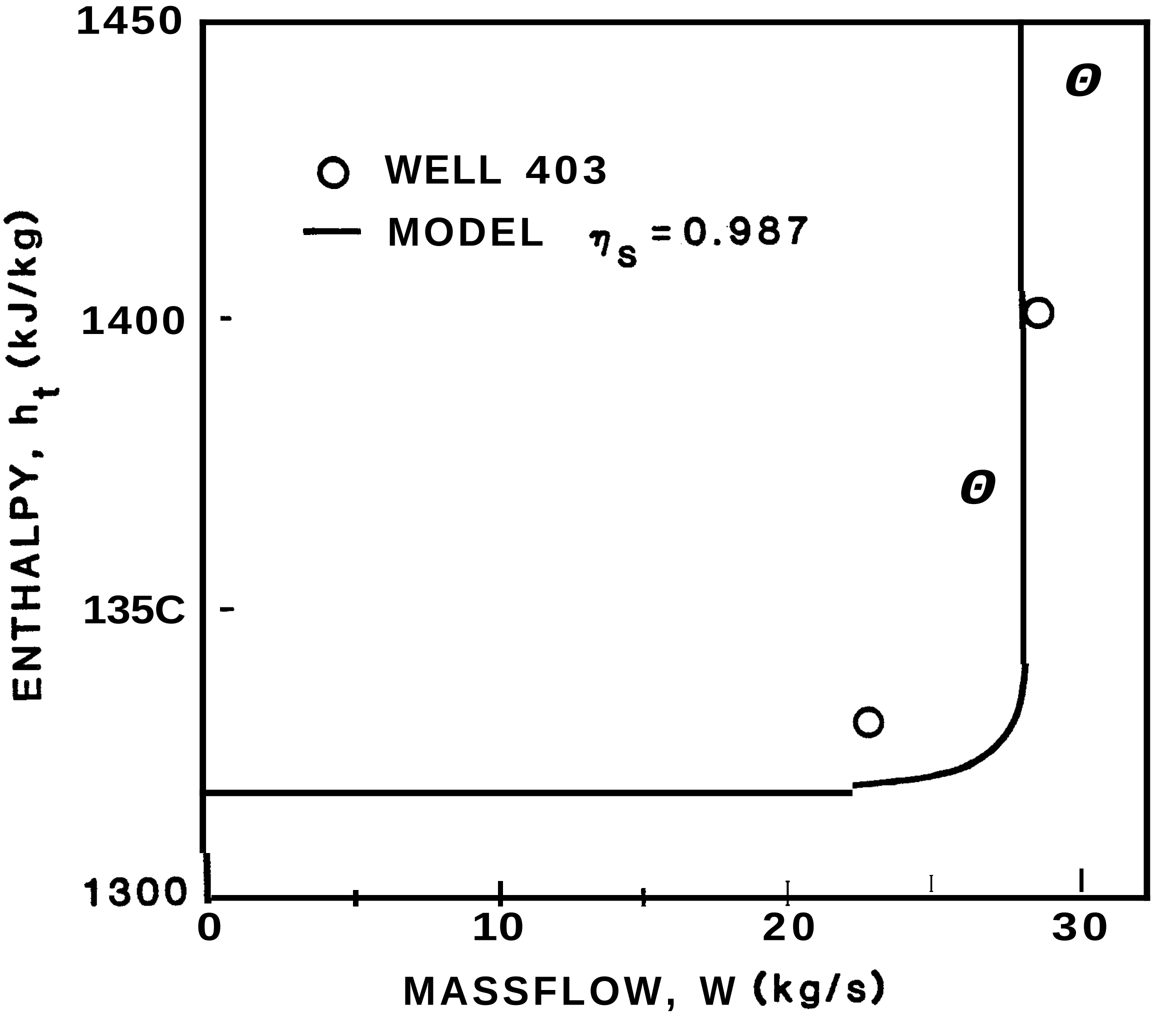

FIGURE 5.8: ENTHALPY/MASSFLOW CROSSPLOT, WELL 403

5.2 Experimental Data

Experimental work on the flow of flashing steam/water mixtures in porous media was one of the aspects of Arihara's (1974) research on non-isothermal flow through consolidated sandstone cores. Seven runs were made; five with a synthetic core and two with a Berea sandstone core. A summary of the core properties is presented in Table 5.8:

TABLE 5.8: PROPERTIES OF CORES USED BY ARIHARA (1974)

	CORE	
	SYNTHETIC	BEREA
Permeability, k (md)	100	400
Porosity, ϕ (%)	35.9	22.0
Diameter, d_c (mm)	50	50
Length, l (mm)	597	597

In all cases, except for run 3, hot pressurized water was introduced into the core and allowed to flash within the core. In run 3 it appears that some flashing may have occurred before the water was injected into the core.

GEOFLOW was used to analyze the data in order to calculate the effective flow area. An effective isentropic efficiency of 0.992 was assumed which approximated an isenthalpic process. The data is presented in Table 5.9.

The average flow area for the synthetic core was found to be 5×10^{-8} m^2 and for the Berea core, 2.1×10^{-8} m^2. These values are orders of magnitude lower than the flow areas calculated for the field examples, suggesting that the experimental setup was not an adequate representation of flow in a geothermal system.

TABLE 5.9 EFFECTIVE FLOW AREA FROM EXPERIMENTAL DATA ARIHARA(1974)

CORE	RUN NO.	INITIAL PRESS.(MPa.a)	INITIAL TEMP.(^oC)	SATURATION PRESS.(MPa.a)	OUTLET PRESS.(MPa.a)	MASSFLOW (kg/s)	MASSFLUX (kg/m^2s)	FLOW AREA (m^2)
SYNTHETIC	1	1.31	180	1.25	0.37	5.62×10^{-4}	1200[illegible]	7.7×10^{-8}
	2	1.31	185	1.12	0.44	9.6×10^{-4}	10148.92	9.5×10^{-8}
	3	1.[illegible]	205	1.81	0.40	$1.[illegible] \times 10^{-4}$	[illegible]000.33	7.3×10^{-9}
	4	1.[illegible]	[illegible]9	1.5[illegible]	0.[illegible]	3.53×10^{-4}	13206.81	2.7×10^{-8}
	5	1.67	193	1.35	1.05	5.50×10^{-4}	11023.40	4.6×10^{-8}
BEREA	6	1.55	203	1.65	0.29	2.85×10^{-4}	14027.[illegible]	2.1×10^{-8}
	7	1.85	208	1.81	1.16	$[illegible] 18 \times [illegible]^{-4}$	15000.[illegible]	2.1×10^{-8}

6. RELATIVE PERMEABILITY FUNCTIONS

The relative permeabilities of steam and water were generated by GEOFLOW at each pressure step to account for the calculated values of flowing enthalpy. The data was calculated for a range of input conditions.

6.1 Effect of the Input Variables

It was found that the calculated relative permeability functions were virtually insensitive to reservoir temperature and effective isentropic efficiency. This may be due to the changing kinematic viscosity ratio(ν_s/ν_w) as the flashing occurs. To illustrate how insensitive the relative permeability functions are to the input variables, values of the steam and water relative permeabilities at 250°C and 300°C for η_s = 0.92 and 0.5 are plotted in Figure 6.1.

The data suggests that it is possible to define a unique set of relative permeability curves. Using a power law curve fit on the water relative permeability, the following functions were derived:

$$S_w > 0.4, \qquad k_{rw} = S_w^{0.6} \qquad (6.1\text{-}1)$$

$$0.4 > S_w > 0.2, \qquad k_{rw} = S_w^{0.7} \qquad (6.1\text{-}2)$$

$$S_w < 0.2, \qquad k_{rw} = S_w^{0.77} \qquad (6.1\text{-}3)$$

$$\text{and:} \qquad k_{rs} = 1 - k_{rw} \qquad (6.1\text{-}4)$$

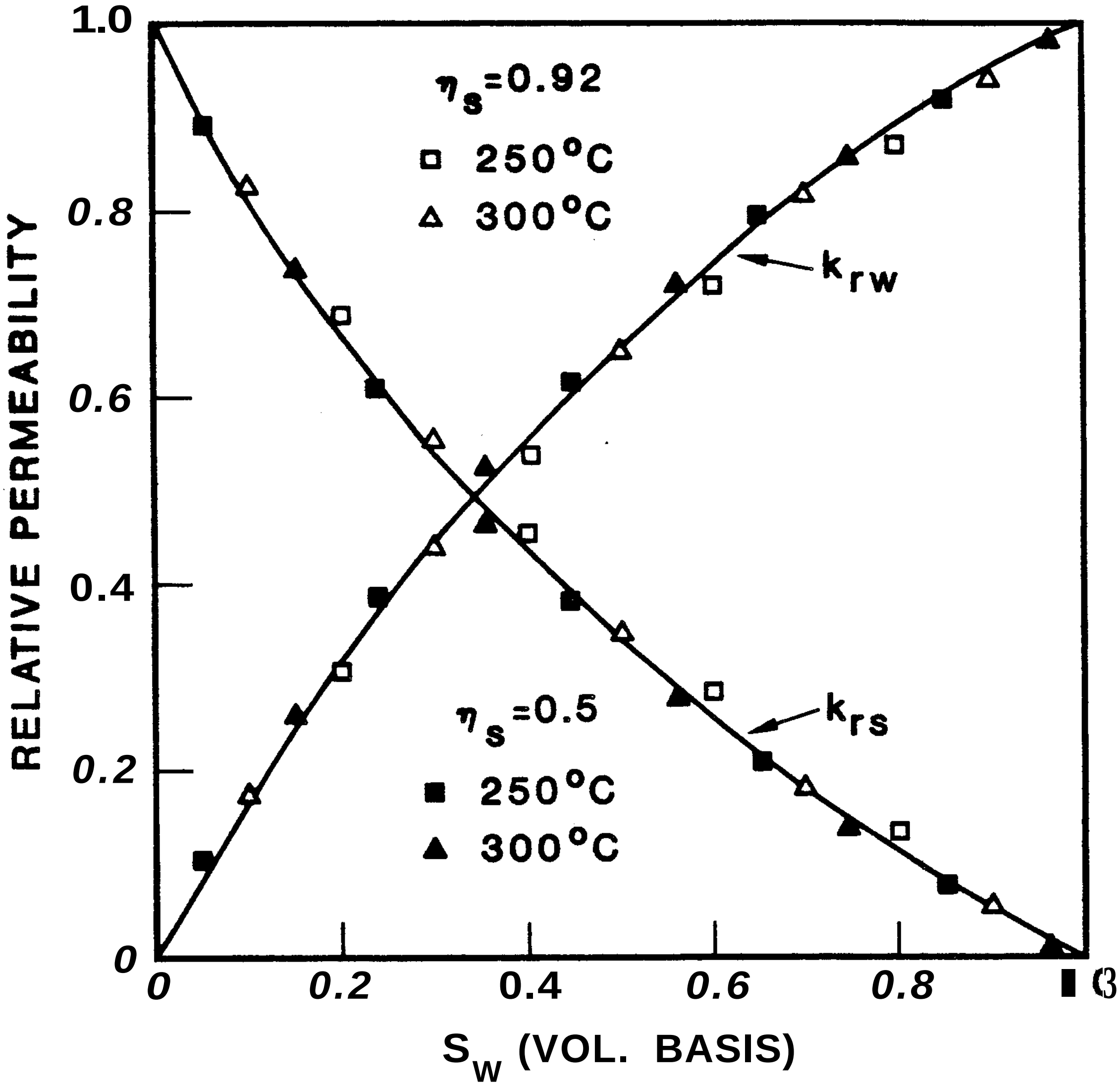

FIGURE 6.1 : RELATIVE PERMEABILITY CURVES FOR STEAM AND WATER AS GENERATED BY GEOFLOW

6.2 Comparison with Corey and X-type Relative Permeability Functions

Bodvarsson, O'Sullivan and Tsang (1981) studied the sensitivity of geothermal recovery processes to relative permeability parameters. Their study considered the Corey and X-type relative permeability functions and included a study of the effect of the residual water and steam saturations.

For the comparison with the relative permeability curves generated by GEOFLOW, only the basic Corey and X-type curves were used. These are shown in Figure 6.2. For the Corey curves a residual water saturation of 0.3 and residual steam saturation of 0.05 had been assumed.

As mentioned in Section 2.2, the relative permeability functions can be estimated from output characteristics, in particular the flowing enthalpy. In the same way the flowing enthalpy can be calculated knowing the relative permeability functions and the fluid properties:

$$h_t = \nu_t \left(h_w \frac{k_{rw}}{\nu_w} + h_s \frac{k_{rs}}{\nu_s} \right) \tag{6.2-1}$$

where:

$$\frac{1}{\nu_t} = \frac{k_{rw}}{\nu_w} + \frac{k_{rs}}{\nu_s} \tag{6.2-2}$$

The relationship between the relative permeabilities and the flowing enthalpy was studied by Bodvarsson et al. (1980), for the basic Corey and X-type curves. They presented their results as a function of the water relative permeability for the specific example of a 250°C reservoir. This is reproduced in Figure 6.3 along with the corresponding data from GEOFLOW. Bodvarsson et al. (1980) considered the Corey and X-type curves to "represent the likely extremes of what the real relative permeability functions may be" and "it is

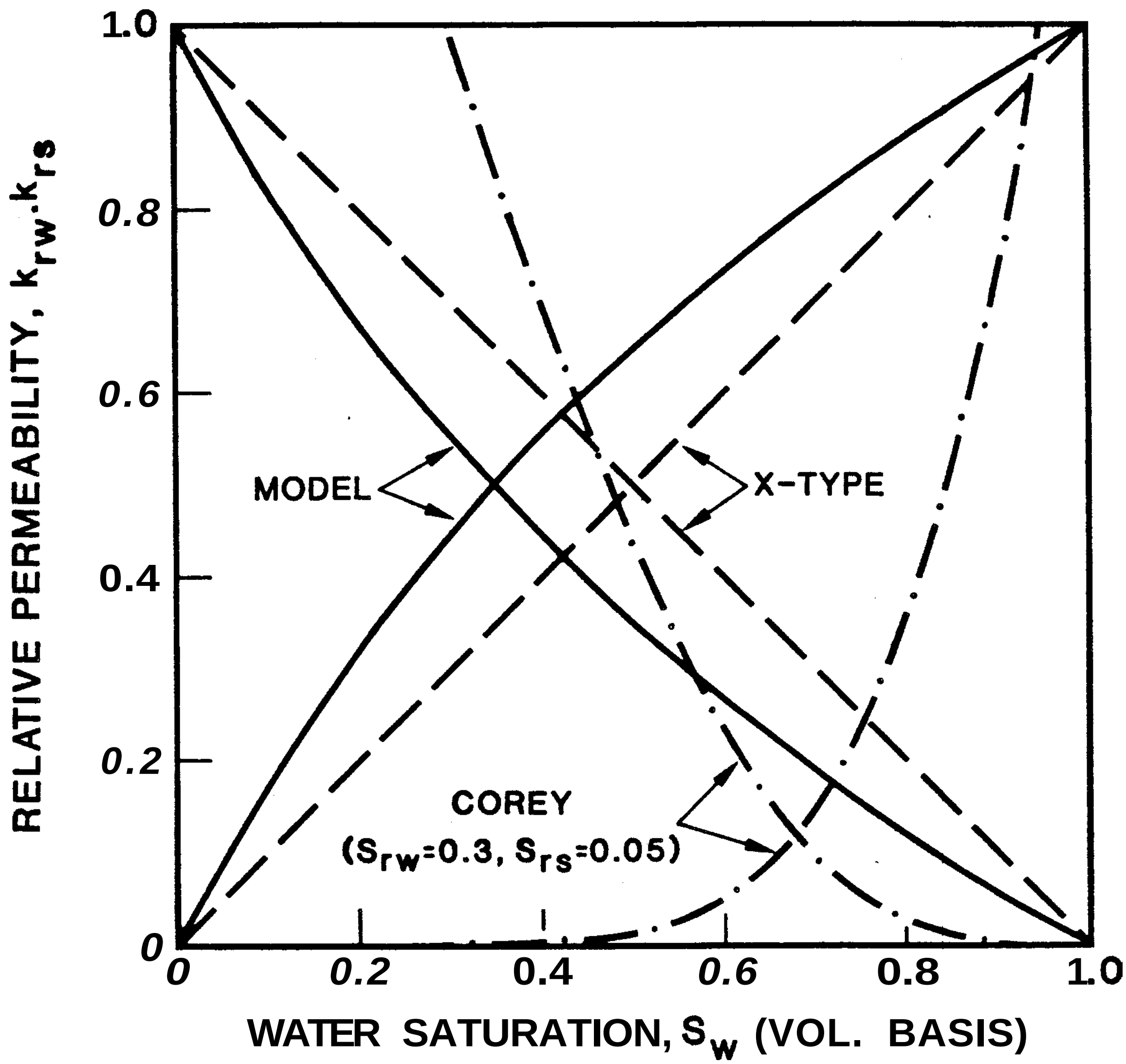

FIGURE 6.2: COREY, X-TYPE AND GEOFLOW RELATIVE PERMEABILITY CURVES

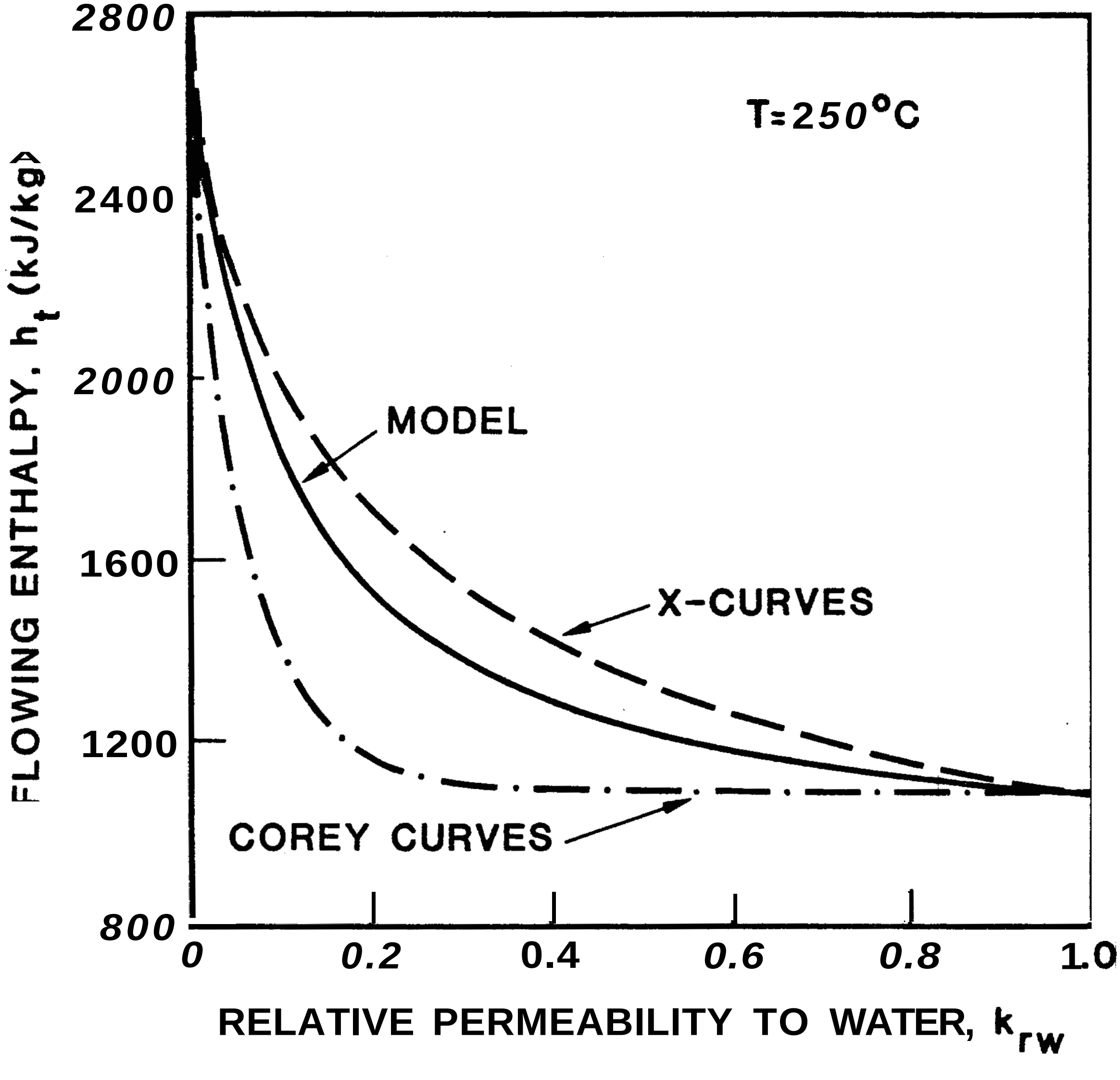

FIGURE 6.3: FLOWING ENTHALPY VS WATER RELATIVE PERMEABILITY, $T_0=250^{\circ}C$
(AFTER BODVARSSON, O'SULLIVAN AND TSANG, 1980)

probable that k_{rw}/h_t values determined from field data will fall within this zone" (the envelope enclosed by the Corey and X-type curves in Figure 6.3). It can be seen that the data from GEOFLOW does in fact fall within this envelope.

6.3 Comparison with Field Derived Curves

Using production data from the Wairakei geothermal field in New Zealand, Horne and Ramey(1978) and Shinohara(1978), using slightly different procedures, derived the relative permeability functions. The main assumption used in their derivations was that flashing did not occur in the reservoir or wellbore. This implies that the wellhead conditions were assumed to reflect the corresponding reservoir conditions.

The relative permeability curves were presented as function of the flowing water mass fraction and in this form they are unsuitable for use in geothermal simulators. Unfortunately it is impossible to convert the data to the inplace water saturation (volume basis) without knowing the slip ratio or the immobile water saturation.

The relative permeability curves from GEOFLOW are available on a flowing water mass fraction basis and can be compared with the curves from Horne and Ramey(1978) and Shinohara(1978) on this basis, as in Figure 6.4. A reservoir temperature of 250°C and effective isentropic efficiency of 0.92 were assumed for the comparison.

The consistency between the shapes of the curves, particularly at high water mass fractions indicates that the assumptions used in GEOFLOW give results in agreement with measured field data from a fractured geothermal reservoir.

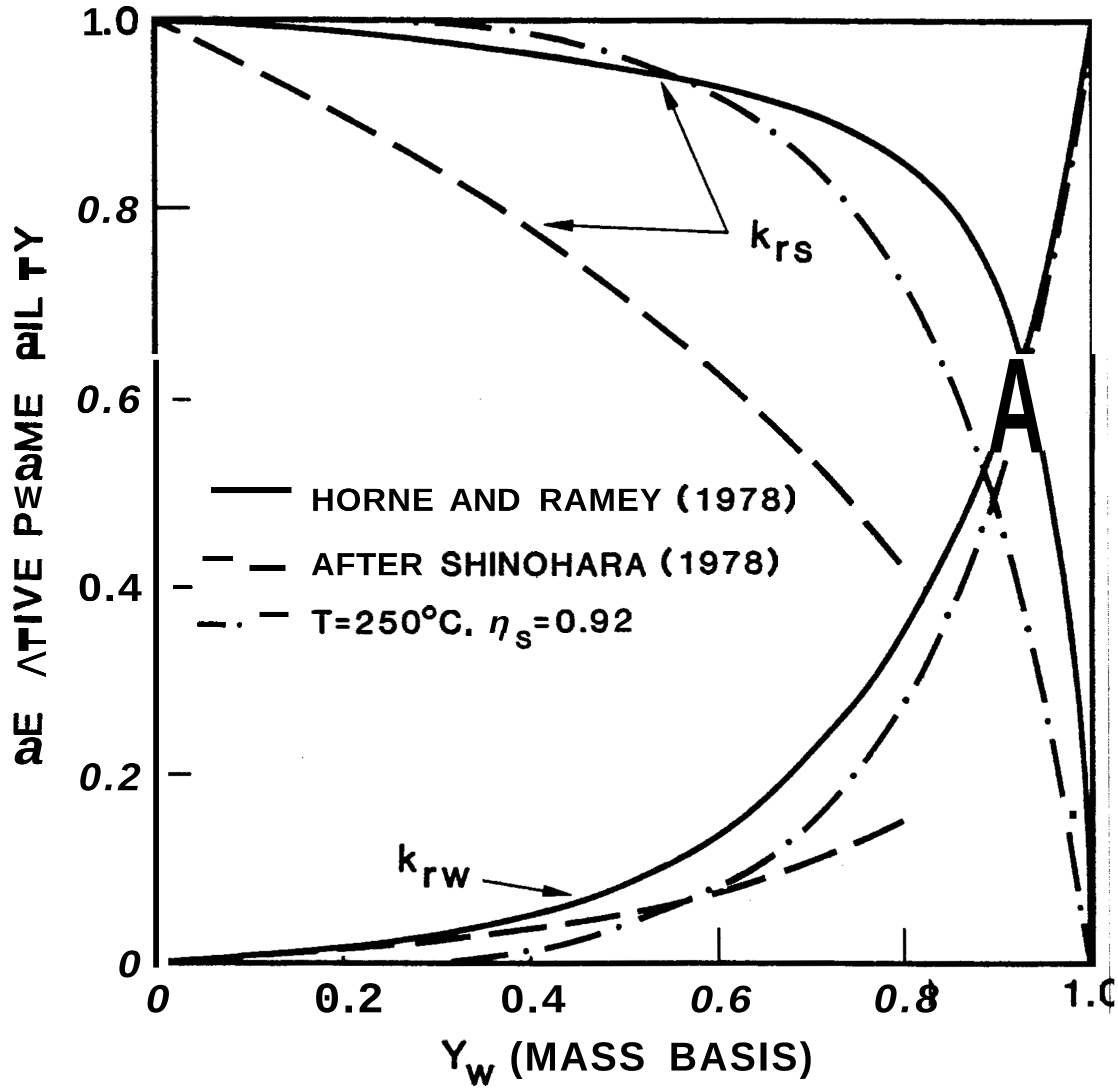

FIGURE *6.4:* **HORNE *AND* RAMEY(1978), SHINOHARA(1978) AND** GEOFLOW RELATIVE PERMEABILITY CURVES

6.4 Comparison with Experimental Relative Permeability Curves

An experimental study of steam/water relative permeability was undertaken by Counsil(1979), using synthetic cores with an average permeability of 32 md. The water saturation within the core was measured using a capacitance probe but due to the low flowrates and radial heat transfer effects, it is believed that a saturation profile existed normal to the flow direction. The probe measured the saturation near the axis of the core, which may have been higher than the average saturation of the cross section.

Counsil(1979) presented three examples of flow data and the derived relative permeability curves. One of these curves is reproduced as Figure 6.5. The other two examples have the same functional form but cover lower ranges of water saturation. The graph in Figure 6.5 shows that the residual water saturation is high, approximately 50%, while the residual steam saturation is not well defined, although it is assumed to be zero in this case, The shape of the curves is similar to the Corey(1954) relative permeability curves for consolidated porous media.

6.5 Comparison with Relative Permeability Curves for Vugular Cores

There has been some work reported in the literature on the effect of stratification, Corey and Rathjens(1956), and heterogeneities such as vugs, Ehrlich(1971) and Sigmund and McCafferty(1979), on relative permeability curves. An example from Sigmund and McCafferty(1979) is reproduced in Figure 6.6 for water displacing oil in a core from a dolomite reservoir. The core contained a compact crystalline matrix and vugs of various sizes. Curves for the other examples in Sigmund and McCafferty(1979), were similar to the Corey-type curves, suggesting that they were in fact homogeneous or had well distributed heterogeneities.

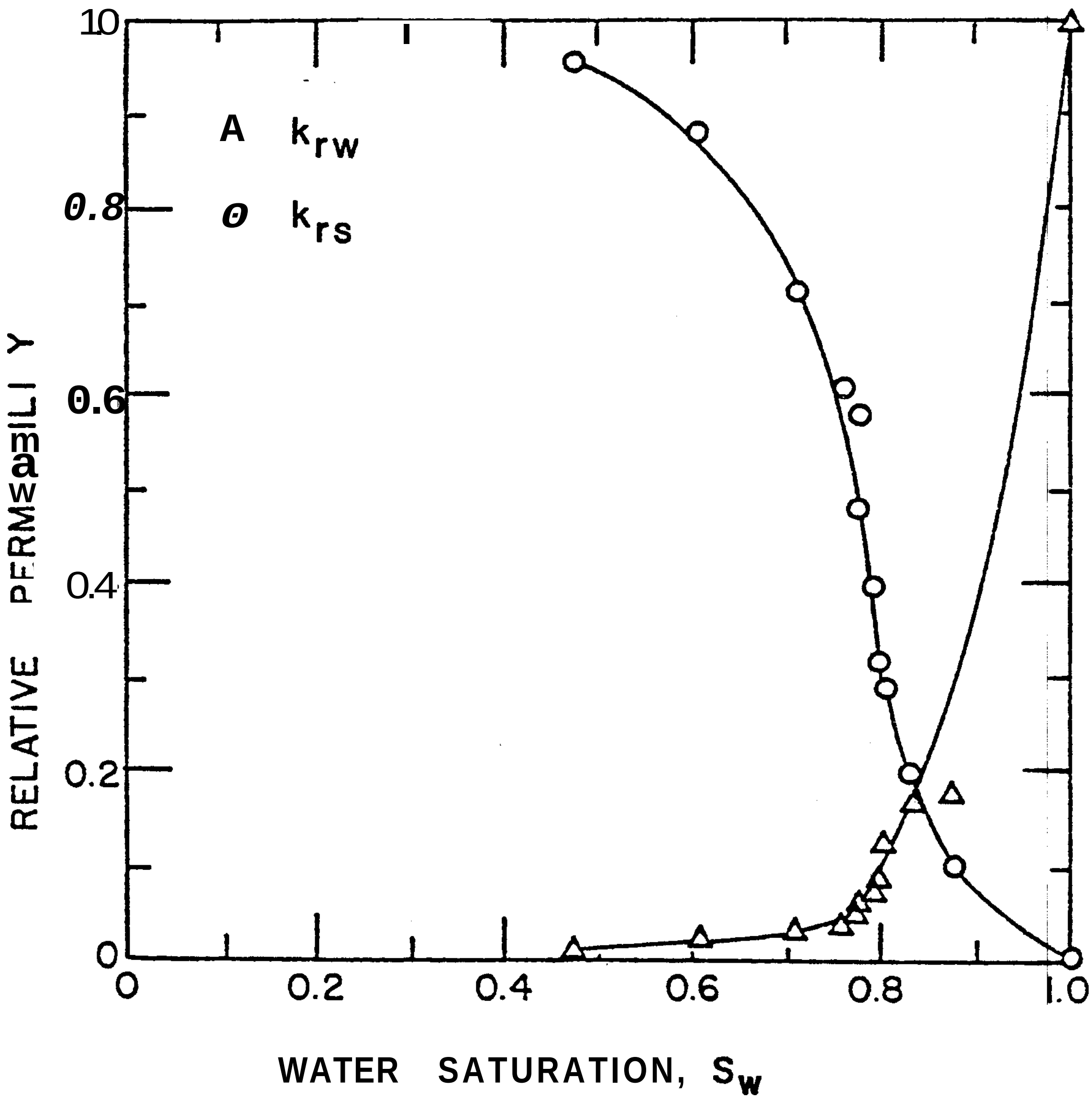

FIGURE 6.5: EXPERIMENTAL RELATIVE PERMEABILITY CURVES FOR STEAM AND WATER (COUNSIL, 1979)

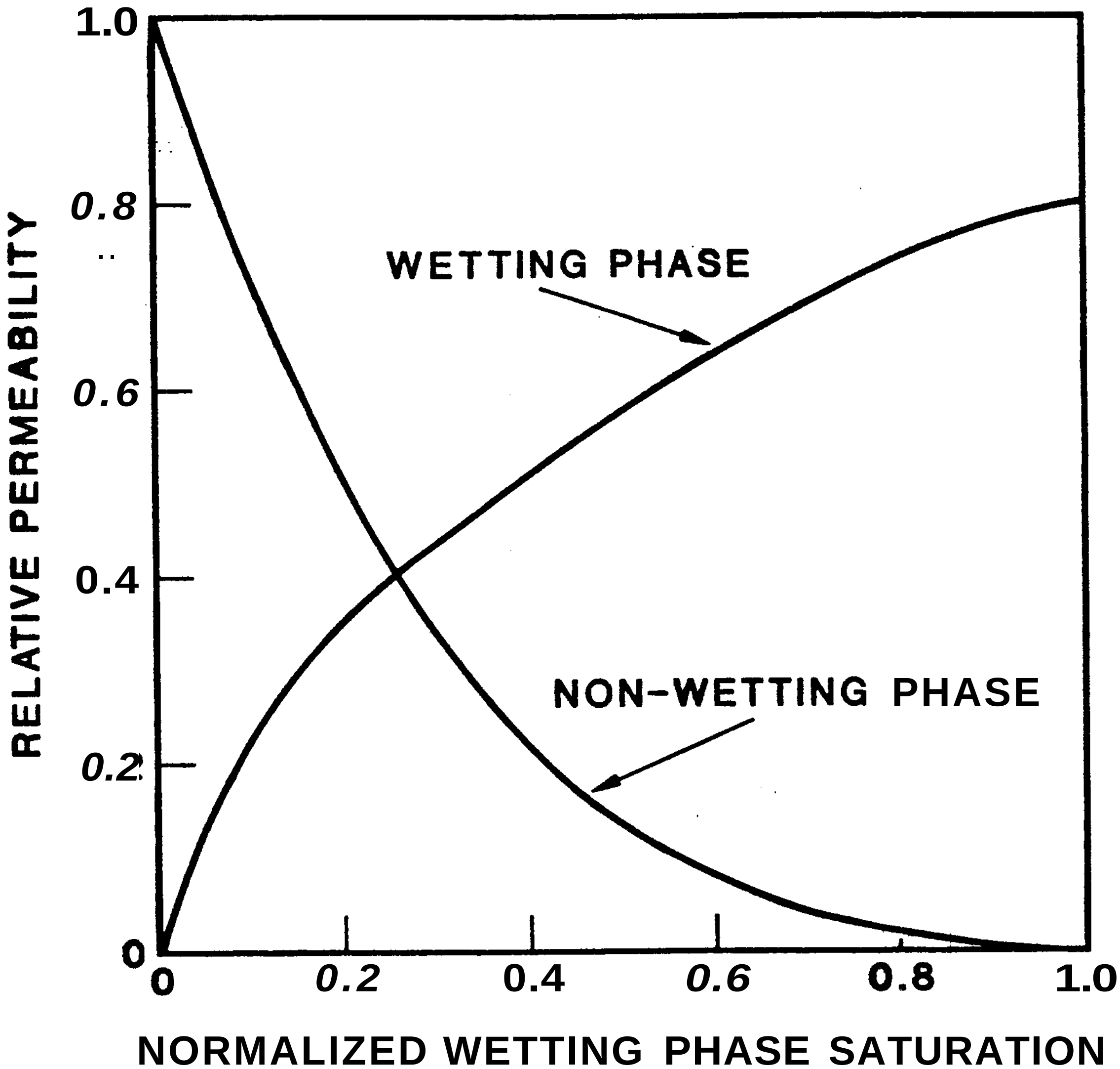

FIGURE 6.6: RELATIVE PERMEABILITY CURVES FOR VUGULAR DOLOMITE CORE (SIGMUND AND McCAFFERTY, 1979)

The shape of the relative permeability curves in Figure 6.6 are similar in shape to the GEOFLOW relative permeability curves, suggesting that a vugular system where the heterogeneities are not well distributed has similar flow properties to the system modelled in GEOFLOW.

The next section discusses the results obtained from using the GEOFLOW program to study the two phase flow of steam and water under simulated geothermal reservoir conditions.

7. DISCUSSION

7.1 Flow Characteristics

One of the aims of this research was to investigate why the flowing enthalpy increased as a non-linear function of the massflow. It appears that this may be explained by the concept of choked flow. In the field examples all the wells exhibited choked flow characteristics at low wellhead pressures but only in well 403 from the Tungonan geothermal field, the Philippines, was both enthalpy and massflow data available. Taking into account the errors involved in the measurement of the enthalpy and massflow and the possibility that more than one zone could be contributing to the total flow, the agreement between GEOFLOW and the field data supports the contention that choked flow may cause this phenomena.

Choking appears to occur when the inplace water saturation is about 0.6-0.7, but it is not immediately apparent where this occurs in relation to the wellbore. It is generally found in simulation studies of radial systems, for example Jonsson(1978), that most of the pressure drop occurs close to the well. This may suggest that choking occurs near the wellbore and furthermore since the Krafla wells can produce saturated or superheated steam it suggests that the choking occurs in the reservoir and not as the fluid enters the wellbore. This is important as it is generally assumed that choking occurs at an abrupt change in geometry, such as at the outlet of a pipe discharging to the atmosphere.

The value of effective isentropic efficiency used to fit the field data was generally found to be greater than 0.9. This suggests either that limited heat is being "mined" from the rock or that most of the heat is lost in irreversible processes, such as friction. It is possible that a steady state situation develops where the flashing front is virtually stationary. Under this condition the heat contained in the rock where the flashing process is occurring will be rapidly depleted and the rock temperature gradient will approximate the fluid temperature gradient. When this situation develops the heat transfer will be close to zero and is reflected by a high effective isentropic efficiency.

It appears that the data from GEOFLOW can be successfully extrapolated into the single phase region to give an indication of the expected flow characteristics. This is important in wells where both two phase and single phase flow conditions can exist.

7.2 Flow Geometry

An important reason for using the field data in this research was to see if GEOFLOW could predict reasonable values for the flow area and effective fracture width. The results ranged from 0.3 - 4.1 mm which do appear to be within the expected order of magnitude. The calculation method of Bodvarsson(1981) for single phase incompressible flow was found to give comparable fracture widths when a friction factor of 1.0 was used. James(1975) formula give consistently high values, suggesting that James' assumption that the kinetic energy term was negligible may not be valid.

The flow areas of $5 \times 10^{-8}\ m^2$ and $2.1 \times 10^{-8}\ m^2$ calculated from the results of Arihara(1974) suggests that his experiments may not reflect the situation in a geothermal reservoir, particularly in the area close to the well, where the flashing is likely to occur. This is probably due to the low permeabilities (100–400 md) of the consolidated cores used in Arihara's study.

7.3 Relative Permeability Curves

It was mentioned in Section 2.2 that the rational for using porous medium type relative permeability functions to model flow in fractured reservoirs, was that heterogeneities should average out if a large enough control volume could be assumed. However, in a geothermal system it appears that flashing, and hence two phase flow, occurs close to the wellbore and only over a relatively short distance. This implies that the use of Corey relative permeability curves to describe the flow in a fractured geothermal reservoir will probably give misleading results.

The relative permeability functions measured in vugular cores show similar properties to the relative permeability curves from GEOFLOW further suggesting that the functional form of the relative permeability curves for fractured systems is very different from the basic Corey-type curves.

Experimental data on steam/water relative permeabilities has been restricted to low permeability consolidated cores and the resulting curves are, not unexpectedly, found to resemble the Corey curves.

The relative permeability curves generated by GEOFLOW are at the other extreme; an open fracture with no steam/water interaction. They do, however, appear to give results that may be closer to reality than either the Corey or X-type curves. They also agree reasonably closely with the field derived curves of Horne and Ramey(1978) and Shinohara(1978). Therefore it is considered that the GEOFLOW curves represent the most appropriate functional form for steam/water relative permeabilities for fractured geothermal system$.

8. CONCLUSIONS

From this study it can be concluded that:

1. Choked flow may occur within a two phase geothermal reservoir, thereby limiting the ultimate exploitation rate.

2. The choked flow condition occurs when the liquid saturation falls below 0.6–0.7.

3. The concept of choked flow may explain observed flow characteristic6 such as the enthalpy rise and constant massflow at low wellhead pressures in two phase geothermal systems.

4. The streamtube model can be used to estimate values for flow area and effective fracture width.

5. The mining of heat from the rock by the flowing fluid does not appear to be a very efficient method of energy recovery from geothermal systems.

6. Relative permeability curves for consolidated sandstone may give misleading information when applied to fractured geothermal reservoirs.

7. Using relative permeability curves of the following form

$$k_{rw} = S_w^{\,n} \qquad \text{where } n = 0.6 - 0.8$$

$$k_{rs} = 1 - k_{rw}$$

may better simulate energy recovery processes in fractured geothermal reservoirs than the relative permeability functions presently used in geothermal reservoir simulation.

8. The relative permeability curves from **GEOFLOW** are not temperature dependent and therefore represent a single set of curves applicable to any geothermal system.

9. RECOMMENDATIONS FOR FUTURE WORK

At present GEOFLOW assumes that the reservoir initially contains either saturated or compressed water. The field examples indicate that it would be an advantage to modify GEOFLOW to accept two phase initial reservoir conditions. This could be accomplished by either using the initial water mass fraction or the inplace fluid enthalpy as additional input parameters.

It would be difficult to modify GEOFLOW beyond considering two phase initial conditions. If further terms were incorporated in the energy balance it would require some definition of the system geometry and GEOFLOW would lose the advantage of being a completely general thermodynamic model. However the effective isentropic efficency should be analyzed to see what extra information it can provide about the system. For example, in the case of BR-21 the low value of effective isentropic efficiency suggested that the reservoir was naturally two phase.

A common problem in the analysis of geothermal well behaviowr, is the existence of multiple production zones. It would therefore be useful to derive a multiple zone model based on GEOFLOW.

An attempt was made to use the derived relative permeability curves in the geothermal simulator, GEONZ, described in Horne, Ogbe, Temeng and Ramey Jnr.(1980). Due to technical problems no useful results were obtained. It is recommended that this work should be continued and the results compared with simulations using Corey and X-type relative permeability curves. The simulations should be based on transient massflow and enthalpy measurements from field data.

Experimental studies on the relative permeability of steam and water need to be continued. However, the experiments should be modified to reflect the likely flow conditions in a fractured geothermal reservoir. Therefore the synthetic cores should be constructed so that they adequately represent the heterogeneities within the reservoir. The size of the experimental apparatus and the required massflow through the system should also be considered, particularly where heat transfer effects are likely to be important.

10. NOMENCLATURE

A	flow area	m^2
C_p	specific heat at constant pressure	kJ/kg^oC
d	wellbore diameter	m
d_c	core diameter	mm
f	friction factor	
G	total massflux	kg/m^2s
h	enthalpy	kJ/kg
h_i	enthalpy after i^{th} pressure step	kJ/kg
h_t	total mixture flowing enthalpy	kJ/kg
k	permeability	md
k_{rw}	water relative permeability	
k_{rs}	steam relative permeability	
l	core length	mm
P	pressure	MPa.a
P_i	pressure after i^{th} pressure step	MPa.a
Q	heat transferred	kJ/kg
s	entropy	kJ/kg^oC
s_i	entropy after i^{th} pressure step	kJ/kg^oC
S^*	normalized liquid saturation	
S_{rw}	residual water saturation	
S_{rs}	residual steam saturation	
S_w	water saturation	
T	temperature	^oC
T_f	fluid temperature	^oC
v_i	velocity after i^{th} pressure step	m/s
w_f	effective fracture width	mm
W	total massflow	kg/s
x	steam mass fraction	
y_i	steam mass fraction in i^{th} streamtube	
Y	water mass fraction	
Y_i	water mass fraction after i^{th} pressure step	

A	difference	
η_s	effective isentropic efficiency	
ρ	density	kg/m^3
E	slip ratio	
μ	dynamic viscosity	Pa.s
ν	kinematic viscosity	m^2/s
ν_t	total mixture kinematic viscosity	m^2/s
ϕ	porosity	

SUPERSCRIPTS

'	water
''	steam
*	property after heat transfer step
—	average value

SUBSCRIPTS

i,n	i^{th} streamtube after n^{th} pressure step
n	n^{th} pressure step
0	initial condition
s	steam
sat	property at saturation conditions
w	water
wf	well flowing (downhole)
wh	wellhead property

11. REFERENCES

Arihara, N.: "A Study of Non-Isothermal Single and Two-Phase Flow Through Consolidated Sandstones", Ph.D. Thesis, Petroleum Engineering Department, Stanford University, Stanford, California (November 1974).

Bodvarsson, G.: "Interstitial Fluid Pressure Signal Propagation along Fracture Ladders", Proc., Seventh Workshop on Geothermal Reservoir Engineering, Stanford University, Stanford, California, 139-141, (15-17 December 1981).

Bodvarsson, G.S., O'Sullivan, M.J. and Tsang, C.F.: "The Sensitivity of Geothermal Reservoir Behaviour to Relative Permeability Parameters", Proc., Sixth Workshop on Geothermal Reservoir Engineering, Stanford University, Stanford, California, 224-237, (16-19 December 1980).

Butz, J. and Plooster, M. : "Subsurface Investigations at the Roosevelt KGRA, Utah", Report No. DOE/ET/28389-1, performed under DOE Contract No. AS08-77ET28389 by Denver Research Institute, University of Denver, Denver, Colorado, (October 1979).

Corey, A.T. : "The Interrelation Between Gas and Oil Relative Permeabilities", Producers Monthly, 38-41, (November 1954).

Corey, A.T. and Rathjens, C.H. : "Effect of Stratification on Relative Permeability", Trans., AIME, 207, 358-360, (1956).

Counsil, J.R. : "Steam-Water Relative Permeability", Ph.D. Thesis, Petroleum Engineering Department, Stanford University, Stanford, California (May 1979)

Ehrlich, R.: "Relative Permeability Characteristics of Vugular Cores - Their Measurement and Significance", paper SPE 3553 presented at the 46th Annual Fall Meeting of the Society of Petroleum Engineers, New Orleans, La. (October 1971).

Grant, M.A. and Sorey, M.L. : "The Compressibility and Hydraulic Diffusivity of a Water-Steam Flow", Water Resoures Research, 15, 3, 684-686 (June 1979).

Grant, M.A., Applied Mathematics Division, New Zealand Department of Scientific and Industrial Research, personal communication (1982).

Horne, R.N. and Ramey Jnr., H.J.: "Steam/Water Relative Permeabilities from Production Data", Trans., Geothermal Resources Council Annual Meeting, 2, 291-293 (July 1978).

Horne, R.N., Ogbe, D.O., Temeng, K. and Ramey Jnr., H.J.: "Geothermal Reservoir Engineering Computer Code Comparison and Validation Using the GEONZ Simulator Program", Final Report, performed under DOE Contract No. DE-AC03-80SF11450 by the Petroleum Engineering Department, Stanford University, Stanford, California, (November 1980).

James, R.: "Steam-Water Critical Flow Through Pipes", Proc., Institution of Mechanical Engineers, 176, 26, 741-748 (1962).

James, R. : "Drawdown Test Results Differentiate Between Crack Flow and Porous Bed Permeability", 2nd United Nations Symposium on the Development and Utilization of Geothermal Resources, San Francisco, 3, 1693-1696 (1975).

Jonsson, V.: "Simulation of the Krafla Geothermal Field", Report No. LBL-7076, UC-66a, performed under DOE Contract No. W-7405-ENG-48 by Lawrence Berkeley Laboratory, University of California, Berkeley, California (August 1978).

Miller, F.G. : "Steady Flow of Two-Phase Single-Component Fluids through Porous Media", Trans., AIME, 192, 205-216 (1951).

Moody, F.J.: "Maximum Flow-Rate of a Single-Component Two-Phase Mixture", Trans., ASME, Journal of Heat Transfer, 134-142 (February 1965).

Nathenson, M.: "Flashing Flow in Hot Water Geothermal Wells", Journal of Research, U.S. Geological Survey, 2, 6, 743-751 (November-December 1974)

PNOC.: unpublished data (1981)

Reynolds, W.C.: Thermodynamic Properties in S.I., Department of Mechanical Engineering, Stanford University, Stanford, California (1979).

Reynolds, W. C. and Perkins, H. C. : Engineering Thermodynamics (2nd Edition), McGraw-Hill Book Company, New York (1977).

Rumi, O.: "Some Considerations on the Flowrate/Pressure Curve of the Steam Wells of Larderello", Geothermics, 1, 1, 13-23 (1972).

Ryley, D.J.: "The Mass Discharge of a Geofluid from a Geothermal Reservoir-Well System with Flashing Flow in the Wellbore", Geothermics, 9, 221-235 (1980).

Schmidt, E.: Properties of Steam and Water in S.I. Units, Springer-Verlag (New York) Inc., R Oldenburg, Munchen (1969).

Shinohara, K. : "Calculation and Use of Steam/Water Relative Permeabilities in Geothermal Reservoirs", M.S. Report, Petroleum Engineering Department, Stanford University, Stanford, California (June 1978).

Sigmund, P.M. and McCafferty, F.G.: "An Improved Unsteady-State Procedure for Determining the Relative Permeability Characteristics of Heterogeneous Porous Media", Journal of the Society of Petroleum Engineers, 19, 1, 15-25 (February 1979).

Smith, M.C. and Ponder, G.M. (Editors): "Hot Dry Rock Geothermal Energy Development Program, Annual Report, Fiscal Year 1981", Report No. LA-9287-HDR, UC-66a, performed under DOE Contract No. W-7405-ENG-36 by the Los Alamos National Laboratory, Los Alamos, New Mexico (April 1982).

Sorey, M.L., Grant, M.A. and Bradford, E.: "Nonlinear Effects in Two Phase Flow to Wells in Geothermal Reservoirs", Water Resources Research, 16, 4, 767-777 (August 1980).

Stefansson, V. and Steingrimsson, B.: "Production Characteristics of Wells Tapping Two Phase Reservoirs at Krafla and Namafjall", Proc., Sixth Workshop on Geothermal Reservoir Engineering, Stanford University, Stanford, California, 49-59 (16-19 December 1980).

Tsang, C.F.. and Wang, J.S.Y.: "State-of-the-Art of Models for Geothermal Recovery Processes", Journal of Energy Resources Technology, 103, 12, 291-295 (December 1981).

Wallis, G.B. and Richter, H.J.: "An Isentropic Streamtube Model for Flashing Two Phase Vapor-Liquid Flow", Journal of Heat Transfer, 100, 11, 595-600 (November 1978).

APPENDIX A

TEXT OF PAPER

BY

WALLIS AND RICHTER

G. B. Wallis
H. J. Richter
Thayer School of Engineering,
Dartmouth College,
Hanover, N. H. 03755

An Isentropic Streamtube Model for Flashing Two-Phase Vapor-Liquid Flow

Introduction

"Flashing" can occur when liquid flows into a region where the local pressure is below the saturation pressure corresponding to the liquid temperature. As a result of the depressurization, vapor is formed. If the drop in pressure is large a two-phase flow with considerable vapor content is created. In some applications, such as a postulated break in the coolant circuit of a pressurized water reactor or in a boiler feedwater system, the downstream pressure can be only a small fraction of the upstream saturation pressure and the discharge rate is limited by choked flow at or near the smallest cross section of the passage.

Flashing occurs in several stages. If the incoming liquid is subcooled, the initial stage is the nucleation of the first vapor, usually in the form of bubbles. These bubbles grow rapidly and tend to agglomerate, forming continuous regions of vapor that are accelerated more rapidly than the denser liquid. If the void fraction becomes large enough, a vapor core, probably containing some liquid droplets, is likely to develop, while the liquid may be displaced to the wall. The development of these successive flow patterns depends on many phenomena including the initial "nucleation centers" present in the fluid, three dimensional inertial effects that may cause phase separation, trace impurities that inhibit agglomeration, fluid properties that determine rates of interphase heat, mass and momentum transfer and so on. Since analysis of these effects is difficult, it is convenient to have available a few self-consistent analyses of certain "limiting cases" that may approximately describe the overall characteristics and may form the basis for more elaborate studies.

This paper presents a new model for the flashing flow of a two-phase liquid-vapor mixture under the influence of steep pressure gradients. A method for predicting choked or "critical" flow is developed. The theory describes an idealized situation in which there are no irreversible processes. The description is thermodynamically and mechanically consistent and requires no additional assumptions beyond straightforward ones of reversible equilibrium flow without mixing, heat transfer or friction across streamlines.

It is not claimed that thii model gives a realistic picture of the details of the flow. However, it provides a useful "ideal case" for comparison with practical situations in which several irreversible processes occur. It also appears to predict critical flbw rates at least as well as previous theories and avoids some of the earlier conceptual difficulties.

Previous Work

Three approaches, each of them treating the flow as one-dimensional, have previously been taken to this critical flow problem:

1 *Homogeneous Equilibrium Flow.* The two-phase flow is treated by the familiar methods used to analyze single phase flow. The phases are assumed to be intimately mixed and to have equal velocities and temperatures.

2 Slip *Flow.* The vapor and liquid are allowed to have different velocities. The ratio between these velocities is specified in various ways, often without taking account of the physics of the flow.

3 *Separated Flow.* Separate one-dimensional conservation laws are written for each phase. These equations contain "interaction terms" describing heat, mass and momentum transfer between the phases. The more sophisticated theories may contain descriptions of bubble nucleation and growth. Average phase temperatures and velocities are unequal.

The first two approaches have been followed about as far as is feasible by numerous previous workers [1–4]. The homogeneous equilibrium model is self-consistent and compatible with an assumption of reversibility; its disadvantage is inaccuracy since it fails to account for differences in behavior between the phases. The slip flow model requires some additional assumption. since the constraint of equal velocity is relaxed. Usually this appears as a formula for calculating the velocity ratio (v_g/v_f); for example, Fauske [1] equated it to $(\rho_f/\rho_g)^{1/2}$ while Zivi [4] or Moody [2] chose $(\rho_f/\rho_g)^{1/3}$. Any assumption about relative motion tends to conflict with the notion of reversibility (which is often assumed at the same time) since, when phase change *occurs,* the transferred mass is required to be suddenly accelerated from the liquid velocity to the vapor velocity, presumably by irreverisble friction or mixing. The one-dimensional approach is forced to compromise somewhere and it is apparently impossible to conserve energy, momentum and entropy without introducing concepts such as "effective interface velocity" or apparent interfacial forces that may appear artificial [5].

The separated flow model is the subject of much current research and may eventually provide more accurate and realistic predictions. However, at present, proven methods of formulating the "interaction terms," including both reversible and irreversible components, do not exist.

Contributed by the Heat Transfer Division for publication in the JOURNAL OF HEAT TRANSFER. Manuscript received by the Heat Transfer Division January 26, 1978.

The Present Theory

The model which we will describe gets around the difficulties with the usual slip flow theory by allowing velocity and thermodynamic state to vary normal to the main flow direction.

The vapor flow is assumed to develop into different streamtubes that are independent of each other. These streamtubes form at the liquid-vapor interface (Fig. 1). There is no friction, mixing nor heat transfer across streamlines, nor is there any impulsive velocity change upon evaporation (or condensation). Flow in each vapor streamtube is isentropic, yet each streamtube is different because it originates from a different point on the liquid-vapor interface (and hence at a different saturation temperature when pressure changes are present in the flow field). The liquid is assumed to have a uniform velocity and temperature across a single streamtube and to be in equilibrium with the vapor which contacts it. The pressure is assumed to be uniform across the cross section normal to the main flow direction. It is also assumed that the flow is sufficiently one-dimensional for the neglect of velocity components perpendicular to the main flow direction.

Saturated Inlet Stagnation Conditions. Assuming saturated liquid at the entrance into a nozzle, the pressure drop by a certain small amount Δp will cause the first flashing, creating a vapor-liquid mixture. The assumption is now that the first vapor formed due to the pressure drop Δp will flow in a streamtube (which we have arbitrarily located at the centerline of the nozzle). A further decrease by another Δp will flash more liquid and form a second streamtube in which initially saturated steam flows, decreasing the amount of liquid assumed to flow along the wall (or indeed anywhere in the nozzle as long as it forms a continuous stream; for example the liquid could flow as a jet down the center of the nozzle, surrounded by the vapor).

The vapor in the center streamtube created in the preceding pressure drop step will expand isentropically as a result of this further pressure drop by Δp. The initially saturated steam will condense partially but the liquid fraction is very small. Therefore this small amount of liquid, probably droplets, will be assumed to have the same velocity as the steam in this streamtube.

Each discrete drop in pressure will create one new streamtube in which initially saturated steam flows. At the same time the homogeneous mixtures in each existing streamtube expand isentropically as indicated in the enthalpy-entropy diagram (Fig. 2). If the step Δp is taken very small a continuous expansion and flow field is created. For computation purposes a finite step size is chosen, sufficiently small for it to have negligible effect on the overall result. (With decreasing step size certain calculation instabilities were observed depending upon the accuracy of the steam tables used in this computer program. This led to some oscillations in the results. However, the predictions of the choked flow condition and the corresponding velocity profile were insensitive to these variations fox Δp smaller than 1 bar. as shown in Fig. 7).

Let us normalize on the basis of unit mass flow rate. Denote the fraction of the total mass flow rate in the ith vapor streamtube, created in the ith Δp step. by y_i and the corresponding normalized liquid flow rate after the ith flash by Y_i. Then the ith flashing "stage" consists of isentropic conversion of a liquid flow rate Y_{i-1} with velocity v_{i-1}, enthalpy h_{i-1}', and entropy s_{i-1}', to a liquid rate Y_i, with properties v_i, h_i', and s_i', and a vapor flow rate y_i, with properties v_i, h_i'' and s_i'' (see Fig. 3).

Mass is conserved if:

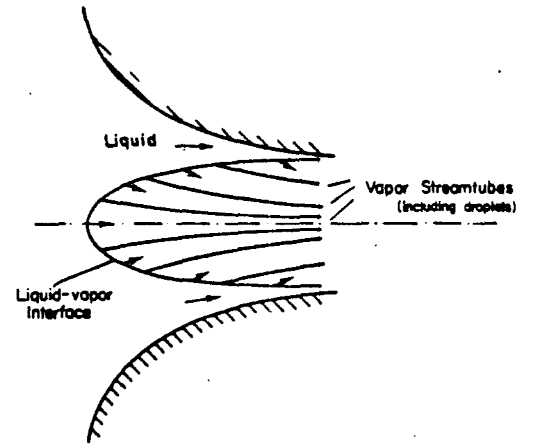

Fig. 1 Development of streamtubes in a nozzle

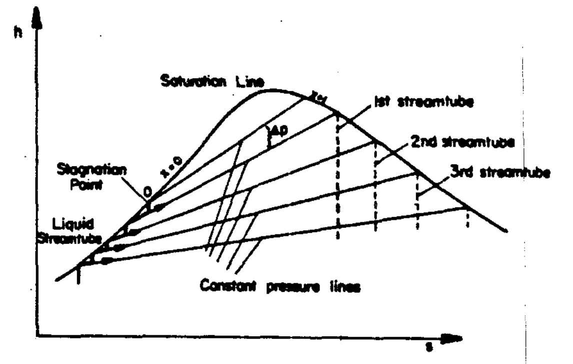

Fig. 2 Enthalpy-entropy diagram with paths for different streamtubes

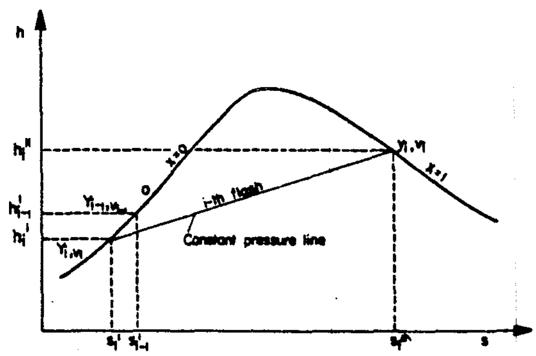

Fig. 3 Details of the ith flash on an enthalpy-entropy diagram

Nomenclature

G = mass flux
G_c = critical mass flux
h' = enthalpy of saturated water
h'' = enthalpy of saturated steam
p = pressure
p_{sat} = saturation pressure
s' = entropy of saturated water
s'' = entropy of saturated steam
T = temperature
v = velocity
x = quality
x_0 = initial quality
Y = normalized liquid mass flow rate (dimensionless)
y_i = traction of total mass flow rate in ith streamtube (vapor + droplets)
y_0 = initial moisture content $y_0 = 1 - x_0$
W = mass flow rate
ρ' = density of saturated water
ρ'' = density of saturated steam
ϵ = slip ratio

Subscripts

0 = stagnation value
i, n = numbers of steps

$$Y_{i-1} = Y_i + y_i \quad (1)$$

Entropy is conserved if:

$$Y_{i-1}s_{i-1}' = Y_i s_i' + y_i s_i'' \quad (2)$$

and energy is conserved if:

$$Y_{i-1}\left(h_{i-1}' + \frac{v_{i-1}^2}{2}\right) = Y_i\left(h_i' + \frac{v_i^2}{2}\right) + y_i\left(h_i'' + \frac{v_i^2}{2}\right) \quad (3)$$

Combining (1) and (2) we may solve for y_i:

$$y_i = Y_{i-1}\frac{s_{i-1}' - s_i'}{s_i'' - s_i'} \quad (4)$$

while combination of (1) and (3) gives v_i:

$$v_i^2 = v_{i-1}^2 + 2\left[h_{i-1}' - h_i' - \frac{y_i}{Y_{i-1}}(h_i'' - h_i')\right] \quad (5)$$

Since the thermodynamic properties are known from the pressure steps, (4) and (5) can be used to calculate y_i and v_i in successive stages of flashing. Y_i follows from (1).

An interesting interpretation of (5) is possible if we use the thermodynamic identity,

$$h_i'' - h_i' = T_i(s_i'' - s_i') \quad (6)$$

Substituting (4) in (5) and using (6) yields

$$\frac{v_i^2 - v_{i-1}^2}{2} = h_{i-1}' - h_i' - T_i(s_{i-1}' - s_i') \quad (7)$$

If Δp is small this is equivalent to

$$v\Delta v = \Delta h' - T\Delta s' = \frac{\Delta p}{\rho'} \quad (8)$$

which is just what would be expected if Bernoulli's equation had been applied to the liquid (a reasonable approach since there is no force besides the pressure that acts on the liquid stream and no reaction from the fleshing vapor since it suffers no finite change in velocity).

Once the vapor is created it expands isentropically with s_i, the specific entropy of the ith streamtube. equal to s_i''. the vapor specific entropy at the originating pressure (Fig. 4). The initial conditions, the pressure at which the streamtube is created and the flow rate y_i are known, therefore the quality, enthalpy, velocity, density and flow area of the streamtube can be calculated as a function of downstream pressure.

For the ith streamtube, created in the ith Δp step. the quality at the nth Δp step downstream is

$$x_{i,n} = \frac{s_i - s_n'}{s_n'' - s_n'} \quad (9)$$

The enthalpy is then

$$h_{i,n} = (1 - x_{i,n})h_n' + x_{i,n}h_n'' \quad (10)$$

and the velocity

$$v_{i,n} = [2(h_i - h_{i,n}) + v_i^2]^{1/2} \quad (11)$$

Since the homogeneous density in the ith streamtube is

$$\rho_{i,n} = \frac{1}{\dfrac{(1 - x_{i,n})}{\rho_n'} + \dfrac{x_{i,n}}{\rho_n''}} \quad (12)$$

The total mass flow per unit overall cross-section area is obtained as the reciprocal of the sum of the areas of all streamtubes, per unit normalized flow as

$$G = \left[\sum_{i=1}^{n}\frac{y_i}{\rho_{i,n}v_{i,n}} + \frac{Y_n}{\rho_n' v_n}\right]^{-1} \quad (13)$$

The criterion for critical flow is

$$\frac{dG}{dp} = 0 \quad (14)$$

i.e., the mass flow per unit area is a maximum.

Since the fluid in each streamtube has a different velocity, with the vapor that is first created being the fastest, a velocity profile is developed in the nozzle.

Subcooled Inlet Conditions. This method can be extended to predict flows in which subcooled liquid enters the nozzle. The liquid is accelerated in the nozzle isentropically and Benouilli's equation can be used until the saturation pressure is reached. At that point the same calculation procedure as indicated earlier for saturated liquid can be applied starting with a finite velocity equal to $[2(p_0 - p_{sat})/\rho_f]^{1/2}$ at the onset of flashing.

Two-Phase Inlet Conditions. A similar approach can be adopted when a steam-water mixture enters the nozzle. The only boundary condition necessary in this case is some assumption about the vapor and liquid velocities at the entrance.

In the absence of better information we have assumed equal phase velocities at the nozzle inlet.

The calculation procedure is illustrated on an enthalpy-entropy diagram in Fig. 5. For the first pressure drop by a certain small amount Δp it is assumed that the phases have equal velocities. Thereafter two streamtubes form and the previous calculation procedure is followed.

An Example

This calculation procedure will be illustrated by means of an example. The initial state is chosen as saturated water with zero velocity and an entrance pressure of $p_0 = 3.98$ MPa, corresponding to $T_0 = 250°C$. The pressure drop step size Δp is 0.1 MPa. Fig. 6 shows the predicted mass flux versus the pressure drop. It can be seen that a maximum is reached at about a pressurt drop of 1.05 MPa. Fig. 7 shows the corresponding velocity profile at thii "critical flow" condition for a cylindrical duct and a total flow rate of W = 1 kg/s; two different predictions are shown for Δp = 0.1 MPa and Δp = 0.05 MPa.

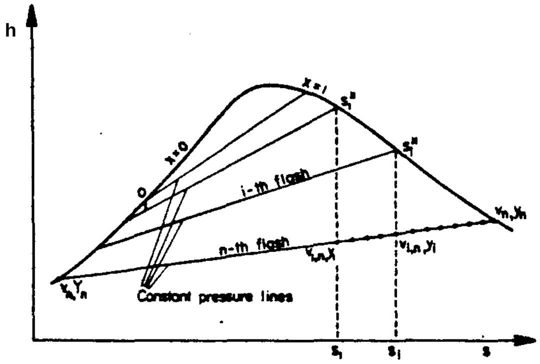

Fig. 4 States of streamtubes after the nth flash

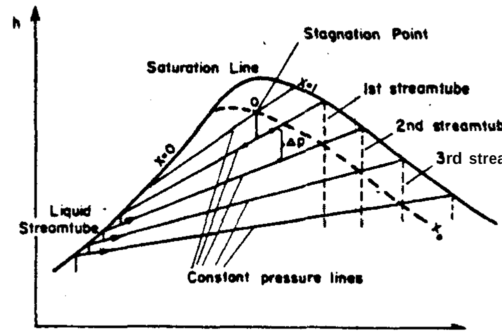

Fig. 5 Enthalpy-entropy diagram with paths for different streamtubes. A vapor-liquid mixture with a quality of x_0 enters the nozzle

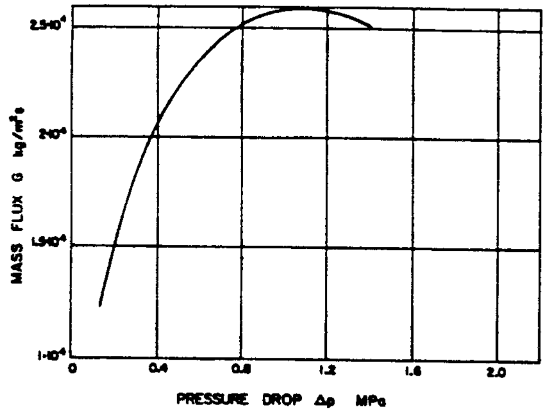

Fig. 6 Mass flux versus pressure drop for water flashing from a stagnation temperature of T_0 = 250° C. (P_0 = 3.98 MPa)

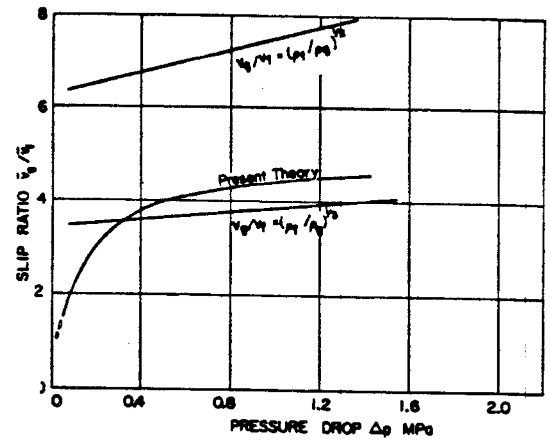

Fig. 8 Slip ratio versus pressure drop for water expanding from T_0 = 250°C, p_0 = 3.98 MPa

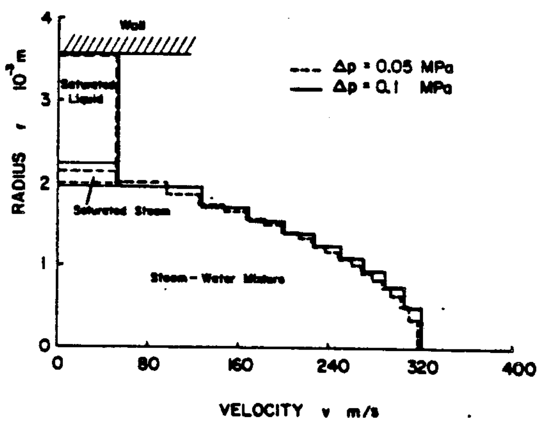

Fig. 7 Predicted velocity profiles in the throat of a nozzle for two different pressure drop steps, Δp (W = 1 kg/s, P_0 = 3.98 MPa. T_0 = 250 °C - - - - - Δp = 0.05 MPa —— Δp = 0.1 MPa)

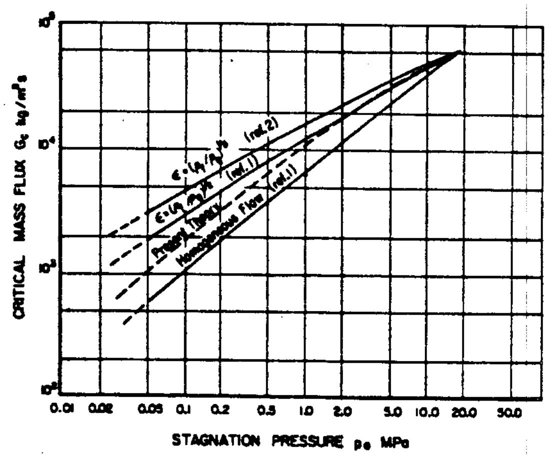

Fig. 9 Critical mass flux versus stagnation pressure for saturated water at inlet

We also calculated average phase velocities at each step, using the definitions

$$\bar{v}_{g,n} = \frac{\sum_1^n y_i v_{i,n} x_{i,n}}{\sum_1^n y_i x_{i,n}} \tag{15}$$

$$\bar{v}_{f,n} = \frac{\sum_1^n y_i v_{i,n}(1 - x_{i,n}) + Y_n v_n}{\sum_1^n y_i(1 - x_{i,n}) + Y_n} \tag{16}$$

and deduced an effective slip ratio,

$$\epsilon_n = \frac{\bar{v}_{g,n}}{\bar{v}_{f,n}} \tag{17}$$

The result is compared with two previous theories in Fig. 8.

Prediction of Critical Mass Flux

Calculations were pursued for saturated water expanding from various stagnation pressures. In Fig. 9 the critical mass flux G_c is plotted versus the stagnation pressure p_0 at the entrance to the nozzle. The present theory is compared with the homogeneous theory and two classical slip flow theories. The results obtained from this theory are between the extremes of homogenous flow and the maximum flux for a slip ratio of the cube root of the density ratio.

Comparison with Data

Fig. 10 shows comparison with experiments using saturated water

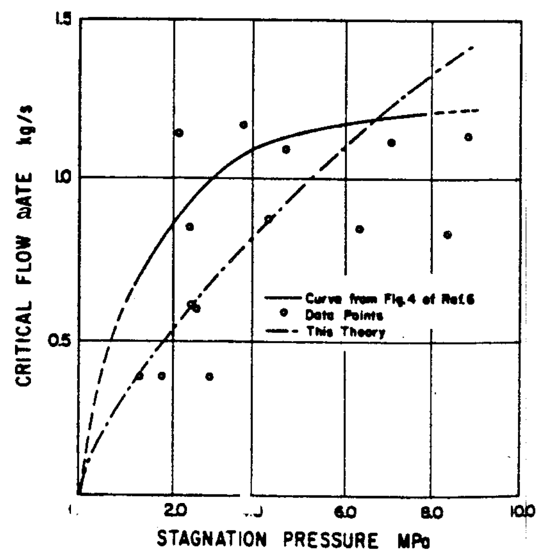

Fig. 10 Comparison between this theory and experiments by Schrock, et al. [6] for saturated water at inlet into the nozzle

entering a nozzle (Schrock, Starkman, et al. [6]).[1] The predictions of the streamtube model seem to give better agreement with the widely scattered data than the curve plotted in reference [6].

Comparison of the streamtube model with other experimental results from the same authors [6, 7] for a different shaped nozzle for saturated as well as subcooled water entering the nozzle shows good agreement (Fig. 11).

Earlier data of Starkman, Schrock, et al. [8] for steam-water mixtures of different qualities at the nozzle entrance are compared with the etreamtube model in Fig. 12. The agreement is very good for low pressures.

In the paper by Deich, et al. [9] experiments in nozzles were described for different moisture contents, $y_0 = 1 - x_0$, at the inlet (Fig. 13). The agreement with the present theory is good for low qualities and the data appear to lie between our predictions and the calculations based on the homogeneous equilibrium model.

Even comparisons with tube data as described by Moody show rather good agreement (Fig. 14). Since inertia effects tend to dominate near critical flow the details of the upstream flow in the pipe can probably be neglected as long as the pipe is not too long. The same figure also shows Moody's theory which uses a slip ratio equal to $(\rho_f/\rho_g)^{1/3}$. In order to obtain these predictions, which are based on quality at the point of critical flow, wt varied the "effective inlet stagnation quality" at each pressure until choking wm predicted at the desired exit quality.

[1] These data were taken from [6], an ASME preprint, but do not appear in the JOURNAL OF HEAT TRANSFER version of the paper [7]. We have checked with the senior author that these data are valid.

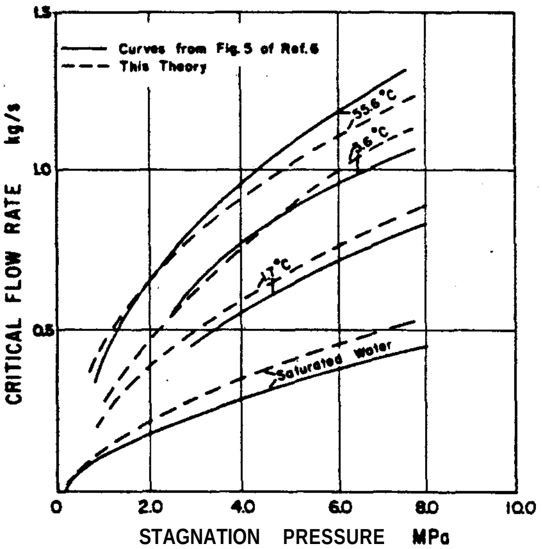

Fig. 11 Comparison between this theory and experiments by Schrock, et al. [6] for saturated and subcooled water at inlet into the nozzle

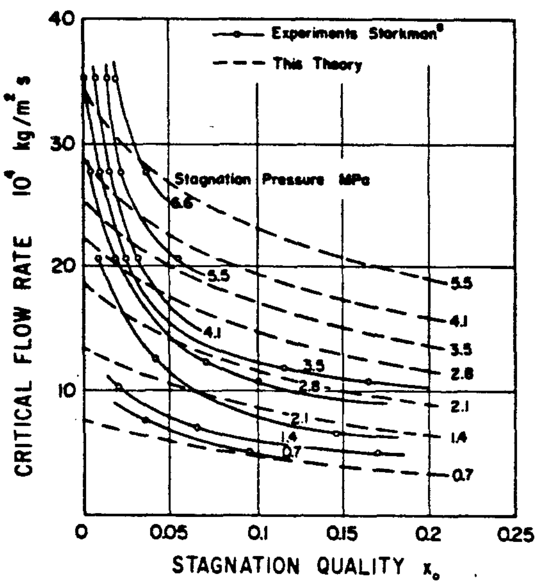

Fig. 12 Comparison between this theory and experiments by Starkman, et al. [8] for saturated water and steam-water mixtures entering the nozzle

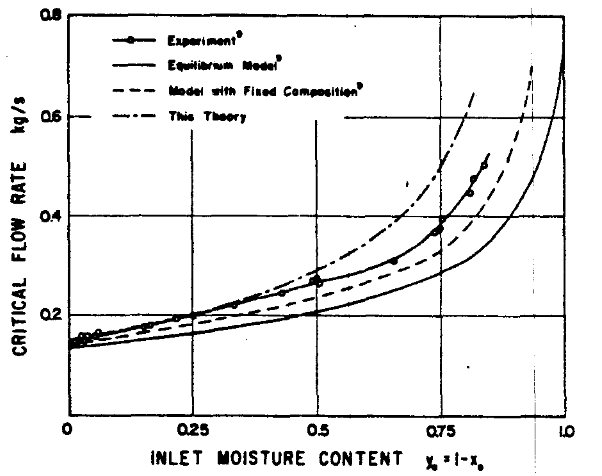

Fig. 13 Comparison between this theory, experiments by Deich, et al. [9] for different steam-water mixtures at inlet of the nozzle and two theories by Deich, et al.

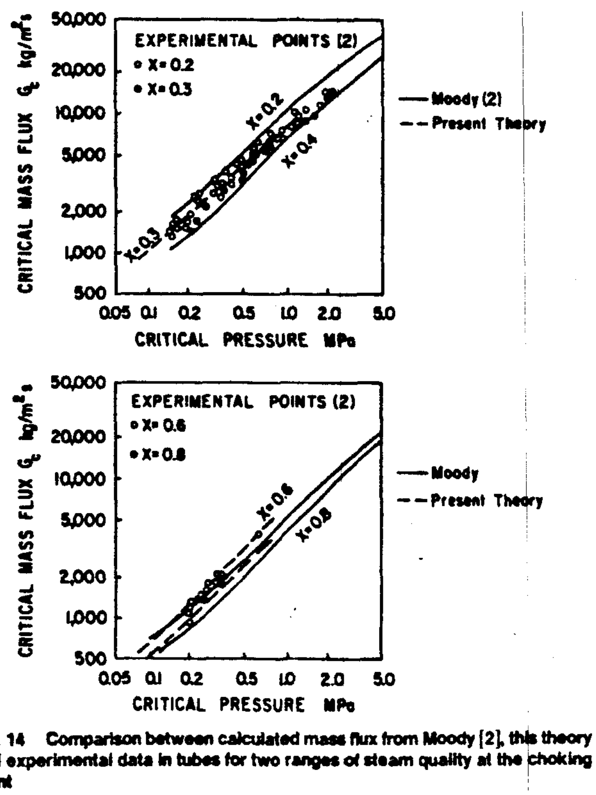

Fig. 14 Comparison between calculated mass flux from Moody [2], this theory and experimental data in tubes for two ranges of steam quality at the choking point

Conclusions

This present model for prediction of choked or critical flow is more consistent in its assumptions than many other models and predicts observed critical flow rates competitively. It does not represent the details of choking realistically but it *can* be considered as a certain ideal limit, comparable to the isentropic predictions of the characteristics of compression or expansion machines, which do not give the complete picture either but are very helpful for providing standards for comparison with actual performance and as starting points for the development of more elaborate theories.

Acknowledgment

The authors gratefully acknowledge the support for this work from the Electric Power Research Institute (EPRI), Contract (RP-443-2).

References

1 Fauske, H. K. "Critical Two-Phase, Steam-Water Flow," ANL-6633, 1963, pp. 79–89.

2 Moody, F. J., "Maximum Flow Rate of a Single Component, Two-Phase Mixture," ASME JOURNAL OF HEAT TRANSFER, 1965, pp. 134–142.

3 Levy, S. "Prediction of Two-Phase Critical Flow Rate," ASME JOURNAL OF HEAT TRANSFER, 1965, pp. 53-58.

4 Zivi, S. M., "Estimation of Study State Steam Void Fraction by Means of the Principle of Minimum Entropy Production," ASME JOURNAL OF HEAT TRANSFER, 1964, pp. 247–252.

5 Wallis, G. B. *One Dimensional Two-Phase Flow.* McGraw-Hill, New York, 1969, pp. 73-80.

6 Schrock, V. E., E S. Starkman and R. A. Brown, "Flashing Flow of Initially Subcooled Water in Convergent-Divergent Noel— " ASME paper 76-HT-12.

7 Schrock, V. E. E S. Starkman md R A Brown, "Flashing Flow of Initially Subcooled Water in Convergent-DivergentNoel— " ASME JOURNAL OF HEAT TRANSFER, Vol. 99, May, 1977, pp. 263–268.

8 Starkman, E S., V. E Schrock, K. F. Neusen, and D. J. Maneely, "Expansion of a Very Low Quality Two-Phase Fluid Through / Convergent-Divergent Nozzle," *Journal of Basic Engineering*, June, 1964, pp. 247–256

9 Deich, M. E., V. S. Danilin, G. V. Tsiklauri, and V. K. Shanin, "Investigation of the Flow of Wet Steam in Axi-Symmetric Laval Nozzles over / Wide Range of Moisture Content," *High Temperature 7*, Vol. 2, 1969, pp. 294–299.

APPENDIX B

LISTING OF PROGRAM

GEOFLOW

WITH TYPICAL OUTPUT

```
//GEOFLOW JOB
// EXEC WATFIV
//SYSIN DD *
$WATFIV
C      STREAM TUBE MODEL TO CALCULATE STEAM/WATER
C      MASS FLOW-RATES ASSUMING ISENTROPIC EXPANSION
C      FOLLOWED BY HEAT TRANSFER AT CONSTANT PRESSURE
C
C      BASED ON PAPER BY WALLIS, G.B. AND RICHTER, H.J. (1978)
C
C      STEAM/WATER THERMODYNAMIC PROPERTIES CALCULATED
C      USING SUBROUTINES DEVELOPED BY PROF. W.C.REYNOLDS,
C      MECHANICAL ENGINEERING DEPT.,STANFORD UNIVERSITY
C
C      AUTHOR: A.J.MENZIES
C
       IMPLICIT REAL*8 (A-H,O-Z)
       DIMENSION VI(200),YW(200),YS(200),P(200),CPW(200),CPS(200)
       DIMENSION X(200),HA(200),VA(200),DA(200),HB(200),VB(200)
       DIMENSION TI(20)
       COMMON
      $  /A/ VW(200),VS(200),SW(200),SWS(200),SS(200)
      $  /B/ HW(200),HWS(200),HS(200),TA(200)
C
C      INPUT VARIABLES
C
C      PI - INITIAL PRESSURE
C      PS - SATURATION PRESSURE
C      DP - SIZE OF PRESSURE STEP
C       N - NO. OF PRESSURE STEPS
C     EIE - ISENTROPIC EFFICIENCY
C
C
       READ(5,50) (TI(J),J=1,20)
 50    FORMAT(20A4)
       WRITE(6,60) (TI(J),J=1,20)
 60    FORMAT(///////,19X,20A4,///)
       READ(5,100) PI,PS,DP,N,EIE
 100   FORMAT(2F7.3,F5.1,I3,F5.3)
       WRITE(6,150)
 150   FORMAT(19X,'INIT. PRESS.',10X,'SATN. PRESS.',10X,'DELTA P.',
      $10X,'ISEN. EFFICIENCY')
       WRITE(6,160) PI,PS,DP,EIE
 160   FORMAT(20X,F7.3,' MPa.a',9X,F7.3,' MPa.a',7X,F5.1,' kPa',
      $18X,F5.3,///)
       WRITE(6,200)
 200   FORMAT(1X,'PRESS.',10X,'TEMP.',11X,'MASS FLUX',12X,
      C'SLIP RATIO',7X,'ENTHALPY',9X,'YW',9X,'SATW',11X,
      C'KS',11X,'KW')
C
       PI=PI*1D03
       PS=PS*1D03
       FHT=1.-EIE
       PA=PS
       I=1
       CALL STEAM(PA,I)
C
       IF(PI.EQ.PS) VI(1)=0.
       IF(PI.GT.PS) VI(1)=DSQRT(2.*VW(I)*(PI-PS))
C
       YW(1)=1.
C
       M=N+1
       P(1)=PS
       DO 10 I=2,M
       P(I)=P(I-1)-DP
       PA=P(I)
       CALL STEAM(PA,I)
C
       PB=P(I)/1000.
       PB2=PB*PB
       PB3=PB2*PB
       IF(PB.LT.2.)  GO TO 5
       IF(PB.LT.7.)  GO TO 6
C
       CPW(I)=3.2028+0.5352*PB-0.0483*PB2+2.4122D-3*PB3
       CPS(I)=-3.0874+2.2944*PB-0.2316*PB2+0.01*PB3
       GO TO 7
 5     CPW(I)=4.2072+0.2236*PB-0.02319*PB2
       CPS(I)=2.0098+0.6689*PB-0.08314*PB2
```

```
      GO TO 7
 6    CPW(I)=4.3137+0.1155*PB+5.7979D-3*PB2
      CPS(I)=2.3794+0.3074*PB+0.01033*PB2
 7    TD=TA(I)-273.15D0
      IF(TD.LT.220.) GO TO 8
      IF(TD.LT.290.) GO TO 9
C
      VISW=87.5233+0.3404*TD-1.1072D-3*(TD**2.)
      VISS=108.0263-0.6619*TD+1.2262D-3*(TD**2.)
      GO TO 11
 8    VISW=629.5949-5.2018*TD+0.01823*(TD**2.)-2.3066D-5*(TD**3.)
      VISS=8.2206+0.03988*TD-1.3636D-5*(TD**2.)
      GO TO 11
 9    VISW=338.6224-1.4286*TD+2.0076D-3*(TD**2.)
      VISS=14.3811-1.5957D-2*TD+1.1288D-4*(TD**2.)
C
 11   QTS=FHT*CPS(I)*(TA(1)-TA(I))
      DELSS=QTS/TA(I)
      QTW=FHT*CPW(I)*(TA(1)-TA(I))
      DELSW=QTW/TA(I)
C
      DO 20 J=2,I
C
      IF(I.EQ.J) GO TO 30
C
      HB(J)=HA(J)
      VB(J)=VA(J)
      X(J)=(SS(J)-SW(I))/SWS(I)
      IF(X(J).LE.1.) GO TO 25
      HA(J)=HS(I)+TA(I)*(SS(J)-SS(I))
      X(J)=1.
      GO TO 22
 25   HA(J)=(1.-X(J))*HW(I)+X(J)*HS(I)
 22   VI3=2000.*(HB(J)-HA(J))+VB(J)**2.
      VA(J)=DSQRT(VI3)
      DA(J)=1./((1.-X(J))*VW(I)+X(J)*VS(I))
C
      GO TO 26
C
 30   YS(J)=YW(J-1)*(SW(J-1)-SW(J))/SWS(J)
      YW(J)=YW(J-1)-YS(J)
      VI1=(HW(J-1)-HW(J))-(HWS(J)*(YS(J)/YW(J-1)))
      VI2=(VI(J-1)**2.+2000.*VI1)
      VI(J)=DSQRT(VI2)
      DA(J)=1./VS(I)
      X(J)=1.
      VA(J)=VI(I)
      HA(J)=HS(I)
      HW(J)=HW(J)+QTW
      SW(J)=SW(J)+DELSW
 26   HA(J)=HA(J)+QTS
      SS(J)=SS(J)+DELSS
C
 20   CONTINUE
C
      GW=YW(I)*VW(I)/VI(I)
      GS=0.
      VS1=0.
      VS2=0.
      VW1=0.
      VW2=0.
      HS1=0.
      HW1=0.
      DS1=0.
C
      DO 40 J=2,I
C
      GS=GS+(YS(J)/(DA(J)*VA(J)))
      VS1=VS1+(YS(J)*VA(J)*X(J))
      VS2=VS2+(YS(J)*X(J))
      VW1=VW1+(YS(J)*VA(J)*(1.-X(J)))
      VW2=VW2+(YS(J)*(1.-X(J)))
      HS1=HS1+YS(J)*X(J)*HA(J)
      HW1=HW1+YS(J)*HA(J)*(1.-X(J))
      DS1=DS1+YS(J)*DA(J)
C
 40   CONTINUE
C
      G=1./(GS+GW)
      VSA=VS1/VS2
```

```
      VWA=(VW1+(YW(I)*VI(I)))/(VW2+YW(I))
      SR=VSA/VWA
      HW1=HW1+YW(I)*HW(I)
      HAVE=HW1+HS1
      DS1=DS1/(1.-YW(I))
      DW1=1./VW(I)
      DWDS=DW1/DS1
      VFF=(DWDS/SR)*((1.-YW(I))/YW(I))
      VFF=1./VFF
      VF=1.-(1./(VFF+1.))
      PWPS=(1./SR)*(VF/(1.-VF))*(VISW/VISS)
      PS=1./(PWPS+1.)
      PW=1.-PS
      IF(HAVE.LE.HS(I)) GO TO 41
      SR=-1.
      PS=1.
      PW=0.
 41   PE=PA/1000.
      TB=TA(I)-273.15D0
C
      WRITE(6,300) PE,TB,G,SR,HAVE,YW(I),VF,PS,PW
 300  FORMAT(1X,F6.3,9X,F6.2,11X,F8.2,15X,F5.2,10X,F7.2,8X,F5.3
     C,8X,F5.3,8X,F5.3,8X,F5.3)
C
 10   CONTINUE
C
      RETURN
      END
C
      SUBROUTINE STEAM(PA,I)
C
C    SUBROUTINE FOR CALCULATION OF
C    STEAM/WATER PROPERTIES
C
      IMPLICIT REAL*8 (A-H,O-Z)
      DIMENSION VWS(200)
      COMMON
     $  /A/ VW(200),VS(200),SW(200),SWS(200),SS(200)
     $  /B/ HW(200),HWS(200),HS(200),TA(200)
C
      COMMON /CRIT/ R,TC,VC,PC
      EXTERNAL PH2O,SH2O,DH2O
      R=461.51
      TC=647.286
      VC=1./317.0
      PC=22.089D6
      T=550
      V=.07
      P=PA*1D03
      CALL SAT(T,P,DPDT,2,SH2O)
      CALL PROP(T,P,V,U,H,S,2,PH2O)
      CALL DH2O (T,DF)
      VW(I)=1./DF
      VS(I)=V
      VWS(I)=VS(I)-VW(I)
      HS(I)=H/1000.
      HWS(I)=T*VWS(I)*DPDT/1000.
      HW(I)=HS(I)-HWS(I)
      SS(I)=S/1000.
      SWS(I)=HWS(I)/T
      SW(I)=SS(I)-SWS(I)
      TA(I)=T
      RETURN
      END
C***********************************************************
C           THE FOLLOWING ROUTINES ARE GENERAL ROUTINES GIVEN IN TPSI
      SUBROUTINE PROP(T,P,V,U,H,S,NOP,PH2O)
C
C          ROUTINE FOR THERMODYNAMIC PROPERTIES EVALUATION
C
C          NOP DETERMINES THE TWO INPUT PROPERTIES. TRIAL VALUES FOR
C          T AND V MUST ALWAYS BE PROVIDED.
C          IF NOP=1, ENTER WITH T,V
C          IF NOP=2, ENTER WITH T,P, AND TRIAL V
C          IF NOP=3, ENTER WITH P,V, AND TRIAL T
C          IF NOP=4, ENTER WITH V,H, AND TRIAL T
C          IF NOP=5, ENTER WITH T,H, AND TRIAL V
C          IF NOP=6, ENTER WITH S,V, AND TRIAL T
C          IF NOP=7, ENTER WITH S,T, AND TRIAL V
C          IF NOP=8, ENTER WITH S,P, AND TRIAL T,V
```

```
C           IF NOP=9, ENTER WITH H,P, AND TRIAL T,V
C           IF NOP=10,ENTER WITH S,H, AND TRIAL T,V
C
C           THE INTERNAL PARAMETERS ERP,ERH, AND ERS CONTROL THE
C           ACCURACY OF P, H, AND S ITERATIONS.
C
C           THE USER MUST FILL COMMON BLOCK CRIT WITH THE GAS.
C           CONSTANT R AND THE CRITICAL T,V,P.
C
C           PH2O(T,P,V,U,H,S) IS THE USER'S SUBSTANCE-SPECIFIC
C           ROUTINE THAT CALCULATES P,U,H,S FOR INPUT T,V.
C
C           ALL QUANTITIES ARE DOUBLE PRECISION.
C
      IMPLICIT REAL*8  (A-H,O-Z)
      COMMON /CRIT/ R,TC,VC,PC
      DATA ERP,ERH,ERS/3*0.0001D0/
C           INITIALIZATIONS
      DT=0.DO
      KBR=0
      DVBF=1.0D0
      VMIN=0.DO
      VMAX=1.0D30
      PMIN=1.0D30
      PMAX=0.DO
      DVS1=2.0D0*VC
      DVS2=0.7D0*VC
      KTR=1
C           LOOP POINT
    1 RT=R*T
      CALL PH2O(T,PX,V,UX,HX,SX)
C           TEST FOR CONVERGENCE
      GO TO (10,20,20,40,40,60,60,80,90,100),  NOP
   10 GO TO 700
   20 IF (DABS(P-PX).LT.(ERP*P))  GO TO 700
      GO TO 104
   40 IF (DABS(H-HX).LT.(ERH*RT))  GO TO 700
      GO TO 104
   60 IF (DABS(S-SX).LT.(ERS*R))  GO TO 700
      GO TO 104
   80 IF ((DABS(S-SX).LT.(ERS*R)).AND.(DABS(P-PX).LT.(ERP*P))) GO TO 700
      GO TO 104
   90 IF ((DABS(H-HX).LT.(ERH*RT)).AND.(DABS(P-PX).LT.(ERP*P)))
     1      GO TO 700
      GO TO 104
  100 IF ((DABS(S-SX).LT.(ERS*R)).AND.(DABS(H-HX).LT.(ERH*RT)))
     1 GO TO 700
      GO TO 104
  104 IF (KTR.GT.20)  GO TO 850
C           CALCULATE THE NECESSARY PARTIAL DERIVATIVES
      IF (PX.LT.0.D0)  GO TO 300
      GO TO (880,120,110,110,120,110,120,110,110,110),  NOP
C           PERTURB T
  110 DT=0.001D0*T
      T1=T+DT
      V1=V
      CALL PH2O(T1,P1,V1,U1,H1,S1)
      GO TO ~880~880~140~140~880~140~880~120NOP120~120~~
C           PERTURB V
  120 DV=0.001D0*V
      IF (V.LE.VC)  DV=-DV
      V2=V+DV
      T2=T
      CALL PH2O(T2,P2,V2,U2,H2,S2)
  140 GO TO (880,220,230,240,250,260,270,280,290,296),  NOP
  220 DPDV=(P2-PX)/DV
      IF (DPDV.GT.0.D0)  GO TO 300
C           THE POINT IS GOOD - UPDATE LIMITS
      IF ((PX.GT.P).AND.(V.GT.VMIN)) VMIN=V
      IF ((PX.LT.P).AND.(V.LT.VMAX))  VMAX=V
      IF (V.EQ.VMIN)  PMIN=PX
      IF (V.EQ.VMAX)  PMAX=PX
      IF (VMIN.GE.VMAX)  GO TO 840
      IF ((VMIN.GT.0.D0).AND.(VMAX.LT.1.0D30))  KBR=1
      DVBF=1.0D0
      IF (DPDV.EQ.0.D0)  GO TO 226
      DV=(P-PX)/DPDV
      DT=0.DO
      GO TO 400
C           DPDV=0 AT A GOOD POINT - TREAT BY BRACKETING
```

```
  226 DVBF=0.5D0
      GO TO 300
  230 DPDT=(P1-PX)/DT
      DT=(P-PX)/DPDT
      DV=0.D0
      GO TO 400
  240 DHDT=(H1-HX)/DT
      DT=(H-HX)/DHDT
      DV=0.D0
      GO TO 400
  250 DHDV=(H2-HX)/DV
      DV=(H-HX)/DHDV
      DT=0.D0
      GO TO 400
  260 DSDT=(S1-SX)/DT
      DT=(S-SX)/DSDT
      DV=0.D0
      GO TO 400
  270 DSDV=(S2-SX)/DV
      DV=(S-SXI/DSDV
      DT=0.D0
      GO TO 400
  280 DSDT=(S1-SX)/DT
      DSDV=(S2-SX)/DV
      DPDT=(P1-PX)/DT
      DPDV=(P2-PX)/DV
      DET=DSDT*DPDV-DPDT*DSDV
      DT=((S-SX)*DPDV-(P-PX)*DSDV)/DET
      DV=(DSDT*(P-PX)-DPDT*(S-SX))/DET
      GO TO 400
  290 DHDT=(H1-HX)/DT
      DHDV=(H2-HX)/DV
      DPDT=(P1-PX)/DT
      DPDV=(P2-PX)/DV
      DET=DHDT*DPDV-DPDT*DHDV
      DT=((H-HX)*DPDV-(P-PX)*DHDV)/DET
      DV=(DHDT*(P-PX)-DPDT*(H-HX))/DET
      GO TO 400
  296 DHDT=(H1-HX)/DT
      DHDV=(H2-HX)/DV
      DSDT=(S1-SX)/DT
      DSDV=(S2-SX)/DV
      DET=DHDT*DSDV-DSDT*DHDV
      DT=((H-HX)*DSDV-(S-SX)*DHDV)/DET
      DV=(DHDT*(S-SX)-DSDT*(H-HX))/DET
      GO TO 400
C          SPECIAL TREATMENT FOR NOP=2, DESIGNED TO AVOID BAD ROOTS
  300 IF (KBR.EQ.0)  GO TO 320
C          CALCULATE SLOPE FROM BRACKETING VALUES
      DPDV=(PMAX-PMIN)/(VMAX-VMIN)
      V=VMAX
      PX=PMAX
      DV=DVBF*(P-PX)/DPDV
      DT=0.D0
      DVBF=0.5D0*DVBF
      GO TO 400
C          NOT YET BRACKETED - ALTER V TO SEEK GOOD POINT
  320 IF (V.LE.VC)  DV=-0.05D0*V
      IF (V.GT.VC)  DV=0.2D0*V
      IF (VMIN.GT.0.D0)  DV=0.2D0*V
      IF (VMAX.LT.1.0D30)  DV=-0.05D0*V
      GO TO 400
C          REGULATE THE MAXIMUM CHANGE
  400 DVM=0.2D0*V
      IF (V.LT.DVS1)  DVM=0.5D0*DVM
      IF (V.LT.DVS2)  DVM=0.5D0*DVM
      DTM=0.1D0*T
      IF (NOP.NE.2)  GO TO 440
C          SPECIAL PRECAUTIONS FOR NOP=2
      IF (KBR.EQ.0)  GO TO 440
      VT=V+DV
      IF ((VT.GE.VMIN).AND.(VT.LE.VMAX))  GO TO 440
C          BRACKETING LIMITATION
      DV=VMIN+(P-PMIN)*(VMAX-VMIN)/(PMAX-PMIN) - V
  440 DVA=DABS(DV)
      DTA=DABS(DT)
      IF (DVA.GT.DVM)  DV=DV*DVM/DVA
      IF (DTA.GT.DTM)  DT=DT*DTM/DTA
      T=T+DT
      V=V+DV
```

```
      KTR=KTR+1
      GO TO 1
C           NORMAL RETURN
  700 GO TO (710,720,720,740,740,760,760,780,790,796),  NOP
  710 P=PX
      U=UX
      H=HX
      S=SX
      RETURN
  720 U=UX
      H=HX
      S=SX
      RETURN
  740 P=PX
      U=UX
      S=SX
      RETURN
  760 P=PX
      U=UX
      H=HX
      RETURN
  780 H=HX
      U=UX
      RETURN
  790 S=SX
      U=UX
      RETURN
  796 P=PX
      U=UX
      RETURN
C           ERROR WRITES
  840 WRITE (6,842)  T,P,V,VMIN,VMAX
  842 FORMAT ('OPROP  ERROR - T,P,V,VMIN,VMAX= ',5D15.5)
      RETURN
  880 WRITE (6,882)
  882 FORMAT ('0PROGRAM ERROR IN PROP')
      RETURN
  850 WRITE (6,852)  NOP,T,P,V,H,S,PX,HX,SX
  852 FORMAT ('0PROP NOT CONVERGENT FOR NOP = ',I3/
     1  1H ,7X,'T',14X,'P',14X,'V',14X,'H',14X,'S',14X,'PX',13X,
     2  'HX',13X,'SX'/1H ,8E15.5)
      RETURN
      END
C**********************************************************************
      SUBROUTINE SAT(T,P,DPDT,NOP,SH2O)
C
C          SATURATION PRESSURE-TEMPERATURE ROUTINE
C
C          FOR NOP=1, CALCULATES PSAT(T) AND DP/DT ON SAT. LINE.
C          FOR NOP=2, CALCULATES TSAT(P) AND DP/DT; A TRIAL T IS NEEDED.
C
C          THE INTERNAL PARAMETER ERR CONTROLS THE ITERATION ACCURACY.
C
C          THE USER MUST FILL COMMON BLOCK CRIT WITH THE GAS
C          CONSTANT R AND THE CRITICAL T,V,P.
C
C          SH2O(T,P,DPDT) IS THE USER'S SUBSTANCE-SPECIFIC ROUTINE
C          THAT CALCULATES P,DPDT FOR INPUT T.
C
C          ALL QUANTITIES ARE DOUBLE PRECISION.
C______________________________________________________________________
      IMPLICIT REAL*8  (A-H,O-Z)
      COMMON /CRIT/  R,TC,VC,PC
      GO TO (1,2),  NOP
C           SPECIFIED T
    1 IF (T.GT.TC)  GO TO 70
      CALL SH2O(T,P,DPDT)
      RETURN
C           SPECIFIED P - START WITH THE TRIAL T
    2 IF (P.GT.PC)  GO TO 74
      KTR=0
      ERR=1.0D-6*P
   10 IF (T.GT.TC)  T=TC-0.001D0
      CALL SH2O(T,PX,DPDT)
      DP=P-PX
      IF (DABS(DP).LT.ERR)  GO TO 20
      IF (KTR.GT.20)  GO TO 80
      DT=DP/DPDT
      DTA=DABS(DT)
      DTM=0.1D0*T
```

```
      IF (DTA.GT.DTM)  DT=DT*DTM/DTA
      T=T+DT
      KTR=KTR+1
      GO TO 10
   20 RETURN
C         ERROR WRITES
   70 WRITE (6,92)  T
      RETURN
   74 WRITE (6,94)  P
      RETURN
   80 LJRITE (6,90)  T,P,DPDT,PX
      RETURN
   90 FORMAT ('0SAT NOT CONVERGENT FOR T,P,DPDT,PX=',4D15.5)
   92 FORMAT ('0SAT CALLED FOR T=',F6.1,'  >TC; GARBAGE RETURN')
   94 FORMAT ('0SAT CALLED FOR P=',1PD12.4,'  >PC; GARBAGE RETURN')
      END
C********* THERMODYNAMIC PROPERTIES OF H2O, NH3, AND CO2 ***
C
C         DEVELOPED BY W.C.  REYNOLDS, STANFORD UNIVERSITY
C         PROGRAMS USED FOR "THERMODYNAMIC PROPERTIES IN SI"
C
C**********THERMODYNAMIC PROPERTIES PACKAGE FOR H2O
      SUBROUTINE PH2O(T,P,V,U,H,S)
      IMPLICIT REAL*8  (A-H,O-Z)
      DATA R/461.51D0/
      RO=1.0D0/V
      CALL GH2O(T,CV,UG,SG)
      CALL QH2O(T,RO,TAU,Q,DQDTAU,DQDRO)
      C0=RO*R*T
      P=C0*(1.0D0+RO*Q+RO*RO*DQDRO)
      TDQDT=TAU*DQDTAU
      U=C0*TDQDT+UG
      S=RO*R*(TDQDT-Q) - R*DLOG(RO)+SG
      H=U+P*V
      RETURN
      END
      SUBROUTINE QH2O(T,RHO,TAU,Q,DQDT,DQDR)
C        CALCULATES Q,DQ/DRHO,DQ/DTAU FOR INPUT TK AND RHO - FULL SI
      IMPLICIT REAL*8 (A-H,O-Z)
      DIMENSION A(10,7),JM(10)
      DATA JM/4*7,4*2,2*7/
      DATA TAUP/2.5D0/
      DATA R/461.51D0/
      DATA T0,TAUC,RHOA1,RHOAJ,E,A/1.D3,1.544912D0,634.D0,1.D3,4.8D-3,
     1 2.94929370D-02,-1.32139170D-04, 2.74646320D-07,-3.60938280D-10,
     2 3.42184310D-13,-2.44500420D-16, 1.55185350D-19, 5.97284870D-24,
     3-4.10308480D-01,-4.16058600D-04,-5.19858600D-03, 7.77791820D-06,
     4-3.33019020D-08,-1.62546220D-11,-1.77310740D-13, 1.27487420D-16,
     5 1.37461530D-19, 1.55978360D-22, 3.37311800D-01,-2.09888660D-04,
     6 6.83353540D-03,-2.61497510D-05, 6.53263960D-08,-2.61819780D-11,
     7 0.00000000D-01, 0.00000000D-01, 0.00000000D-01, 0.00000000D-01,
     8-1.37466180D-01,-7.33968480D-04,-1.56410400D-04,-7.25461080D-07,
     9-9.27342890D-09, 4.31258400D-12, 0.00000000D-01, 0.00000000D-01,
     X 0.00000000D-01, 0.00000000D-01, 6.78749830D-03, 1.04017170D-05,
     1-6.39724050D-03, 2.64092820D-05,-4.77403740D-08, 5.63231300D-11,
     2 0.00000000D-01, 0.00000000D-01, 0.00000000D-01, 0.00000000D-01,
     3 1.36873170D-01, 6.45818800D-04,-3.96614010D-03, 1.54530610D-05,
     4-2.91424700D-08, 2.95687960D-11, 0.00000000D-01, 0.00000000D-01,
     5 0.00000000D-01, 0.00000000D-01, 7.98479700D-02, 3.99175700D-04,
     6-6.90485540D-04, 2.74074160D-06,-5.10280700D-09, 3.96360850D-12,
     7 0.00000000D-01, 0.00000000D-01, 0.00000000D-01, 0.00000000D-01,
     8 1.30412530D-02, 7.15313530D-05/
      TAU=T0/T
      SQ=0.DO
      SQR=0 .DO
      SQT=0 .DO
      EXA=E*RHO
      EX=0.DO
      IF (EXA.LT.70.0D0)  EX=DEXP(-EXA)
      DO 40 J=1,7
      B=0 .DO
      DB=0.DO
      IF (J.EQ.1)  RHOA=RHOA1
      IF (J.GT.1)  RHOA=RHOAJ
      C1=1.0D0
      C2=RHO-RHOA
      IF (DABS(RHO-RHOA).LT.(1.0D-08*RHOA))  C2=0.D0
      DO 10 I=1,8
      IF (J.GT.JM(I))  GO TO 10
      B=B+A(I,J)*C1
```

```
      IF (I.EQ.1)  GO TO 4
      DIN1=I-1
      DB=DB+A(I,J)*C3*DIM1
    4 C3=C1
      C1=C1*C2
   10 CONTINUE
      C1=1.0D0
      C2=RHO
      DO 14 I=9,10
      IF (J.GT.JM(I))  GO TO 14
      C5=EX*A(I,J)*C1
      B=B+C5
      DB=DB-E*C5
      IF (I.EQ.9)  GO TO 12
      DB=DB+EX*A(I,J)*C3
   12 C3=C1
      C1=C1*C2
   14 CONTINUE
      IF (J.GT.1)  GO TO 22
C         J=1
      TF=1.0D0
      DTF=0.D0
      GO TO 30
   22 IF (J.GT.2)  GO TO 24
C         J=2
      TMTC=TAU-TAUC
      TF=TMTC
      DTF=1.0D0
      TMTP=TAU-TAUP
      IF (DABS(TMTP).LT.(1.0D-8*TAUP))  TMTP=0.D0
      C7=TMTC*TMTP
      C8=TMTP
      C9=TMTC
      GO TO 30
C         J>2
   24 TF=C7
      DTF=C8+(J-2)*C9
      C7=C7*TMTP
      C8=C8*TMTP
      C9=C9*TMTP
   30 SQ=SQ+TF*B
      SQR=SQR+TF*DB
   40 SQT=SQT+DTF*B
      Q=SQ
      DQDR=SQR
      DQDT=SQT
      RETURN
      END
      SUBROUTINE GH2O(TX,CV,UG,SG)
      IMPLICIT REAL*8  (A-H,O-Z)
      DIMENSION B(6)
      DATA R,B/461.51D0,4.6D4,101 .249D0,8.3893D-1,-2.19989D-4,
     1  2.46619D-7,-9.7047D-11/
      DATA U0,S0/-0.23750207D7,-0 66965776D4/
      DATA T0/273.16D0/
      DATA L/0/
      IF (L.EQ.0)  GO TO 40
    1 T=TX
    2 DLT=DLOG(T)
      T2=T*T
      T3=T2*T
      T4=T3*T
      T5=T4*T
      T202=0.5D0*T2
      T303=T3/3.0D0
      T404=0.25D0*T4
      T505=0.2D0*T5
      UG=+B(1)*DLT+B(2)*T+B(3)*T202+B(4)*T303+B(5)*T404+B(6)*T505
      SG=-B(1)/T+B(2)*DLT+B(3)*T+B(4)*T202+B(5)*T303+B(6)*T404
      IF (L.EQ.0)  GO TO 42
      UG=UG-UG0
      SG=SG-SG0
      CV=B(1)/T+B(2)+B(3)*T+B(4)*T2+B(5)*T3+B(6)*T4
      RETURN
   40 T=T0
      R=R
      GO TO 2
   42 L=1
      UG0=UG+U0
      SG0=SG+S0
```

```
      GO TO 1
      END
      SUBROUTINE SH2O(T,P,DPDT)
      IMPLICIT REAL*8 (A-H,O-Z)
      DIMENSION F(8)
      DIMENSION FA(8)
      DATA TOK/1.0D3/
      DATA TPK,TCK,PC,F/338.15D0,647.286D0,22.088D6,0.74192420D3,
     1  -0.29721000D2,0.11552860D2,-0.8685635D0,-0.10940980D0,
     2  0.43999300D0,-0.25206580D0,0.5218684D-1/
      TK=T
      S1=0.D0
      S2=0.D0
      C1=1.0D0
      C2=0.01D0*(TK-TPK)
      IF (DABS(C2).LT.(1.0D-10*TPK))  C2=0.D0
      C3=1.D0
      DO 4 I=1,8
      S1=S1+F(I)*C1
      IF (I.EQ.1)  GO TO 4
      S2=S2+F(I)*C3*(I-1)
      C3=C3*C2
    4 C1=C1*C2
      TAUX=TOK*1.0D-05/TK
      TMTC=TK-TCK
      Z=TAUX*TMTC*S1
      DZ=-Z/TK+TAUX*S1+TAUX*TMTC*S2*0.01D0
      EX=DEXP(Z)
      P=PC*EX
      DPDT=P*DZ
      RETURN
      END
      SUBROUTINE DH2O(T,RF)
      IMPLICIT REAL*8  (A-H,O-Z)
      DIMENSION G(8)
      DATA RHOC,G/317.0D0,0.36711257D1,-0.28512396D2,0.22265240D3,
     1  -0.88243852D3,0.20002765D4,-0.26122557D4,0.18297674D4,
     2  -0.53350520D3/
      DATA TCK/647.286D0/
      IF (T.EQ.TCK)  GO TO 30
      OT=1.0D0/3.0D0
      X=(1.D0-T/TCK)**OT
      IF (X.LT.1.0D-6)  X=0.D0
      CO=X
      SUM=1.0D0
      DO 20 I=1,8
      SUM=SUM+G(I)*CO
   20 CO=CO*X
      RHOF=RHOC*SUM
      GO TO 40
   30 RHOF=RHOC
      GO TO 40
   40 RF=RHOF
      RETURN
      END
C          END THERMODYNAMIC PROPERTIES PACKAGE FOR H2O
SDATA
INITIAL RESERVOIR TEMPERATURE = 270 C
005.506005.506050.01000.800
```

INITIAL RESERVOIR TEMPERATURE = 270 C

INIT. PRESS.	SATN. PRESS.	DELTA P.	ISEN EFFICIENCY
5.506 MPa.a	5.506 MPa.a	50.0 kPa	0.800

PRESS.	TEMP.	MASS FLUX	SLIP RATIO	ENTHALPY	YW	SATW	KS	KW
5.456	269.51	8732.05	1.00	1185.82	0.998	0.952	0.009	0.991
5.406	268.92	11430.62	2.32	1186.95	0.996	0.955	0.020	0.980
5.356	268.33	14258.27	2.57	1188.66	0.993	0.933	0.033	0.967
5.306	267.73	16034.41	2.76	1190.97	0.991	0.910	0.047	0.953
5.256	267.13	17409.77	2.85	1193.88	0.987	0.885	0.063	0.937
5.206	266.53	18479.39	2.91	1197.39	0.984	0.857	0.081	0.919
5.156	265.92	19297.52	2.95	1201.50	0.980	0.828	0.099	0.901
5.106	265.31	19903.71	2.98	1206.20	0.975	0.798	0.119	0.881
5.056	264.69	20103.77	3.05	1211.53	0.971	0.770	0.140	0.860
5.006	264.07	20441.66	3.05	1217.42	0.966	0.737	0.162	0.838
4.956	263.44	20640.29	3.05	1223.92	0.960	0.704	0.185	0.815
4.906	262.81	20707.88	3.06	1231.01	0.955	0.672	0.209	0.791
4.856	262.17	20666.77	3.06	1238.71	0.949	0.640	0.233	0.767
4.806	261.53	20536.90	3.07	1247.00	0.942	0.609	0.257	0.743
4.756	260.88	20335.27	3.08	1255.89	0.936	0.579	0.281	0.719
4.706	260.23	20076.25	3.09	1265.38	0.929	0.549	0.306	0.694
4.656	259.57	19771.97	3.10	1275.46	0.921	0.521	0.330	0.670
4.606	258.91	19432.60	3.10	1286.14	0.914	0.493	0.355	0.645
4.556	258.24	19066.68	3.11	1297.41	0.906	0.467	0.379	0.621
4.506	257.57	18681.33	3.12	1309.28	0.898	0.442	0.403	0.597
4.456	256.89	18271.94	3.14	1321.74	0.889	0.418	0.426	0.574
4.406	256.20	17868.76	3.14	1334.78	0.881	0.395	0.449	0.551
4.356	255.51	17461.59	3.15	1348.41	0.872	0.373	0.472	0.528
4.306	254.82	17049.29	3.16	1362.63	0.863	0.352	0.494	0.506
4.256	254.11	16637.87	3.17	1377.43	0.853	0.332	0.516	0.484
4.206	253.40	16230.05	3.18	1392.81	0.844	0.314	0.537	0.463
4.156	252.68	15827.71	3.19	1408.78	0.834	0.296	0.557	0.443
4.106	251.96	15432.31	3.20	1425.31	0.824	0.280	0.576	0.424
4.056	251.23	15044.97	3.21	1442.43	0.814	0.264	0.595	0.405
4.006	250.49	14656.88	3.23	1460.12	0.803	0.250	0.614	0.386
3.956	249.75	14289.80	3.24	1478.37	0.793	0.235	0.631	0.369
3.906	249.00	13933.57	3.24	1497.18	0.782	0.222	0.648	0.352
3.856	248.24	13586.91	3.25	1516.55	0.771	0.209	0.665	0.335
3.806	247.47	13249.91	3.26	1536.48	0.760	0.197	0.681	0.319
3.756	246.70	12922.80	3.28	1556.97	0.749	0.186	0.696	0.304
3.706	245.92	12605.72	3.29	1578.01	0.738	0.176	0.710	0.290
3.656	245.13	12298.73	3.30	1599.59	0.726	0.166	0.724	0.276
3.606	244.33	11996.98	3.32	1621.73	0.715	0.157	0.737	0.263
3.556	243.52	11712.87	3.33	1644.38	0.703	0.148	0.750	0.250
3.506	242.71	11436.42	3.34	1667.58	0.691	0.139	0.763	0.237
3.456	241.88	11168.69	3.35	1691.30	0.679	0.132	0.774	0.226
3.406	241.05	10909.88	3.37	1715.55	0.667	0.124	0.785	0.215

3.356	240.20	10659.80	3.38	1740.32	0.656	0.117	0.796	0.204
3.306	239.35	10418.19	3.40	1765.61	0.643	0.111	0.806	0.194
3.256	238.49	10184.76	3.41	1791.40	0.631	0.104	0.816	0.184
3.206	237.61	9957.35	3.43	1817.72	0.619	0.099	0.825	0.175
3.156	236.73	9739.49	3.44	1844.51	0.607	0.093	0.834	0.166
3.106	235.83	9529.29	3.46	1871.80	0.595	0.088	0.843	0.157
3.056	234.93	9325.93	3.47	1899.58	0.583	0.083	0.851	0.149
3.006	234.01	9129.05	3.49	1927.84	0.571	0.078	0.858	0.142
2.956	233.08	8938.40	3.51	1956.59	0.559	0.074	0.866	0.134
2.906	232.14	8753.73	3.52	1985.80	0.546	0.070	0.873	0.127
2.856	231.19	8574.81	3.54	2015.49	0.534	0.066	0.879	0.121
2.806	230.22	8401.36	3.56	2045.63	0.522	0.062	0.886	0.114
2.756	229.24	8233.14	3.57	2076.23	0.510	0.058	0.892	0.108
2.706	228.25	8069.87	3.59	2107.28	0.498	0.055	0.898	0.102
2.656	227.24	7911.28	3.61	2138.77	0.486	0.052	0.903	0.097
2.606	226.21	7757.11	3.63	2170.70	0.475	0.049	0.908	0.092
2.556	225.18	7607.08	3.65	2203.07	0.463	0.046	0.913	0.087
2.506	224.12	7460.95	3.67	2235.86	0.451	0.043	0.918	0.082
2.456	223.05	7318.97	3.69	2269.05	0.440	0.041	0.923	0.077
2.406	221.96	7180.69	3.71	2302.66	0.428	0.038	0.927	0.073
2.356	220.86	7045.60	3.73	2336.68	0.417	0.036	0.931	0.069
2.306	219.74	6913.58	3.75	2371.10	0.405	0.034	0.935	0.065
2.256	218.59	6784.46	3.77	2405.91	0.394	0.032	0.938	0.062
2.206	217.43	6658.04	3.79	2441.11	0.383	0.030	0.942	0.058
2.156	216.25	6534.11	3.81	2476.69	0.372	0.028	0.945	0.055
2.106	215.05	6412.48	3.84	2512.65	0.361	0.026	0.948	0.052
2.056	213.82	6292.89	3.85	2548.95	0.350	0.025	0.951	0.049
2.006	212.57	6175.51	3.88	2585.62	0.340	0.023	0.954	0.046
1.956	211.30	6059.83	3.90	2622.46	0.329	0.022	0.957	0.043
1.906	210.00	5946.02	3.92	2659.64	0.319	0.020	0.960	0.040
1.856	208.67	5833.48	3.95	2697.15	0.309	0.019	0.962	0.038
1.806	207.32	5722.08	3.97	2734.97	0.299	0.018	0.965	0.035
1.756	205.93	5611.70	4.00	2773.09	0.289	0.016	0.967	0.033
1.706	204.52	5501.85	-1.00	2811.48	0.280	0.015	1.000	0.000
1.656	203.07	5392.95	-1.00	2850.14	0.270	0.014	1.000	0.000
1.606	201.59	5284.49	-1.00	2889.06	0.261	0.013	1.000	0.000
1.556	200.07	5176.30	-1.00	2928.22	0.251	0.012	1.000	0.000
1.506	198.51	5068.24	-1.00	2967.58	0.242	0.011	1.000	0.000
1.456	196.92	4960.17	-1.00	3007.16	0.234	0.011	1.000	0.000
1.406	195.27	4851.39	-1.00	3046.87	0.225	0.010	1.000	0.000
1.356	193.59	4742.44	-1.00	3086.75	0.216	0.009	1.000	0.000
1.306	191.85	4632.75	-1.00	3126.75	0.208	0.008	1.000	0.000
1.256	190.06	4522.15	-1.00	3166.85	0.200	0.008	1.000	0.000
1.206	188.22	4410.52	-1.00	3207.02	0.192	0.007	1.000	0.000
1.156	186.31	4297.00	-1.00	3247.19	0.184	0.006	1.000	0.000
1.106	184.34	4182.15	-1.00	3287.37	0.177	0.006	1.000	0.000
1.056	182.29	4065.36	-1.00	3327.49	0.169	0.005	1.000	0.000
1.006	180.17	3946.49	-1.00	3367.53	0.162	0.005	1.000	0.000
0.956	177.96	3824.71	-1.00	3407.38	0.155	0.004	1.000	0.000
0.906	175.66	3700.33	-1.00	3447.03	0.148	0.004	1.000	0.000
0.856	173.26	3572.78	-1.00	3486.40	0.141	0.004	1.000	0.000
0.806	170.75	3441.52	-1.00	3525.38	0.135	0.003	1.000	0.000
0.756	168.10	3306.33	-1.00	3563.90	0.128	0.003	1.000	0.000
0.706	165.32	3166.71	-1.00	3601.83	0.122	0.003	1.000	0.000
0.656	162.37	3021.99	-1.00	3639.02	0.116	0.002	1.000	0.000
0.606	159.24	2871.77	-1.00	3675.30	0.110	0.002	1.000	0.000
0.556	155.90	2715.30	-1.00	3710.46	0.104	0.002	1.000	0.000
0.506	152.31	2551.83	-1.00	3744.20	0.099	0.001	1.000	0.000

STATEMENTS EXECUTED= 783314
CORE USAGE OBJECT CODE= 25976 BYTES,ARRAY AREA= 36232 BYTES,TOTAL AREA AVAILABLE= 221184 BYTES

APPENDIX C

OUTPUT FROM

GEOFLOW

FOR FIELD EXAMPLES

WELL:'UTAH-STATE' 14-2 FIELD: ROOSEVELT HOT SPRINGS, UTAH, USA

INIT. PRESS.	SATN. PRESS.	OE A P.	ISEN EFFICIENCY
9.845 MPa	4.0[illegible]4 MPa.a	300 kPa	0.995

PRESS.	TEMP.	MASS FLUX	SLIP RATIO	ENTHALPY	YW	SATW	KS	KW
4.644	259.42	8904.58	1.00	1134.97	0.998	0.939	0.011	0.989
4.594	258.75	12133.08	2.49	1134.93	0.996	0.950	0.022	0.978
4.544	258.08	14522.63	2.99	1134.91	0.994	0.937	0.033	0.967
4.494	257.41	16444.46	3.23	1134.90	0.992	0.922	0.044	0.956
4.444	256.73	18011.67	3.40	1134.90	0.990	0.908	0.056	0.944
4.394	256.04	19305.77	3.52	1134.91	0.988	0.893	0.067	0.933
4.344	255.35	20602.91	3.56	1134.93	0.986	0.876	0.078	0.922
4.294	254.65	21649.90	3.62	1134.97	0.984	0.861	0.089	0.911
4.244	253.94	22560.94	3.67	1135.02	0.982	0.846	0.101	0.899
4.194	253.23	23361.45	3.71	1135.08	0.980	0.830	0.112	0.888
4.144	252.51	24065.74	3.75	1135.15	0.978	0.815	0.124	0.876
4.094	251.79	24684.89	3.78	1135.24	0.976	0.800	0.135	0.865
4.044	251.05	25061.77	3.86	1135.35	0.974	0.788	0.146	0.854
3.994	250.32	25573.51	3.87	1135.45	0.972	0.771	0.158	0.842
3.944	249.57	26033.27	3.88	1135.57	0.970	0.756	0.169	0.831
3.894	248.82	26421.62	3.89	1135.70	0.967	0.740	0.181	0.819
3.844	248.06	26744.89	3.91	1135.84	0.965	0.725	0.193	0.807
3.794	247.29	27010.78	3.93	1135.99	0.963	0.710	0.204	0.796
3.744	246.51	27226.01	3.95	1136.15	0.961	0.696	0.216	0.784
3.694	245.73	27396.13	3.97	1136.33	0.959	0.682	0.228	0.772
3.644	244.94	27525.59	3.99	1136.52	0.956	0.667	0.239	0.761
3.594	244.14	27592.68	4.02	1136.72	0.954	0.654	0.251	0.749
3.544	243.33	27653.79	4.03	1136.93	0.952	0.639	0.262	0.738
3.494	242.51	27693.45	4.05	1137.14	0.949	0.625	0.274	0.726
3.444	241.68	27695.76	4.06	1137.37	0.947	0.611	0.286	0.714

```
STATEMENTS EXECUTED=   45573
CORE USAGE      OBJECT CODE=   25976 BYTES,ARRAY AREA=   36232 BYTES,TOTAL AREA AVAILABLE=  221180  BYTES
DIAGNOSTICS       NUMBER OF ERRORS=       0, NUMBER OF WARNINGS=0       0, NUMBER OF EXTENSIONS=      0
COMPILE TIME=    0.20 SEC,EXECUTION TIME=     0.87 SEC,       9.5'.06     THURSDAY     19 AUG 82     W TFIV - JUN 1977 V1L6
        C$STOP
```

WELL: BR-21 FIELD: BROADLANDS, NEW ZEALAND

INIT. PRESS.	SATN. PRESS.	DELTA P.	ISEN. EFFICIENCY
4.600 MPa.a	4.600 MPa.a	50.0 kPa	0.380

PRESS.	TEMP.	MASS FLUX	SLIP RATIO	ENTHALPY	YW	SATW	KS	KW
4.550	258.16	8472.37	1.00	1130.19	0.998	0.938	0.011	0.989
4.500	257.49	11601.10	2.28	1132.91	0.995	0.933	0.027	0.973
4.450	256.81	13561.71	2.69	1137.03	0.992	0.901	0.048	0.952
4.400	256.12	14965.59	2.86	1142.54	0.987	0.862	0.072	0.928
4.350	255.43	15985.06	2.93	1149.45	0.982	0.810	0.100	0.900
4.300	254.73	16547.50	2.99	1157.77	0.976	0.769	0.131	0.869
4.250	254.03	16815.61	3.03	1167.48	0.969	0.720	0.165	0.835
4.200	253.32	16857.47	3.06	1178.59	0.962	0.671	0.200	0.800
4.150	252.60	16725.87	3.08	1191.10	0.953	0.622	0.237	0.763
4.100	251.87	16464.32	3.10	1205.01	0.944	0.575	0.274	0.726
4.050	251.14	16108.45	3.11	1220.31	0.934	0.530	0.312	0.688
4.000	250.41	15628.62	3.14	1237.02	0.924	0.490	0.349	0.651
3.950	249.66	15185.82	3.14	1255.09	0.913	0.44[illegible]	0.386	0.614
3.900	248.91	14714.16	3.14	1274.53	0.901	0.411	0.422	0.578
3.850	248.15	14223.55	3.14	1295.36	0.888	0.376	0.457	0.543
3.800	247.38	13727.00	3.15	1317.55	0.875	0.344	0.490	0.510
3.750	246.61	13234.20	3.16	1341.10	0.862	0.315	0.523	0.477
3.700	245.82	12751.89	3.16	1365.99	0.848	0.288	0.554	0.446
3.650	245.03	12284.59	3.17	1392.23	0.833	0.264	0.583	0.417
3.600	244.23	11821.87	3.19	1419.81	0.818	0.242	0.610	0.390
3.550	243.42	11401.32	3.19	1448.68	0.802	0.221	0.637	0.363
3.500	242.61	10994.73	3.19	1478.87	0.786	0.203	0.661	0.339
3.450	241.78	10606.27	3.20	1510.35	0.770	0.186	0.685	0.315
3.400	240.95	10237.80	3.21	1543.12	0.754	0.170	0.706	0.294
3.350	240.10	9889.13	3.22	1577.15	0.737	0.156	0.727	0.273
3.300	239.25	9559.68	3.22	1612.43	0.719	0.148	0.746	0.254
3.250	238.38	9248.72	3.23	1648.96	0.702	0.132	0.764	0.236
3.200	237.51	8950.55	3.25	1686.72	0.684	0.121	0.780	0.220
3.150	236.62	8675.64	3.26	1725.68	0.666	0.111	0.796	0.204
3.100	235.73	8416.47	3.26	1765.82	0.648	0.102	0.810	0.190

```
STATEMENTS EXECUTED=   169.15
CORE USAGE      OBJECT CODE=   25976 BYTES,ARRAY AREA=    36232 BYTES,TOTAL AREA AVAILABLE=  221184  BYTES
DIAGNOSTICS       NUMBER OF ERRORS=      0, NUMBER OF WARNINGS=       0, NUMBER OF EXTENSIONS=       0
COMPILE TIME=    0.20 SEC,EXECUTION TIME=      1.00 SEC,       9.56.44     THURSDAY      19 AUG 82     WATFIV - JAN 1977 V1L6
        C$STOP
```

WELL: K≤-12 FI≤LD: X⊼AF[illegible] ICELAND

INIT. ⊐⊼ES[illegible] 12.600 M[illegible].a | SATN. PRE[illegible] 11.289 X[illegible].a | D≤LTA P. 5o.0 kPa | ISEN ≤FFICIENCY 0.950

PRESS.	TEMP.	MASS FLUX	SLIP RATIO	ENTHALPY	YW	SATW	KS	KW
11.239	319.77	8192.27	1.00	1462.26	0.998	0.984	0.004	0.996
11.189	319.43	11453.10	1.66	1462.40	0.997	0.980	0.009	0.991
11.139	319.10	13914.89	1.87	1462.65	0.995	0.972	0.014	0.986
11.089	318.76	15946.93	1.97	1463.01	0.993	0.964	0.019	0.981
11.039	318.42	17694.21	2.03	1463.48	0.991	0.955	0.024	0.976
10.989	318.08	19231.61	2.07	1464.05	0.989	0.946	0.029	0.971
10.939	317.73	20603.84	2.09	1464.73	0.987	0.937	0.035	0.965
10.889	317.39	21840.18	2.11	1465.52	0.985	0.927	0.041	0.959
10.839	317.05	22961.08	2.13	1466.41	0.983	0.917	0.047	0.953
10.789	316.70	23981.57	2.14	1467.42	0.980	0.906	0.053	0.947
10.739	316.35	24913.11	2.15	1468.53	0.978	0.895	0.060	0.940
10.689	316.00	25764.72	2.16	1469.74	0.975	0.884	0.066	0.934
10.639	315.65	26543.70	2.16	1471.06	0.973	0.873	0.073	0.927
10.589	315.30	27256.11	2.17	1472.49	0.970	0.862	0.080	0.920
10.539	314.95	27907.07	2.17	1474.02	0.968	0.850	0.087	0.913
10.489	314.60	28500.97	2.18	1475.66	0.965	0.838	0.095	0.905
10.439	314.24	29041.76	2.18	1477.41	0.962	0.826	0.102	0.898
10.389	313.88	29532.99	2.19	1479.26	0.959	0.814	0.110	0.890
10.339	313.53	29977.81	2.19	1481.21	0.956	0.802	0.118	0.882
10.289	313.17	30379.07	2.20	1483.27	0.953	0.790	0.125	0.875
10.239	312.81	30739.40	2.20	1485.44	0.950	0.778	0.133	0.867
10.189	312.45	31061.20	2.21	1487.71	0.947	0.765	0.142	0.858
10.139	312.08	31346.72	2.21	1490.08	0.944	0.753	0.150	0.850
10.089	311.72	31598.05	2.22	1492.56	0.940	0.741	0.158	0.842
10.039	311.35	31745.77	2.23	1495.16	0.937	0.729	0.166	0.834
9.989	310.98	31965.52	2.23	1497.84	0.934	0.716	0.175	0.825
9.939	310.62	32147.48	2.23	1500.63	0.930	0.704	0.184	0.816
9.889	310.25	32292.72	2.23	1503.52	0.927	0.691	0.193	0.807
9.839	309.87	32403.38	2.24	1506.52	0.923	0.679	0.201	0.799
9.789	309.50	32481.86	2.24	1509.62	0.919	0.667	0.210	0.790
9.739	309.13	32530.55	2.25	1512.83	0.916	0.655	0.219	0.781
9.689	308.75	32552.59	2.26	1516.14	0.912	0.643	0.228	0.772
9.639	308.37	32575.87	2.26	1519.55	0.908	0.631	0.237	0.763
9.589	307.99	32580.45	2.26	1523.07	0.905	0.619	0.246	0.754
9.539	307.61	32567.11	2.27	1526.68	0.901	0.607	0.255	0.745
9.489	307.23	32536.77	2.27	1530.40	0.897	0.595	0.265	0.735
9.439	306.85	32490.44	2.28	1534.22	0.893	0.584	0.274	0.726
9.389	306.46	32429.10	2.28	1538.15	0.889	0.572	0.283	0.717
9.339	306.07	32353.71	2.28	1542.17	0.885	0.561	0.292	0.708
9.289	305.69	32265.21	2.29	1546.30	0.880	0.550	0.301	0.699
9.239	305.30	32164.48	2.29	1550.53	0.876	0.539	0.311	0.689
9.189	304.90	32052.37	2.30	1554.86	0.872	0.528	0.320	0.680

9.139	304.51	31929.68	2.30	1559.29	0.868	0.517	0.329	0.671
9.089	304.12	31797.39	2.31	1563.83	0.864	0.506	0.338	0.662
9.039	303.72	31655.84	2.31	1568.46	0.859	0.496	0.348	0.652
8.989	303.32	31505.90	2.32	1573.20	0.855	0.486	0.357	0.643
8.939	302.92	31348.23	2.32	1578.04	0.850	0.475	0.366	0.634
8.889	302.52	31183.45	2.33	1582.97	0.846	0.466	0.375	0.625
8.839	302.12	31012.16	2.34	1588.01	0.842	0.456	0.384	0.616
8.789	301.71	30834.91	2.34	1593.15	0.837	0.446	0.393	0.607
8.739	301.30	30652.21	2.35	1598.38	0.832	0.437	0.402	0.598
8.689	300.89	30464.58	2.35	1603.72	0.828	0.427	0.411	0.589
8.639	300.48	30272.46	2.36	1609.15	0.823	0.418	0.420	0.580
8.589	300.07	30076.30	2.37	1614.69	0.819	0.409	0.429	0.571
8.539	299.66	29876.52	2.37	1620.32	0.814	0.400	0.438	0.562
8.489	299.24	29673.49	2.38	1626.06	0.809	0.392	0.447	0.553
8.439	298.82	29467.58	2.38	1631.89	0.805	0.383	0.456	0.544
8.389	298.40	29259.14	2.39	1637.81	0.800	0.375	0.465	0.535
8.339	297.98	29048.48	2.40	1643.84	0.795	0.367	0.473	0.527
8.289	297.56	28827.88	2.41	1649.98	0.790	0.359	0.482	0.518
8.239	297.13	28617.90	2.41	1656.19	0.785	0.351	0.490	0.510
8.189	296.70	28404.59	2.42	1662.50	0.781	0.343	0.499	0.501
8.139	296.27	28187.85	2.42	1668.92	0.776	0.336	0.507	0.493
8.089	295.84	27967.80	2.43	1675.43	0.771	0.328	0.515	0.485
8.039	295.41	27744.72	2.44	1682.05	0.766	0.321	0.524	0.476
7.989	294.97	27532.28	2.44	1688.73	0.761	0.314	0.532	0.468
7.939	294.53	27313.78	2.45	1695.53	0.756	0.307	0.540	0.460
7.889	294.09	27094.95	2.46	1702.42	0.751	0.300	0.548	0.452
7.839	293.65	26870.24	2.47	1709.43	0.746	0.294	0.556	0.444
7.789	293.21	26651.41	2.48	1716.50	0.741	0.287	0.564	0.436
7.739	292.76	26433.21	2.48	1723.68	0.736	0.281	0.572	0.428
7.689	292.31	26215.58	2.49	1730.94	0.731	0.274	0.579	0.421
7.639	291.86	25998.56	2.50	1738.30	0.726	0.268	0.587	0.413
7.589	291.41	25782.20	2.50	1745.75	0.721	0.262	0.595	0.405
7.539	290.95	25566.58	2.51	1753.29	0.716	0.256	0.602	0.398
7.489	290.49	25351.78	2.52	1760.92	0.711	0.250	0.609	0.391
7.439	290.03	25137.88	2.53	1768.65	0.706	0.245	0.617	0.383
7.389	289.57	24924.95	2.54	1776.46	0.701	0.239	0.625	0.375
7.339	289.10	24713.08	2.54	1784.37	0.695	0.234	0.632	0.368
7.289	288.64	24502.32	2.55	1792.36	0.690	0.228	0.639	0.361
7.239	288.17	24292.74	2.56	1800.45	0.685	0.223	0.646	0.354
7.189	287.69	24084.40	2.57	1808.62	0.680	0.218	0.653	0.347
7.139	287.22	23877.34	2.58	1816.88	0.675	0.213	0.659	0.341
7.089	286.74	23671.63	2.59	1825.22	0.670	0.208	0.666	0.334
7.039	286.26	23467.30	2.59	1833.65	0.665	0.204	0.673	0.327
6.989	285.78	23264.38	2.60	1842.15	0.659	0.199	0.679	0.321
6.939	285.29	23063.21	2.61	1850.74	0.654	0.194	0.685	0.315
6.889	284.81	22863.39	2.62	1859.42	0.649	0.190	0.692	0.308
6.839	284.31	22664.97	2.63	1868.18	0.644	0.186	0.698	0.302
6.789	283.82	22467.36	2.64	1877.05	0.639	0.182	0.704	0.296
6.739	283.32	22271.94	2.65	1885.97	0.634	0.177	0.710	0.290
6.689	282.83	22077.98	2.66	1894.99	0.629	0.173	0.716	0.284
6.639	282.32	21885.17	2.67	1904.10	0.623	0.169	0.722	0.278
6.589	281.82	21694.20	2.68	1913.28	0.618	0.165	0.727	0.273
6.539	281.31	21504.82	2.69	1922.55	0.613	0.161	0.733	0.267
6.489	280.80	21316.91	2.69	1931.90	0.608	0.158	0.739	0.261
6.439	280.29	21130.53	2.70	1941.34	0.603	0.154	0.744	0.256
6.389	279.77	20945.66	2.71	1950.85	0.598	0.151	0.749	0.251
6.339	279.25	20762.29	2.72	1960.45	0.592	0.147	0.755	0.245
6.289	278.73	20580.42	2.74	1970.14	0.587	0.144	0.760	0.240
6.239	278.20	20399.56	2.75	1979.90	0.582	0.140	0.765	0.235
6.189	277.67	20220.45	2.76	1989.73	0.577	0.137	0.770	0.230

6.139	277.14	20042.98	2.77	1999.64	0.572	0.134	0.775	0.225
6.089	276.60	19867.08	2.78	2009.63	0.567	0.131	0.780	0.220
6.039	276.06	19692.70	2.79	2019.70	0.562	0.128	0.784	0.216
5.989	275.52	19519.81	2.80	2029.84	0.557	0.125	0.789	0.211
5.939	274.97	19348.39	2.81	2040.06	0.552	0.122	0.794	0.206
5.889	274.42	19178.39	2.82	2050.36	0.547	0.119	0.798	0.202
5.839	273.87	19009.80	2.83	2060.73	0.542	0.116	0.802	0.198
5.789	273.31	18842.60	2.84	2071.17	0.536	0.113	0.807	0.193
5.739	272.75	18676.76	2.85	2081.69	0.531	0.111	0.811	0.189
5.689	272.19	18512.30	2.86	2092.28	0.526	0.108	0.815	0.185
5.639	271.62	18349.13	2.87	2102.94	0.521	0.106	0.819	0.181
5.589	271.05	18187.27	2.89	2113.67	0.516	0.103	0.823	0.177
5.539	270.47	18027.39	2.90	2124.49	0.511	0.101	0.827	0.173
5.489	269.89	17867.08	2.91	2135.35	0.506	0.098	0.831	0.169
5.439	269.31	17709.12	2.92	2146.29	0.501	0.096	0.835	0.165
5.389	268.72	17552.15	2.93	2157.29	0.497	0.093	0.839	0.161
5.339	268.13	17396.55	2.94	2168.37	0.492	0.091	0.842	0.158
5.289	267.53	17242.10	2.96	2179.51	0.487	0.089	0.846	0.154
5.239	266.93	17088.79	2.97	2190.72	0.482	0.087	0.850	0.150
5.189	266.32	16936.60	2.98	2201.99	0.477	0.085	0.853	0.147
5.139	265.71	16785.50	2.99	2213.33	0.472	0.083	0.856	0.144
5.089	265.10	16635.47	3.01	2224.73	0.467	0.081	0.860	0.140
5.039	264.48	16487.44	3.02	2236.20	0.462	0.079	0.863	0.137
4.989	263.86	16338.89	3.03	2247.72	0.458	0.077	0.866	0.134
4.939	263.23	16191.56	3.05	2259.30	0.453	0.075	0.869	0.131
4.889	262.59	16045.34	3.06	2270.94	0.448	0.073	0.873	0.127
4.839	261.96	15900.17	3.07	2282.64	0.443	0.071	0.876	0.124
4.789	261.31	15755.97	3.09	2294.40	0.439	0.069	0.879	0.121
4.739	260.66	15612.70	3.10	2306.21	0.434	0.068	0.881	0.119
4.689	260.01	15470.32	3.11	2318.08	0.429	0.066	0.884	0.116
4.639	259.35	15328.78	3.13	2330.01	0.424	0.064	0.887	0.113
4.589	258.69	15188.05	3.14	2341.99	0.420	0.063	0.890	0.110
4.539	258.02	15048.10	3.16	2354.02	0.415	0.061	0.893	0.107
4.489	257.34	14908.90	3.17	2366.11	0.411	0.060	0.895	0.105
4.439	256.66	14770.47	3.18	2378.25	0.406	0.058	0.898	0.102
4.389	255.97	14633.10	3.20	2390.44	0.401	0.057	0.900	0.100
4.339	255.28	14495.37	3.21	2402.67	0.397	0.055	0.903	0.097
4.289	254.58	14358.90	3.23	2414.96	0.392	0.054	0.905	0.095
4.239	253.87	14223.04	3.24	2427.29	0.388	0.052	0.908	0.092
4.189	253.16	14087.75	3.26	2439.66	0.383	0.051	0.910	0.090
4.139	252.44	13953.01	3.27	2452.08	0.379	0.050	0.912	0.088
4.089	251.71	13818.79	3.29	2464.55	0.374	0.048	0.914	0.086
4.039	250.98	13686.26	3.31	2477.08	0.370	0.047	0.917	0.083
3.989	250.24	13552.34	3.32	2489.62	0.366	0.046	0.919	0.081
3.939	249.50	13419.14	3.34	2502.20	0.361	0.045	0.921	0.079
3.889	248.74	13286.51	3.35	2514.82	0.357	0.043	0.923	0.077
3.839	247.98	13154.37	3.37	2527.49	0.353	0.042	0.925	0.075
3.789	247.21	13022.65	3.39	2540.19	0.348	0.041	0.927	0.073
3.739	246.43	12891.29	3.40	2552.92	0.344	0.040	0.929	0.071
3.689	245.65	12760.23	3.42	2565.69	0.340	0.039	0.931	0.069
3.639	244.86	12629.44	3.44	2578.49	0.335	0.038	0.933	0.067
3.589	244.05	12499.26	3.46	2591.33	0.331	0.037	0.934	0.066
3.539	243.24	12368.81	3.47	2604.19	0.327	0.036	0.936	0.064
3.489	242.43	12238.19	3.49	2617.07	0.323	0.035	0.938	0.062
3.439	241.60	12108.13	3.51	2629.99	0.319	0.034	0.940	0.060
3.389	240.76	11978.17	3.53	2642.93	0.315	0.033	0.941	0.059
3.339	239.91	11848.28	3.54	2655.89	0.311	0.032	0.943	0.057
3.289	239.06	11718.42	3.56	2668.87	0.307	0.031	0.945	0.055
3.239	238.19	11588.56	3.58	2681.88	0.303	0.030	0.946	0.054
3.189	237.31	11459.45	3.60	2694.91	0.299	0.029	0.948	0.052

3.139	236.43	11329.00	3.62	2707.94	0.295	0.028	0.949	0.051
3.089	235.53	11198.71	3.64	2720.99	0.291	0.027	0.951	0.049
3.039	234.62	11068.43	3.66	2734.05	0.287	0.026	0.952	0.048
2.989	233.70	10938.07	3.68	2747.12	0.283	0.026	0.954	0.046
2.939	232.76	10807.54	3.70	2760.20	0.279	0.025	0.955	0.045
2.889	231.82	10677.76	3.72	2773.30	0.275	0.024	0.956	0.044
2.839	230.86	10545.90	3.74	2786.38	0.271	0.023	0.958	0.042
2.789	229.89	10414.25	3.76	2799.47	0.268	0.023	0.959	0.041
2.739	228.90	10282.59	-1.00	2812.56	0.264	0.022	1.000	0.000
2.689	227.90	10150.55	-1.00	2825.64	0.260	0.021	1.000	0.000
2.639	226.89	10018.12	-1.00	2838.72	0.256	0.020	1.000	0.000
2.589	225.86	9885.32	-1.00	2851.79	0.253	0.020	1.000	0.000
2.539	224.82	9752.13	-1.00	2864.85	0.249	0.019	1.000	0.000
2.489	223.76	9617.36	-1.00	2877.88	0.245	0.018	1.000	0.000
2.439	222.68	9482.74	-1.00	2890.90	0.242	0.018	1.000	0.000
2.389	221.59	9347.46	-1.00	2903.90	0.238	0.017	1.000	0.000
2.339	220.48	9211.49	-1.00	2916.87	0.235	0.017	1.000	0.000
2.289	219.35	9074.78	-1.00	2929.81	0.231	0.016	1.000	0.000
2.239	218.20	8937.32	-1.00	2942.72	0.227	0.015	1.000	0.000
2.189	217.03	8799.09	-1.00	2955.59	0.224	0.015	1.000	0.000
2.139	215.84	8660.12	-1.00	2968.42	0.220	0.014	1.000	0.000
2.089	214.63	8520.43	-1.00	2981.20	0.217	0.014	1.000	0.000
2.039	213.40	8378.22	-1.00	2993.91	0.214	0.013	1.000	0.000
1.989	212.14	8236.04	-1.00	3006.48	0.210	0.013	1.000	0.000
1.939	210.86	8092.85	-1.00	3018.98	0.207	0.012	1.000	0.000
1.889	209.55	7948.45	-1.00	3031.41	0.204	0.012	1.000	0.000
1.839	208.21	7802.84	-1.00	3043.76	0.200	0.011	1.000	0.000
1.789	206.85	7656.04	-1.00	3056.02	0.197	0.011	1.000	0.000
1.739	205.45	7508.13	-1.00	3068.19	0.194	0.010	1.000	0.000
1.689	204.03	7357.30	-1.00	3080.21	0.190	0.010	1.000	0.000
1.639	202.57	7205.90	-1.00	3092.12	0.187	0.009	1.000	0.000
1.589	201.08	7052.87	-1.00	3103.88	0.184	0.009	1.000	0.000
1.539	199.55	6898.16	-1.00	3115.50	0.181	0.009	1.000	0.000
1.489	197.97	6741.81	-1.00	3126.95	0.178	0.008	1.000	0.000
1.439	196.36	6583.07	-1.00	3138.20	0.174	0.008	1.000	0.000
1.389	194.71	6422.62	-1.00	3149.25	0.171	0.007	1.000	0.000
1.339	193.00	6260.06	-1.00	3160.07	0.168	0.007	1.000	0.000

```
STATEMENTS EXECUTED= 203978
CORE USAGE        OBJECT CODE=   25976 BYTES,ARRAY AREA=   36232 BYTES,TOTAL AREA AVAILABLE=  22 18C  BYTES
DIAGNOSTICS          NUMBER OF ERRORS=      0, NUMBER OF WARNINGS=       0, NUMBER OF EXTENSIONS=       0
COMPILE TIME=     0.21 SEC, EXECUTION TIME=     14.26 SEC,       9.54.41     THURSDAY      19 AUG 82    WATFIV - JUN 1977 V1L6
        C$STOP
```

WELL: C03 FIELD : TUNGONAN PHILIPPINES

INIT. PRESS.	SATN. PRESS.	DELTA P.	ISEN. EFFICIENCY
11.680 MPa.a	8.000 MPa.a	50.0 kPa	0.987

PRESS.	TEMP.	MASS FLUX	SLIP RATIO	ENTHALPY	YW	SATW	KS	KW
7.950	294.63	8641.44	1.00	1316.99	0.998	0.973	0.006	0.994
7.900	294.19	11926.46	1.97	1316.98	0.997	0.972	0.012	0.988
7.850	293.75	13838.51	2.39	1317.02	0.995	0.966	0.017	0.983
7.800	293.30	16037.28	2.49	1317.07	0.994	0.956	0.024	0.976
7.750	292.86	17901.42	2.56	1317.15	0.992	0.946	0.030	0.970
7.700	292.41	19519.02	2.61	1317.26	0.990	0.936	0.036	0.964
7.650	291.96	20947.69	2.65	1317.40	0.988	0.926	0.043	0.957
7.600	291.51	22224.79	2.68	1317.57	0.987	0.915	0.049	0.951
7.550	291.05	23376.19	2.70	1317.77	0.985	0.905	0.056	0.944
7.500	290.59	24420.69	2.72	1318.00	0.983	0.895	0.062	0.938
7.450	290.13	25372.53	2.74	1318.27	0.981	0.884	0.069	0.931
7.400	289.67	26242.80	2.76	1318.56	0.979	0.874	0.076	0.924
7.350	289.21	27040.38	2.77	1318.88	0.977	0.864	0.083	0.917
7.300	288.74	27772.50	2.78	1319.23	0.975	0.853	0.089	0.911
7.250	288.27	28445.17	2.80	1319.61	0.974	0.843	0.096	0.904
7.200	287.80	29063.45	2.81	1320.03	0.972	0.832	0.103	0.897
7.150	287.32	29631.66	2.82	1320.47	0.970	0.822	0.111	0.889
7.100	286.85	30153.54	2.83	1320.94	0.968	0.812	0.118	0.882
7.050	286.37	30632.33	2.84	1321.44	0.966	0.801	0.125	0.875
7.000	285.88	31070.89	2.85	1321.97	0.964	0.791	0.132	0.868
6.950	285.40	31471.76	2.86	1322.53	0.962	0.780	0.140	0.860
6.900	284.91	31837.31	2.87	1323.12	0.960	0.770	0.147	0.853
6.850	284.42	32169.41	2.87	1323.74	0.958	0.759	0.154	0.846
6.800	283.93	32398.72	2.90	1324.41	0.956	0.750	0.162	0.838
6.750	283.43	32717.88	2.89	1325.07	0.954	0.739	0.169	0.831
6.700	282.94	32975.37	2.90	1325.78	0.951	0.728	0.177	0.823
6.650	282.43	33166.85	2.91	1326.52	0.949	0.718	0.184	0.816
6.600	281.93	33380.84	2.91	1327.28	0.947	0.707	0.192	0.808
6.550	281.42	33549.10	2.92	1328.08	0.945	0.697	0.200	0.800
6.500	280.91	33692.72	2.93	1328.91	0.943	0.687	0.208	0.792
6.450	280.40	33812.90	2.94	1329.76	0.941	0.677	0.216	0.784
6.400	279.88	33911.58	2.94	1330.65	0.938	0.667	0.223	0.777
6.350	279.36	33989.87	2.95	1331.56	0.936	0.657	0.231	0.769
6.300	278.84	34004.36	2.97	1332.52	0.934	0.648	0.239	0.761
6.250	278.32	34046.49	2.98	1333.49	0.932	0.638	0.247	0.753
6.200	277.79	34075.61	2.98	1334.49	0.929	0.627	0.255	0.745
6.150	277.26	34088.31	2.99	1335.52	0.927	0.617	0.263	0.737
6.100	276.72	34084.21	2.99	1336.58	0.925	0.607	0.271	0.729
6.050	276.18	34063.68	3.00	1337.66	0.922	0.597	0.279	0.721
6.000	275.64	34027.39	3.01	1338.78	0.920	0.588	0.287	0.713
5.950	275.09	33976.07	3.01	1339.92	0.918	0.578	0.295	0.705
5.900	274.54	33910.50	3.02	1341.10	0.915	0.568	0.303	0.697

5.850	273.99	33831.42	3.03	1342.30	0.913	0.559	0.311	0.689
5.800	273.44	33739.53	3.04	1343.54	0.910	0.550	0.319	0.681
5.750	272.88	33635.50	3.04	1344.80	0.908	0.540	0.327	0.673
5.700	272.31	33519.80	3.05	1346.09	0.905	0.531	0.335	0.665
5.650	271.74	33393.18	3.06	1347.41	0.903	0.522	0.343	0.657
5.600	271.17	33256.19	3.07	1348.75	0.901	0.513	0.351	0.649
5.550	270.60	33109.34	3.08	1350.13	0.898	0.504	0.359	0.641
5.500	270.02	32951.56	3.08	1351.54	0.895	0.495	0.367	0.633
5.450	269.44	32786.18	3.09	1352.97	0.893	0.486	0.375	0.625
5.400	268.85	32608.02	3.11	1354.44	0.890	0.478	0.383	0.617
5.350	268.26	32425.88	3.11	1355.91	0.888	0.469	0.391	0.609
5.300	267.66	32239.22	3.12	1357.43	0.885	0.461	0.399	0.601
5.250	267.06	32043.78	3.13	1358.97	0.883	0.452	0.407	0.593
5.200	266.46	31840.80	3.13	1360.55	0.880	0.444	0.415	0.585
5.150	265.85	31630.93	3.14	1362.14	0.877	0.436	0.423	0.577
5.100	265.23	31414.61	3.15	1363.77	0.875	0.427	0.431	0.569
5.050	264.62	31192.85	3.17	1365.45	0.872	0.420	0.438	0.562
5.000	263.99	30958.87	3.17	1367.12	0.869	0.412	0.446	0.554
4.950	263.37	30723.68	3.18	1368.83	0.867	0.404	0.454	0.546
4.900	262.73	30485.09	3.19	1370.56	0.864	0.396	0.462	0.538
4.850	262.10	30242.36	3.20	1372.32	0.861	0.388	0.470	0.530
4.800	261.45	29995.31	3.21	1374.11	0.858	0.381	0.478	0.522
4.750	260.81	29743.97	3.22	1375.93	0.856	0.373	0.485	0.515
4.700	260.15	29488.48	3.22	1377.77	0.853	0.366	0.493	0.507
4.650	259.50	29229.04	3.23	1379.64	0.850	0.358	0.501	0.499
4.600	258.83	28965.85	3.24	1381.54	0.847	0.351	0.508	0.492
4.550	258.16	28699.15	3.25	1383.46	0.844	0.344	0.516	0.484
4.500	257.49	28429.14	3.26	1385.41	0.842	0.337	0.523	0.477
4.450	256.81	28157.20	3.28	1387.39	0.839	0.330	0.531	0.469
4.400	256.12	27880.76	3.29	1389.40	0.836	0.323	0.538	0.462
4.350	255.43	27600.00	3.29	1391.42	0.833	0.316	0.546	0.454
4.300	254.73	27319.46	3.31	1393.47	0.830	0.310	0.553	0.447
4.250	254.03	27036.33	3.32	1395.55	0.827	0.303	0.560	0.440
4.200	253.32	26750.95	3.33	1397.65	0.824	0.297	0.568	0.432
4.150	252.60	26463.51	3.34	1399.78	0.821	0.290	0.575	0.425
4.100	251.87	26174.20	3.35	1401.93	0.818	0.284	0.582	0.418
4.050	251.14	25883.16	3.36	1404.11	0.815	0.278	0.589	0.411
4.000	250.41	25596.66	3.38	1406.33	0.812	0.272	0.596	0.404
3.950	249.66	25297.49	3.38	1408.55	0.809	0.266	0.603	0.397
3.900	248.91	24999.90	3.40	1410.79	0.806	0.260	0.610	0.390
3.850	248.15	24702.55	3.41	1413.07	0.803	0.254	0.617	0.383
3.800	247.38	24404.79	3.42	1415.36	0.800	0.248	0.624	0.376
3.750	246.61	24106.33	3.43	1417.68	0.797	0.243	0.631	0.369
3.700	245.82	23807.06	3.44	1420.02	0.794	0.237	0.638	0.362
3.650	245.03	23506.96	3.45	1422.39	0.791	0.232	0.644	0.356
3.600	244.23	23212.17	3.47	1424.79	0.788	0.226	0.651	0.349
3.550	243.42	22903.07	3.48	1427.19	0.785	0.221	0.658	0.342
3.500	242.61	22600.58	3.49	1429.62	0.782	0.216	0.664	0.336
3.450	241.78	22298.44	3.50	1432.07	0.778	0.210	0.671	0.329
3.400	240.95	21995.60	3.52	1434.54	0.775	0.205	0.677	0.323
3.350	240.10	21692.27	3.53	1437.04	0.772	0.200	0.684	0.316
3.300	239.25	21388.59	3.54	1439.55	0.769	0.195	0.690	0.310
3.250	238.38	21084.63	3.56	1442.08	0.765	0.190	0.696	0.304
3.200	237.51	20787.35	3.57	1444.65	0.762	0.186	0.702	0.298
3.150	236.62	20477.48	3.59	1447.21	0.759	0.181	0.708	0.292
3.100	235.73	20170.89	3.60	1449.80	0.756	0.176	0.715	0.285
3.050	234.82	19865.82	3.61	1452.41	0.752	0.172	0.721	0.279
3.000	233.90	19561.42	3.63	1455.03	0.749	0.167	0.727	0.273

STATEMENTS EXECUTED= 806759
CORE USAGE OBJECT CODE= 25976 BYTES, ARRAY AREA= 36232 BYTES, TOTAL AREA AVAILABLE= 221180 BYTES